

**Investigation of the stress tolerance regulatory  
network integration of the NAC transcription factor  
JUNGBRUNNEN1 (JUB1)**

---

**Maryna Welsch**

**Univ.-Diss.**

**zur Erlangung des akademischen Grades**

**"doctor rerum naturalium"**

**(Dr. rer. nat.)**

**in der Wissenschaftsdisziplin "Molekulare Pflanzenphysiologie"**

**eingereicht an der  
Mathematisch-Naturwissenschaftlichen Fakultät  
Institut für Biochemie und Biologie  
der Universität Potsdam  
und  
Max-Planck-Institut für Molekulare Pflanzenphysiologie**

Ort und Tag der Disputation: Potsdam, 09.03.2022

Hauptbetreuer: Prof. Dr. Bernd Müller-Röber  
Betreuerin: Prof. Dr. Salma Balazadeh  
Gutachter: Prof. Dr. Bernd Müller-Röber  
Dr. Friedrich Kragler  
Prof. Dr. Wolfgang Dröge-Laser

Online veröffentlicht auf dem  
Publikationsserver der Universität Potsdam:  
<https://doi.org/10.25932/publishup-54731>  
<https://nbn-resolving.org/urn:nbn:de:kobv:517-opus4-547310>

## Summary

The NAC transcription factor (TF) JUNGBRUNNEN1 (JUB1) is an important negative regulator of plant senescence, as well as of gibberellic acid (GA) and brassinosteroid (BR) biosynthesis in *Arabidopsis thaliana*. Overexpression of *JUB1* promotes longevity and enhances tolerance to drought and other abiotic stresses. A similar role of JUB1 has been observed in other plant species, including tomato and banana. Our data show that *JUB1* overexpressors (*JUB1-OXs*) accumulate higher levels of proline than WT plants under control conditions, during the onset of drought stress, and thereafter. We identified that overexpression of *JUB1* induces key proline biosynthesis and suppresses key proline degradation genes. Furthermore, *bZIP63*, the transcription factor involved in proline metabolism, was identified as a novel downstream target of JUB1 by Yeast One-Hybrid (Y1H) analysis and Chromatin immunoprecipitation (ChIP). However, based on Electrophoretic Mobility Shift Assay (EMSA), direct binding of JUB1 to *bZIP63* could not be confirmed. Our data indicate that *JUB1-OX* plants exhibit reduced stomatal conductance under control conditions. However, selective overexpression of *JUB1* in guard cells did not improve drought stress tolerance in *Arabidopsis*. Moreover, the drought-tolerant phenotype of *JUB1* overexpressors does not solely depend on the transcriptional control of the *DREB2A* gene. Thus, our data suggest that JUB1 confers tolerance to drought stress by regulating multiple components. Until today, none of the previous studies on JUB1's regulatory network focused on identifying protein-protein interactions. We, therefore, performed a yeast two-hybrid screen (Y2H) which identified several protein interactors of JUB1, two of which are the calcium-binding proteins CaM1 and CaM4. Both proteins interact with JUB1 in the nucleus of *Arabidopsis* protoplasts. Moreover, *JUB1* is expressed with *CaM1* and *CaM4* under the same conditions. Since *CaM1.1* and *CaM4.1* encode proteins with identical amino acid sequences, all further experiments were performed with constructs involving the *CaM4* coding sequence. Our data show that JUB1 harbors multiple CaM-binding sites, which are localized in both the N-terminal and C-terminal regions of the protein. One of the CaM-binding sites, localized in the DNA-binding domain of JUB1, was identified as a functional CaM-binding site since its mutation strongly reduced the binding of CaM4 to JUB1. Furthermore, JUB1 transactivates expression of the stress-related gene *DREB2A* in mesophyll cells; this effect is significantly reduced when the calcium-binding protein CaM4 is expressed as well. Overexpression of both genes in *Arabidopsis* results in early senescence observed through lower chlorophyll content and an enhanced expression of senescence-associated genes (*SAGs*) when compared with single *JUB1* overexpressors. Our

data also show that JUB1 and CaM4 proteins interact in senescent leaves, which have increased  $\text{Ca}^{2+}$  levels when compared to young leaves. Collectively, our data indicate that JUB1 activity towards its downstream targets is fine-tuned by calcium-binding proteins during leaf senescence.

## Zusammenfassung

Der NAC Transkriptionsfaktor (TF) JUNGBRUNNEN1 (JUB1) ist ein wichtiger negativer Regulator der Pflanzenseneszenz, Gibberellinsäure- (GA) und Brassinosteroid- (BR) Biosynthese in *Arabidopsis thaliana*. Die Überexpression von JUB1 fördert die Langlebigkeit und erhöht die Toleranz gegenüber Trockenheit und anderen abiotischen Belastungen. Bei anderen Pflanzenarten, einschließlich Tomaten und Bananen, wurde eine ähnliche Rolle von JUB1 beobachtet. Unsere Daten zeigen, dass JUB1 Überexpressionslinien im Vergleich zu WT-Pflanzen sowohl unter Kontrollbedingungen, als auch zu Beginn und während späterer Stadien von Trockenstress größere Mengen an Prolin akkumulieren. Wir haben festgestellt, dass die Überexpression von JUB1 die Schlüsselbiosynthese von Prolin induziert und Schlüsselgene für den Abbau von Prolin unterdrückt. Darüber hinaus wurde bZIP63, ein am Prolinstoffwechsel beteiligter Transkriptionsfaktor, mittels Yeast One-Hybrid-System (Y1H) und Chromatin-Immunopräzipitation (ChIP) als neues nachgeschaltetes Ziel von JUB1 identifiziert. Basierend auf dem Electrophoretic Mobility Shift Assay (EMSA) konnte die direkte Bindung von JUB1 an bZIP63 jedoch nicht bestätigt werden. Unsere Daten zeigen, dass JUB1-OXs unter Kontrollbedingungen eine niedrigere stomatale Leitfähigkeit aufweisen. Allerdings verbessert eine selektive Überexpression von JUB1 in den Schließzellen die Trockenstresstoleranz bei *Arabidopsis* nicht. Darüber hinaus hängt der trockenheitstolerante Phänotyp von JUB1 nicht allein von der transkriptionellen Kontrolle des DREB2A-Gens ab. Unsere Daten legen daher nahe, dass JUB1 durch die Regulierung mehrerer Komponenten Toleranz gegenüber Trockenstress verleiht. Bis heute konzentrierte sich keine der bisherigen Studien zum regulatorischen Netzwerk von JUB1 auf die Identifizierung von Protein-Protein-Interaktionen. Wir führten deshalb einen Hefe-Zwei-Hybrid-Screen (Y2H) durch, der mehrere Protein-Interaktoren von JUB1 identifizierte, von denen zwei Calcium-bindende Proteine sind (CaM1 und CaM4). Beide Proteine interagieren mit JUB1 im Kern von *Arabidopsis*-Protoplasten. Darüber hinaus wird JUB1 mit den CaM1- und CaM4-Genen unter den gleichen Bedingungen exprimiert und kolokalisiert mit den Proteinen im Zellkern von *Arabidopsis thaliana*-Protoplasten. Unsere Daten zeigen, dass JUB1 mehrere CaM-Bindungsstellen aufweist, die sowohl in der N-terminalen, als auch in der C-terminalen Region des Proteins lokalisiert sind. Eine der CaM-Bindungsstellen, die in der DNA-Bindungsdomäne von JUB1 lokalisiert ist, wurde als funktionelle und aktive CaM-Bindungsstelle identifiziert, da ihre Mutation die Bindung von CaM4 an JUB1 stark reduzierte. Darüber hinaus transaktiviert JUB1 die Expression des stressbezogenen Gens DREB2A in Mesophyllzellen. Dieser Effekt wird

deutlich reduziert, wenn auch das Calcium-bindende Protein CaM4 exprimiert wird. Die Überexpression beider Gene in Arabidopsis führt zum frühen Seneszenz-Phänotyp, der durch einen verminderten Chlorophyllgehalt und eine veränderte SAGs-Expression im Vergleich zu einzelnen JUB1-Überexpressoren beobachtet wird. Unsere Daten zeigen auch, dass JUB1- und CaM4-Proteine in den seneszenten Blättern, die im Vergleich zu jungen Blättern erhöhte  $\text{Ca}^{2+}$ -spiegel aufweisen, interagieren. Zusammenfassend weisen unsere Daten darauf hin, dass während der Blattseneszenz die Aktivität von JUB1 gegenüber seinen nachgeschalteten Zielen durch die Calcium-bindenden Proteine fein abgestimmt wird.

## CONTENTS

Summary.....	I
Zusammenfassung.....	III
CONTENTS.....	V
LIST OF FIGURES.....	VIII
LIST OF TABLES.....	IX
ABBREVIATIONS.....	X
<b>1. INTRODUCTION.....</b>	<b>1</b>
<b>1.1. Abiotic stress tolerance and senescence in plants.....</b>	<b>1</b>
<b>1.2. Drought stress and resistance mechanisms.....</b>	<b>5</b>
<b>1.2.1. Accumulation of proline as a mechanism of stress survival.....</b>	<b>8</b>
<b>1.2.2. Stomatal responses upon drought stress.....</b>	<b>11</b>
<b>1.3. Plant response to environmental stimuli <i>via</i> calcium signaling.....</b>	<b>13</b>
<b>1.3.1. Ca<sup>2+</sup> signal transduction and decoding through calcium-binding proteins....</b>	<b>14</b>
<b>1.3.2. Calmodulins and their roles in the plant cell.....</b>	<b>16</b>
<b>1.3.3. Role of the protein-protein interaction between calmodulins and other         proteins.....</b>	<b>17</b>
<b>1.4. JUB1 function in stress-associated networks.....</b>	<b>19</b>
<b>1.5. Aim of the thesis.....</b>	<b>21</b>
<b>2. MATERIALS AND METHODS.....</b>	<b>22</b>
<b>2.1. General methods.....</b>	<b>22</b>
<b>2.2. Plant materials and growth conditions.....</b>	<b>23</b>
<b>2.3. Plasmid construction and plant transformation.....</b>	<b>24</b>
<b>2.4. Gene expression analysis.....</b>	<b>26</b>
<b>2.4.1. RNA isolation and cDNA synthesis.....</b>	<b>26</b>
<b>2.4.2. Quantitative real-time PCR (qRT-PCR).....</b>	<b>27</b>
<b>2.5. Yeast one-hybrid screen.....</b>	<b>27</b>
<b>2.6. Expression and purification of recombinant proteins in <i>E. coli</i>.....</b>	<b>28</b>
<b>2.7. Electrophoretic mobility shift assay (EMSA).....</b>	<b>28</b>
<b>2.8. Chromatin immunoprecipitation (ChIP) assay.....</b>	<b>29</b>
<b>2.10. Isolation and DNA transfection of mesophyll protoplasts.....</b>	<b>29</b>
<b>2.11. Transient transformation of <i>Nicotiana benthamiana</i>.....</b>	<b>30</b>
<b>2.12. Transactivation assay.....</b>	<b>30</b>
<b>2.13. Immunoblot analysis.....</b>	<b>31</b>

2.14. Microscopic analysis .....	32
2.15. Treatments.....	33
2.15.1. Drought treatment .....	33
2.15.2. Salt treatment .....	33
2.16. Determination of proline levels.....	34
2.17. Determination of Relative Water Content (RWC) .....	34
2.18. Measurement of chlorophyll content .....	34
2.19. Measurement of Ca <sup>2+</sup> level in leaves.....	34
2.20. GUS staining assay.....	35
2.21. DAB staining assay .....	35
2.22. Stomatal conductance .....	35
2.23. Statistical analysis .....	36
3. RESULTS .....	37
3.1. Overexpression of <i>JUB1</i> results in resistance to severe drought stress .....	37
3.2. Under control conditions, plants overexpressing <i>JUB1</i> accumulate a high level of proline .....	38
3.3. <i>JUB1-OXs</i> accumulate a high level of proline under drought conditions .....	39
3.4. Expression of proline metabolism genes is altered in <i>JUB1-OXs</i> .....	40
3.5. Identification of the putative downstream targets of <i>JUB1</i> related to proline metabolism.....	42
3.6. <i>bZIP63</i> is a downstream target of <i>JUB1</i> .....	43
3.7. <i>JUB1</i> regulates accumulation of proline, possibly <i>via bZIP63</i> .....	44
3.8. <i>JUB1-OXs</i> exhibit a lower stomatal conductance .....	45
3.9. Expression of <i>JUB1</i> under guard-cell specific promoter <i>KST1</i> does not alter drought tolerance .....	46
3.10. Abiotic stress tolerance phenotype of <i>JUB1</i> overexpressors might depend on the direct induction of <i>DREB2A</i> .....	48
3.11. Characterization of <i>jub1</i> <i>crispr</i> line .....	50
3.12. Identification of proteins interacting with <i>JUB1</i> .....	51
3.13. Localization analysis of <i>CaM1</i> and <i>CaM4</i> proteins.....	51
3.14. Expression analysis of <i>CaM1</i> and <i>CaM4</i> genes.....	52
3.15. <i>JUB1</i> interacts with <i>CaM1</i> and <i>CaM4</i> proteins.....	54
3.16. Identification of <i>CaM</i> -binding sites in the <i>JUB1</i> protein .....	56
3.17. The role of Ca <sup>2+</sup> for <i>JUB1</i> - <i>CaM4</i> protein interaction .....	61



3.18. Characterization of <i>JUB1-OX/CaM4-OX</i> and <i>CaM4-OX</i> lines .....	65
3.19. CaM4 overcomes the JUB1 function upon senescence .....	67
3.20. Characterization of <i>CaM1</i> and <i>CaM4</i> knockout mutants .....	70
4. DISCUSSION .....	72
4.1. Role of the <i>JUB1-OXs</i> in drought stress tolerance.....	72
4.1.1. Regulation of proline accumulation by JUB1 .....	73
4.1.2. Regulation of stomatal conductance in <i>JUB1-OXs</i> .....	74
4.2. The effect of cell-specific overexpression of JUB1 on drought tolerance .....	74
4.3. The effect of transcriptional control of <i>DREB2A</i> gene on drought tolerance of <i>JUB1-OXs</i> .....	75
4.4. JUB1 confers tolerance to drought stress through the regulation of multiple components .....	76
4.5. Interaction between JUB1 and CaM4.....	78
4.6. Localization of active CaM4 binding sites in JUB1 protein.....	80
4.7. Involvement of Ca <sup>2+</sup> in the regulation of the interaction between JUB1 and CaM4 .....	82
4.8. The biological relevance of the JUB1 CaM4 interaction in connection to plant senescence .....	83
5. REFERENCES.....	86
6. SUPPLEMENTAL DATA .....	105
Publication and conference attendance .....	113
Eidesstattliche Erklärung.....	114
Acknowledgments .....	115

## LIST OF FIGURES

Figure 1.1. Molecular basis of leaf growth and senescence..	3
Figure 1.2. The scheme of proline metabolism.....	8
Figure 3.1. <i>JUB1-OXs</i> plants are resistant to severe drought stress. ....	37
Figure 3.2. Accumulation of proline under control conditions.....	39
Figure 3.3. Accumulation of proline under drought conditions.....	40
Figure 3.4. Transcript levels of proline metabolism genes assessed using qRT-PCR.....	41
Figure 3.5. JUB1 activates the promoters of <i>MYB2</i> and <i>bZIP63</i> in yeast..	42
Figure 3.6. <i>bZIP63</i> is a downstream target of JUB1.....	43
Figure 3.7. Characterization of <i>bZIP63-OX</i> lines. ....	44
Figure 3.8. Stomatal conductance in <i>JUB1-OX</i> , <i>jub1-kd</i> , and WT plants..	45
Figure 3.9. Expression of <i>JUB1</i> under a guard-cell specific promoter.....	47
Figure 3.10. Characterization of <i>JUB1-OX/dreb2a-2</i> line.....	48
Figure 3.11. Drought tolerance phenotype of <i>JUB1-OX/dreb2a-2</i> plants. ....	49
Figure 3.12. Characterization of <i>jub1 crispr</i> line.....	50
Figure 3.13. Localization analysis of CaM1 and CaM4 proteins. ....	52
Figure 3.14. Expression analysis of <i>CaM1</i> and <i>CaM4</i> genes. ....	53
Figure 3.15. CaM1 and CaM4 interact with JUB1. ....	54
Figure 3.16. Several CaM-binding sites present in the JUB1 protein. ....	57
Figure 3.17. JUB1 has calmodulin-binding sites in both the N- and C-terminal parts of the protein. ....	58
Figure 3.18. Calmodulin-binding site in the JUB1 DNA-binding domain.....	60
Figure 3.19. Role of Ca <sup>2+</sup> in JUB1-CaM4 protein interaction. ....	62
Figure 3.20. JUB1-CaM4 protein interaction occurs in the senescent leaves..	63
Figure 3.21. Ca <sup>2+</sup> level in young and senescent leaves.....	64
Figure 3.22. Characterization of <i>JUB1-OX/CaM4-OX</i> and <i>CaM4-OX</i> lines.....	66
Figure 3.23. CaM4 overcomes the JUB1 function. ....	68
Figure 3.24. CaM4 reduces JUB1 protein activity towards <i>DREB2A</i> . ....	70
Figure 3.25. Characterization of <i>CaM1</i> and <i>CaM4</i> knockout mutants.....	71
Figure 4.1. Model of JUB1 action leading to drought stress tolerance.....	78
Figure 4.2. Model of JUB1 CaM4 interaction.....	85
Supplemental Figure S1. The sequences of the promoter regions are used in Y1H for the generation of bait constructs. ....	110
Supplemental Figure S2. Expression pattern of <i>CaM1</i> gene. ....	111
Supplemental Figure S3. Expression pattern of <i>CaM4</i> gene..	112

## LIST OF TABLES

Table 3.1. CaM-binding motifs present in the JUB1 protein.....	61
Supplemental Table S1. Primers used for cloning and genotyping. ....	105
Supplemental Table S2. Primers used for the generation of knockout mutants. sgRNAs are underlined. ....	107
Supplemental Table S3. Primers used for qRT-PCR and end-point PCR. ....	108
Supplemental Table S4. Oligonucleotides used for EMSA. Mutated nucleotides within the JUB1 binding site are shown in red. JUB1 binding site is underlined. ....	109
Supplemental Table S5. Primers used for ChIP-qPCR.....	109

## ABBREVIATIONS

$\mu\text{mol m}^{-2}\text{s}^{-1}$	Micromole per square meter per second
3AT	3-amino-1,2,4-triazole
4-MU	4-methyl umbelliferone
ABA	Abscisic acid
ACA	AUTOINHIBITED $\text{CA}^{2+}$ -ATPASE
ADE2	Phosphoribosylaminoimidazole carboxylase
AHL1	AT-HOOK MOTIF NUCLEAR-LOCALIZED PROTEIN 1
ANR	Anthocyanidin reductase
AP2/EREBP	APETALA2/ethylene-responsive element binding proteins
ATAF1	Arabidopsis thaliana ACTIVATING FACTOR1
BAK	BRASSINOSTEROID INSENSITIVE 1-ASSOCIATED RECEPTOR KINASE
bHLH	Basic helix–loop–helix
BiFC	Bimolecular fluorescence complementation
BR	Brassinosteroids
bZIP	Basic Leucine Zipper Domain
BZR1	BRASSINAZOLE-RESISTANT 1
CaM	Calmodulin
CaMB	CaM-binding domain
CAMTA	calmodulin-binding transcription activators families
CBL	Calcineurin-B-like proteins
CCaMK	Calcium and calmodulin-dependent protein kinase
CDPK	Calcium-dependent protein kinases
CDS	Coding sequence
CDTA	Cyclohexane Diamine Tetraacetic Acid
ChIP	Chromatin immunoprecipitation
CIPK	CBL-interacting protein kinases
CML	Calmodulin-like proteins
CNGC	Cyclic nucleotide-gated non-selective cation channel
CO	CONSTANS
Col-0	Columbia-0
CRISPR	Clustered Regularly Interspaced Short Palindromic Repeats
CRKs	CDPK-related kinases
CTDB	Calmodulin Target Database Binding Sites Search and Analysis
DAB	3, 3'-diaminobenzidine, tetrahydrochloride
DAPI	4',6-diamidino-2-phenylindole
DAS	Days after sowing
DELLA	Proteins named after a highly conserved DELLA amino acid motif
DFR1	DROUGHT AND FREEZING RESPONSIVE GENE 1
DHN	DEHYDRIN

DIV	DIVARICATA
DREB2A	DEHYDRATION-RESPONSIVE ELEMENT BINDING PROTEIN 2
DTT	Dithiothreitol
DW	Dry weight
DWF4	DWARF 4
EDTA	Ethylenediaminetetraacetic acid
EF-hand	Helix–loop–helix structural domain
EGTA	Ethylene glycol-bis( $\beta$ -aminoethyl ether)-N,N,N',N'-tetraacetic acid, egtazic acid
EMSA	Electrophoretic mobility shift assay
EPF	EPIDERMAL PATTERNING FACTOR
ERF	ETHYLENE RESPONSIVE FACTOR
FAD	Omega-3 fatty acid desaturase
FT	FLOWERING LOCUS T
FW	Fresh weight
GA	Gibberellin
GA3ox1	GIBBERELLIN 3-OXIDASE 1
GABA	Gamma-aminobutyric acid
GAD	Glutamate decarboxylase
GAI	GIBBERELIC ACID INSENSITIVE
GAPDH	Glyceraldehyde 3-phosphate dehydrogenase
GCH	Glutathione
GI	GIGANTEA
GOLS	GALACTINOL SYNTHASE
GORK	Guard cell outwardly rectifying K <sup>+</sup> channel
GSA	Glutamate-semialdehyde
GSNOR	S-Nitrosoglutathione reductase
GST	Glutathione S-transferase
GUS	$\beta$ -glucuronidase
H2O2	Hydrogen peroxide
HD-HOX	HOX homeodomain
HIS3	Imidazoleglycerol-phosphate dehydratase
HSP	Heat shock protein
HY5	HYPOCOTYL5
IPT	Isopentenyl transferase
IPTG)	Isopropyl- $\beta$ -D-thiogalactoside
IQ	IQ motif (“IQ” refers to the first two amino acids of the motif)
JA	Jasmonic acid
JUB1	JUNGBRUNNEN1
LD	Long-day
LEA	Late embryogenesis abundant
Ler	Landsberg <i>erecta</i>

LEW	Lysis-Equilibration-Wash buffer
LUC	Luciferase
MES	2-(N-morpholino) ethanesulfonic acid
MPK	MITOGEN-ACTIVATED PROTEIN KINASE
MUG	4-Methylumbelliferyl- $\beta$ -D-glucuronide hydrate
MYB	MYB DOMAIN PROTEIN
MYB15	MYB DOMAIN PROTEIN 15
NAC	NAC DOMAIN CONTAINING PROTEIN
NADH	Nicotinamide adenine dinucleotide
NADPH	Nicotinamide adenine dinucleotide phosphate
NCED3	NINE-CIS-EPOXYCAROTENOID DIOXYGENASE 3
ND	Neutral day
NFYA5	UCLEAR FACTOR Y, SUBUNIT A5
NO	Nitric oxide
NSRP	Naturally stress-resistant plants
NTL4	NAC WITH TRANSMEMBRANE MOTIF 1-LIKE 4
OAT	Ornithine-delta-aminotransferase
ORE1	ORESARA1, also called ARABIDOPSIS NAC092 (ANAC092) or AtNAC2
OST1	OPEN STOMATA 1
P5C	Pyrroline-5-carboxylate
P5CDH	Pyrroline-5-carboxylate dehydrogenase
P5CR	Pyrroline-5-carboxylate reductase
P5CS	Pyrroline-5-carboxylate synthetase
PBS	Phosphate-buffered saline
PDH	Proline dehydrogenase
PHL1	PHR1-LIKE 1
PHR1	PHOSPHATE STARVATION RESPONSE 1
PIF4	PHYTOCHROME INTERACTING FACTOR 4
PMB	Plant measuring buffer
PMSF	Phenylmethylsulfonyl fluoride
QTL	Quantitative trait locus
R-GECO	Red fluorescent, genetically-encoded Ca <sup>2+</sup> indicator for optical imaging
RGL1	RGA-LIKE 1
ROS	Reactive oxygen species
RWC	Relative water content
RWC3	RICE WATER CHANNEL 3
SA	Salicylic acid
SAG12	SENESCENCE-ASSOCIATED GENE 12
SD	Minimal synthetic defined base
SDS	Sodium dodecyl sulfate
SDS-PAGE	Sodium dodecyl sulfate-polyacrylamide gel electrophoresis

SNF1	SUCROSE NON-FERMENTING 1
SOC1	SUPPRESSOR OF OVEREXPRESSION OF CO 1
SRO5	SIMILAR TO RCD ONE 5
TA	Transactivation assay
TA3	Transposable element gene
TSF	TWIN SISTER OF FT
TW	Turgid weight
UTR	Untranslated region
WR2	WAX SYNTHESIS REGULATORY 2
WRKY	WRKY DNA-BINDING PROTEIN
WT	Wild type
WUE	Water use efficiency
WW	Water withhold
Y1H	Yeast One-Hybrid-System
Y2H	Yeast Two-Hybrid-System





# 1. INTRODUCTION

## 1.1. Abiotic stress tolerance and senescence in plants

For the last 30 years, climate change has introduced a shift in the distribution and abundance of different species. In the nearest future, the extinction probabilities associated with climate change scenarios indicate that 15–37% of animal and plant species will be committed to extinction (Thomas et al., 2004). Abiotic stress is often associated with a number of different environmental stimuli such as heat stress or cold stress, low or high light, water deficit or flooding, submergence, chemical factors, salinity, mechanical factors, radiation. Climate change will intensify the damage caused by different stresses and cause a situation where several abiotic stresses have a combined effect on plant species (Ferguson, 2019).

Abiotic stress responses in plants involve (Onaga and Wydra, 2016):

- a change in primary metabolism through increased levels of glycolytic and OPPP-derived metabolites due to high energy demand (Sipari et al., 2020);
- an increase in reactive oxygen species (ROS) scavenging to prevent oxidative damage;
- an increased activity of chaperon proteins, e.g., heat shock proteins (HSP) or late embryogenesis abundant proteins (LEA);
- an increased cell cycle activity for cell size maintenance by cytoskeletal proteins;
- an increase in mechanical strength by hardening the cell wall;
- a decrease of specific secondary metabolites for energy conservation (depending on the plant species) (Daneshmand et al., 2009);
- changes in growth-related signaling proteins;
- an increase in transmembrane activity to maintain osmotic and ion balance.

Some of the responses to abiotic stresses are also regarded as defense mechanisms. They are present to some extent in most plant species and connected to stress escape, stress avoidance or intercellular reduction of ROS, and many others. For example, plant responses to drought can be described by complex mechanisms, which mainly include several aspects:

- drought escape *via* shortening the plant life cycle before severe water deficit;
- drought avoidance *via* preservation of a high water potential (e.g., by developing longer root systems, or conserving water potential by e.g. a reduction of stomatal aperture and/or a reduction of leaf area/canopy);
- drought tolerance mainly *via* improving osmotic adjustment ability and increasing cell wall elasticity to maintain tissue turgidity;

- drought resistance *via* altering metabolic paths for survival under severe stress (e.g., increased antioxidant metabolism) (Xu et al., 2010).

Naturally stress-resistant plants (NSRPs) exhibit specific stress defense mechanisms. After identification of promising domestication genes in NSRPs, based on their orthologs in crops, multi-stress-tolerant transgenic plants can be generated using precise gene editing (Zhang et al., 2018). In general, defense against abiotic stresses includes manipulation of the cuticle, unsaturated fatty acids, ROS scavengers, molecular chaperones, and compatible solutes (He et al., 2018). For example, overexpression of the *SHINE* (*SHN*) gene in *Arabidopsis thaliana* activates wax biosynthesis, alters cuticle properties, and confers drought tolerance (Aharoni et al., 2004). Overexpression of the *WAX SYNTHESIS REGULATORY 2* gene (*OsWR2*) in rice enhances tolerance to water deficit by regulating wax and cutin biosynthesis (Zhou et al., 2014). In *Arabidopsis*, the MYB DOMAIN PROTEIN 96 (MYB96) transcription factor was identified as a regulator of cuticular wax biosynthesis under drought conditions (Seo et al., 2011). Increased contents of unsaturated fatty acids were achieved by overexpression of *Lycopersicon esculentum* omega-3 fatty acid desaturase gene (*LeFAD7*) in the thylakoid membrane, which reduced the photoinhibition of photosystem PSI and PSII under chilling at low irradiance in tomato (*Solanum lycopersicum*) (Liu et al., 2008). Overexpression of anthocyanidin reductase (ANR) in tobacco results in increased plant tolerance to oxidative stress *via* induced scavenging of ROS (Luo et al., 2016). Manipulation of molecular chaperone heat shock protein 17.2 (CsHSP17.2) is essential for thermotolerance in *Camellia sinensis* (Wang et al., 2017).

Chaperones play a role not only in the tolerance to heat stress. For example, a report in *Manihot esculenta* indicated that chaperone heat shock protein 90 (MeHSP90) is essential for drought stress resistance. HSP90 regulates abscisic acid (ABA) accumulation and H<sub>2</sub>O<sub>2</sub> concentration through two specific protein inhibitors of HSP90. MeHSP90 recruits WRKY DNA-BINDING PROTEIN 20 (MeWRKY20) and MeCatalase1 to regulate drought stress resistance (Wei et al., 2020). Compatible solutes or osmoprotectants also play an important role in the general defense against abiotic stresses. Overexpression of *GALACTINOL SYNTHASE 2* from *Thellungiella salsuginea* (*TsGOLS2*), which encodes a galactinol synthase, in *Arabidopsis* enhances tolerance to high salinity and osmotic stresses (Sun et al., 2013). Suppression of proline degradation *via* generation of antisense transgenic plants in *Arabidopsis* also resulted in improved tolerance to freezing and salinity (Nanjo et al., 1999). Improved tolerance can also be achieved by activation or suppression of some gene regulatory factors. For example, in transgenic soybean (*Glycine max*), an increase of drought and salt stress tolerance was achieved

*via* overexpression of the Arabidopsis *AtMYB44* gene (Seo et al., 2012). In some cases, increased tolerance may be attained alongside some undesirable traits. Thus, in Arabidopsis, *MYB96* overexpressors exhibit drought and freezing tolerance together with significant dwarfism (Guo et al., 2013). Another powerful approach for generating plants tolerant to stress is the manipulation of  $\text{Ca}^{2+}$  channels or  $\text{Ca}^{2+}$  sensors. It is known that  $\text{Ca}^{2+}$  is involved in plant responses to all abiotic stresses directly or *via* activation of other signaling molecules. A well-known example is a conversion of L-glutamate to gamma-aminobutyrate (GABA), which is catalyzed by glutamate decarboxylase (GAD). GAD activity is regulated by CaM binding, this in turn is essential for the further regulation of GABA metabolism, a known multifunctional anti-stress molecule (Baum et al., 1996). Calmodulins (calcium binding proteins, CaMs) can also inhibit the degradation of the enzymes *S*-nitrosoglutathione reductase (GSNOR), leading to increased nitric oxide (NO) production and salt resistance (Zhou et al., 2016).

Abiotic stresses such as drought, high temperature, salinity, and nutrient deficiencies accelerate plant senescence and affect plant productivity. In plants, senescence is defined as a programmed process of degradation and degeneration of cells, organs, and in some cases, the entire organism which leads to plant death. Senescence can be promoted by different factors, either internal or external. The developmental age of plants also influences the process of senescence, as, during senescence, plants recycle nutrients from their source tissues to their reproductive organs. This is followed by photosynthesis cessation and chlorophyll breakdown that later leads to the degradation of proteins and nucleic acids (**Figure 1.1.**) This process is controlled by complex networks regulating physiological, biochemical, and molecular mechanisms (Munné-Bosch and Alegre, 2004; Woo et al., 2013).

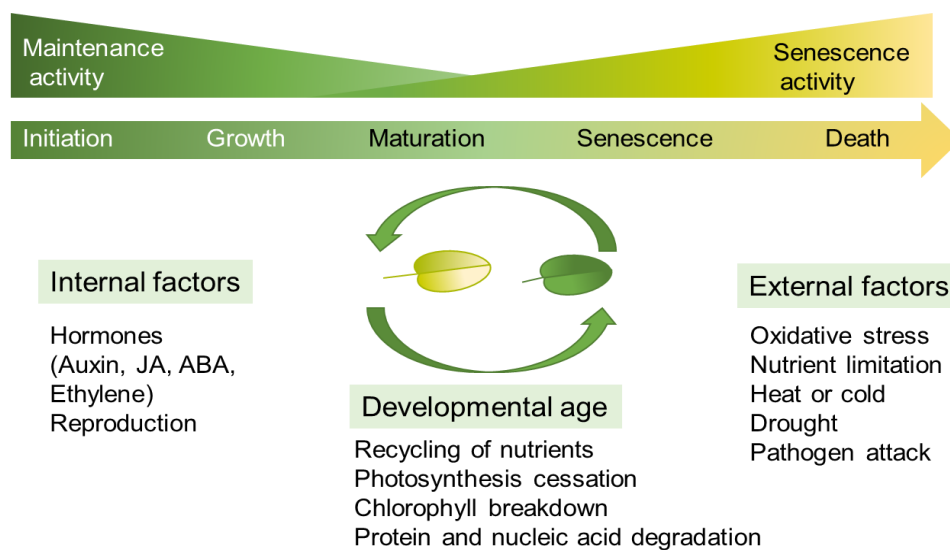


**Figure 1.1. Molecular basis of leaf growth and senescence.** The illustration shows the changes occurring in the plant during plant aging and the processes that involve primarily

maintenance activity at the initiation and growth stages, followed by an increase in the senescence activity at the later stages of development. Leaf senescence is regulated and promoted by developmental age, internal and external factors. JA, jasmonic acid; ABA, abscisic acid. The illustration is modified from Woo et al. (2013).

Several approaches are used to delay senescence in crop plants using gene editing and transgenic plant breeding. For example, protection and maintenance of the chloroplast function or hormone homeostasis modification are often used for this purpose. Suppression of the *Arabidopsis thaliana* *ACTIVATING FACTOR1* (*ATAF1*) and *ORESARA1* (*ORE1*) genes in *Arabidopsis* results in positive regulation of key chloroplast maintenance genes and repression of senescence-promoting transcriptional cascades (Rauf et al., 2013; Garapati et al., 2015). In rice, stress-induced cytokinin synthesis increases drought tolerance and improves grain yield by delaying stress-induced senescence (Reguera et al., 2013).

Stress-induced senescence is often associated in plants with a "stress escape" strategy. By escaping stress, plants facilitate the survival of the next generation. However, agricultural yield or plant productivity undergoes significant losses due to leaf abscission or decreased canopy size (Kooyers, 2015). Often, transcription factors involved in the response to abiotic stresses also play a role in the regulation of senescence. Global transcriptional analysis also indicates a remarkable overlap between stress- and senescence-responsive responses (Wehner et al., 2016; Zheng et al., 2016). A recent example is transcription factor HbWRKY82 from *Hevea brasiliensis* that promotes tolerance to dehydration and salinity stress and regulates the transcriptional expression of several leaf senescence marker genes (Kang et al., 2020). An increase of tolerance to drought and cold stress in eggplant (*Solanum melongena* L.), and a significantly delay in leaf senescence, were achieved by expressing isopentenyl transferase (*IPT*) under the control of the senescence-activated *SENESCENCE-ASSOCIATED GENE 12* (*SAG12*) promoter from *Arabidopsis* (Xiao et al., 2017). Overexpression of *ETHYLENE RESPONSIVE FACTOR 19* (*ERF019*) also delayed plant senescence and improved drought tolerance in *Arabidopsis* (Scarpeci et al., 2017). For *ORE1*, salt-triggered senescence occurs alongside age-dependent leaf senescence. The *ore-1* mutant exhibits delayed-senescence and increased tolerance to various types of oxidative stress and salt stress (Woo et al., 2004; Balazadeh et al., 2010). Rice transcription factor WRKY DNA-BINDING PROTEIN 47 (*OsWRKY47*) was also identified as a positive regulator of the response to water deficit stress; the *oswrky47* mutant exhibits early senescence (Raineri et al., 2015). Another NAC transcription factor, NAC WITH TRANSMEMBRANE MOTIF 1-LIKE 4 (*NTL4*), is associated with senescence regulation and tolerance to drought stress; *ntl4* mutant plants

display reduced leaf senescence and increased drought tolerance (Lee et al., 2012). The genetic engineering of crop plants aims to achieve abiotic stress tolerance without sacrificing plant productivity. Thus, finding a balance between plant growth and stress responses is the main focus in plant breeding nowadays.

## **1.2. Drought stress and resistance mechanisms**

Drought is a predominant abiotic stress affecting many of the crops and causing significant yield losses worldwide (Bodner et al., 2015). Extreme weather changes and evident global warming lead to a shortage in water availability for agriculture, creating an urgent need for the potential development of drought-tolerant crops and more water-efficient cropping systems (Baltes et al., 2017).

Depending on drought stress duration, severity, and its re-occurrence, plants may exhibit different drought symptoms. Drought symptoms also vary depending on plant species, plant age/developmental stage, and other environmental conditions. The most common symptoms occurring in leaves include loss of turgor, wilting, yellowing, and leaf abscission (Farooq et al., 2009). In plants, drought stress affects different aspects of growth and development, which includes changes also in morphological and anatomical characteristics, the relative water content in leaves, photosynthesis rate and chlorophyll content, respiration, mineral nutrition, hormonal balance, the content of lipids, proteins, amino acids and minerals, generation of ROS, and changes in gene expression (Basu et al., 2016; Kumar et al., 2018).

Due to the loss of turgor during drought stress, cell division, elongation, and differentiation are drastically affected. This leads to suppressed cell expansion and elongation, which, together with reduced photosynthetic efficiency, causes diminished plant productivity due to decreased biomass production. A drop in relative water content (RWC), one of the earliest physiological effects of drought in plants, precedes the reduction of photosynthesis and leads to stomatal closing, which subsequently causes a further reduction of photosynthesis due to the limitation in CO<sub>2</sub> uptake. The decrease in photosynthetic CO<sub>2</sub> assimilation also affects respiration rate which leads to decreased energy resources, growth rate, and water absorption from the soil. The closure of stomata also increases leaf temperature, which additionally affects different aspects of metabolism, e.g., abscisic acid and jasmonic acid metabolism. Accumulation of reduced photosynthetic electron transport components caused by the drop in CO<sub>2</sub> leads to ROS production which damages the photosynthetic apparatus and leads to the degradation of the photosynthetic pigment chlorophyll. This, in turn, causes a reduction of the photosynthesis rate (Chernyad'ev, 2005). Drought stress induces the synthesis of ABA in the chloroplast. The role

of ABA is also known in the regulation of stomatal closure, caused by translocation of ABA to guard cells (Kuromori et al., 2018). The protein content decreases upon drought stress due to the stop of their synthesis or by protein degradation directed to maintain energy level in the plants. However, the synthesis of molecular chaperones as well as of enzymes that synthesize osmoprotectants, antioxidants, and other compatible solutes, e.g., proline, increases under drought stress. The nutrient uptake by roots is also decreased and affected by the energy status of the plant during drought stress (Kumar et al., 2018).

Plant responses to drought can be described by complex mechanisms, which mainly include the following aspects:

- drought escape *via* shortening the plant life cycle before severe water deficit;
- drought avoidance *via* preservation of a high-water potential in plants (e.g., by developing elaborate root systems or conserving water potential by a reduction of stomatal conductance and/or leaf area/canopy);
- increasing drought tolerance mainly *via* increasing cell wall elasticity to maintain tissue turgidity, improving osmotic adjustment ability, and altering metabolic paths for survival under severe stress (Verslues et al., 2006; Xu et al., 2010; Osmolovskaya et al., 2018).

Drought escape mechanisms in plants are mainly associated with early flowering, bolting, and remobilization of nutrients to reproductive organs and are mainly determined by the rapid transition from the vegetative to the reproductive stage before the occurrence of severe drought stress. The mechanism observed in many plant species, including *Arabidopsis* and crops such as wheat and barley, may still be present in only some accessions or cultivars. For example, *Arabidopsis Landsberg erecta (Ler)* and *Columbia-0 (Col-0)* ecotypes display different drought-adaptive strategies. *Ler* exhibits an escape strategy, whereas *Col-0* withstands water stress by drought tolerance. The *Ler* ecotype exhibits early flowering and bolting, high sensitivity of rosette leaves to water deficit leading to early leaf senescence. *Col-0* plants demonstrate higher biomass allocation to vegetative organs, root-to-shoot ratio, drought rhizogenesis intensity, RWC, and water use efficiency (WUE) compared with the *Ler* ecotype (Meyre et al., 2001). Some of the genes involved in the regulation of the drought escape mechanism were identified in *Arabidopsis* and other species. The *GIGANTEA (GI)* gene was identified as a key element in drought escape response under long-day conditions. *GI* enables the abscisic acid- and drought-mediated activation of *FLOWERING LOCUS T (FT)/TWIN SISTER OF FT (TSF)* and *SUPPRESSOR OF OVEREXPRESSION OF CO 1 (SOC1)*, and all three genes are required for the drought escape response (Riboni et al., 2013). Quantitative trait

locus (QTL) mapping between *Mimulus guttatus* ecotypes revealed a candidate gene, *DIVARICATA2* (*DIV2*), that might be involved in the flowering regulatory network that contributes to the drought escape mechanism (Hall et al., 2010; Lowry and Willis, 2010).

The preservation of a high-water potential in plants is the main aim of a drought avoidance mechanism. Such an effect can be achieved *via* altering stomatal density or size, transpiration efficiency, and WUE due to e.g. a higher ratio of root to shoot growth. Overexpression of the cotton *MYB DOMAIN PROTEIN 62* (*GaMYB62*) gene in Arabidopsis leads to less water loss, reduced stomatal apertures, and high drought avoidance compared to WT plants (Butt et al., 2017). In rice, *RICE WATER CHANNEL 3* (*RWC3*) aquaporin genes have been associated with an increase in water uptake through changes in the root architecture and root system size to acquire water under drought conditions (Lian et al., 2004). The maintenance of the high-water potential needs a lot of energy. Plants that use this mechanism of drought tolerance generally are small in size. Overexpression of soybean *UCLEAR FACTOR Y, SUBUNIT A5* (*GmNFYA5*) in transgenic Arabidopsis plants causes enhanced drought resistance in seedlings by decreasing stomatal aperture and water loss from leaves (Ma et al., 2020). However, some of the reports indicate that improvement of traits associated with drought avoidance may have no impact on plant productivity. In barley, ectopic overexpression of *EPIDERMAL PATTERNING FACTOR 1* (*HvEPF1*) reduced stomatal density and improved drought tolerance without impacting yield (Hughes et al., 2017).

Improved accumulation of compatible solutes, protective proteins, detoxification of ROS, and metabolic changes also contribute to drought tolerance mechanisms. In rice, *NAC DOMAIN CONTAINING PROTEIN 14* (*OsNAC14*) mediates drought tolerance by recruiting factors involved in DNA damage repair and defense response (Shim et al., 2018). Overexpression of *Saussurea involucreata* *DEHYDRIN* (*SiDHN*) gene in tomato promotes drought tolerance by inhibiting cell membrane damage, protecting chloroplasts, and enhancing ROS scavenging capacity (Guo et al., 2019).

Plant drought resistance is a complex process that can sometimes combine different mechanisms. For example, the direct regulation of the expression of many stress-related genes by overexpression of *AT-HOOK MOTIF NUCLEAR-LOCALIZED PROTEIN 1* (*AHL1*) in rice improves both drought avoidance and drought tolerance (Zhou et al., 2016).

The introduction of drought tolerance to crops requires identifying the regulatory components and the mechanisms controlling the response and tolerance to drought stress.

### 1.2.1. Accumulation of proline as a mechanism of stress survival

One of the other common physiological responses in plants to water deficit is an accumulation of the amino acid proline (Pro) (Patel and Vora, 1985; Verslues and Sharp, 1999; Parida et al., 2008; Verbruggen and Hermans, 2008). The molecular mechanism of proline-mediated stress protection has been proposed to be due to the chemical properties of proline which may act as an osmoprotectant and the ability to balance water stress, stabilize proteins and antioxidants, and to regulate intracellular redox homeostasis, e.g. by directly scavenging ROS, etc. (Liang et al., 2013). Moreover, proline is a precursor for other antioxidant molecules, a potential signaling molecule, and a metal chelator (Sharma et al., 1998; Groppa and Benavides, 2008). The scheme of proline metabolism is shown in **Figure 1.2**. The biosynthesis of proline occurs in the cytosol and chloroplast. The most common pathway for proline biosynthesis is derived from glutamate, in which biosynthesis occurs in two steps. The first step is a conversion of glutamate to glutamate-semialdehyde (GSA), which spontaneously converts to pyrroline-5-carboxylate (P5C) by pyrroline-5-carboxylate synthetase (P5CS), followed by reduction to proline by pyrroline-5-carboxylate reductase (P5CR) (Szabados and Saviouré, 2010; Fichman et al., 2015).

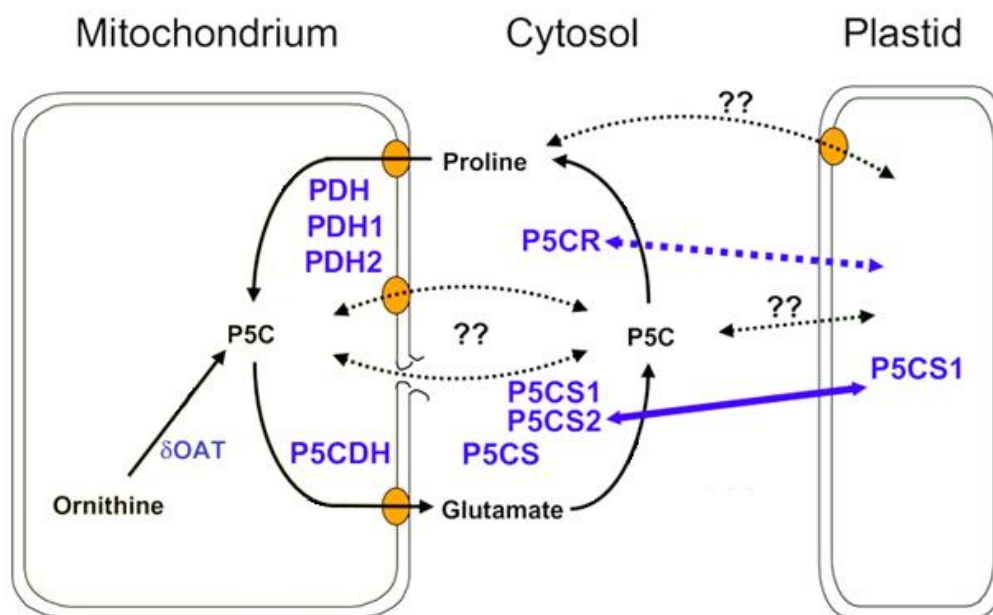


**Figure 1.2. The scheme of proline metabolism.** Illustration of proline metabolism in the cell and its compartments (mitochondrion, cytosol, and plastid). Enzymes and the isoforms are shown in blue. Black arrows indicate metabolic fluxes; blue arrows show the movement of the isoforms or enzymes between compartments. Solid lines indicate previously reported metabolic fluxes; dotted lines indicate presumed metabolic fluxes, movement of the isoforms, or enzymes. Abbreviations: P5C, pyrroline-5-carboxylate; P5SC, pyrroline-5-carboxylate synthetase; PDH, proline dehydrogenase; P5CDH, pyrroline-5-carboxylate dehydrogenase. ??, unknown predicted transporters. The scheme was modified from Funck et al. (2010).



In *Arabidopsis*, P5SC is encoded by two genes, whereas P5CR is encoded by one. P5CS1 is a stress-induced isoform localized in the chloroplasts, is regulated by ABA-dependent and independent signals, and controls the synthesis of proline in the chloroplast. *P5SC2* is a housekeeping gene; the protein it encodes is mainly localized in the cytosol and is essential for seedling growth and embryo maturation. *P5SC* genes have nonredundant functions (Székely et al., 2008; Amini et al., 2015). *P5CR* expression seems to be less associated with proline accumulation; moreover, protein level and proline concentration in stressed plants were not correlated to mRNA levels of *P5CR*. P5CR plays a critical role in cycling proline between chloroplast and cytosol and maintaining proper NADP<sup>+</sup>/NADPH levels. The kinetic properties of P5CR are dependent on the use of either NADH or NADPH as the electron donor (Hua et al., 1997; Miller et al., 2009; Giberti et al., 2014).

Proline degradation occurs in the mitochondria that include proline oxidation to P5C by proline dehydrogenase (PDH) and conversion of P5C into glutamate by pyrroline-5-carboxylate dehydrogenase (P5CDH) (Szabados and Saviouré, 2010; Fichman et al., 2015). While *P5CDH* is a single gene copy, PDH is encoded by two genes in *Arabidopsis*. PDH1 a dominant isoform during most of stresses and is repressed by cold drought and salt stress but induced during the recovery from the stress (Kiyosue et al., 1996; Verbruggen et al., 1996; Kaplan et al., 2007). *PDH2* is specifically upregulated during salt stress, in senescent leaves, and the abscission zone of floral organs (Nakashima et al., 1998). *PDH1* is upregulated by hypoosmolarity and proline treatment. *PDH* genes also have non-redundant functions (Funck et al., 2010; Schertl et al., 2014). *P5CDH* is necessary for proline degradation but not essential for stress tolerance or vegetative plant growth, and for the most part, expression of *P5CDH* remains constant during stress (Deuschle et al., 2004).

The alternative pathway of proline biosynthesis derives from ornithine. The reaction of ornithine transamination to GSA and P5C is catalyzed by ornithine-delta-aminotransferase (OAT) and followed by reduction to proline by P5CR like in the glutamate pathway. The ornithine pathway was suggested to be involved in stress-induced proline accumulation only in some plants and is essential for arginine catabolism but not for proline biosynthesis (Funck et al., 2008; Xue et al., 2009).

Regulation of proline metabolism involves environmental effects, hormones, metabolites, pathogens, and other factors. Proline biosynthesis is upregulated by light and osmotic stress and activated by ABA-dependent and ABA insensitive1(*ABI1*)-controlled pathway (Strizhov et al., 1997; Sharma and Verslues, 2010). *P5CS1* expression is promoted by light, phospholipase C, calcium signaling, and repressed by brassinosteroids (BRs), phospholipase

D, and proline (Abrahám et al., 2003; Thiery et al., 2004; Yoo et al., 2005; Parre et al., 2007). *P5CS2* is activated by avirulent bacteria, salicylic acid, and ROS (Fabro et al., 2004). Exogenous H<sub>2</sub>O<sub>2</sub> treatment also leads to increased proline accumulation and upregulation of the *P5CS1* gene, increased P5CS, and decreased PDH activity (Yang et al., 2009). Proline catabolism is activated in the dark, during stress relief, and by high proline accumulation (Kiyosue et al., 1996).

Transcriptional regulation of proline biosynthesis genes in plants is predicted to be regulated by bZIP, MYB, bHLH, WRKY, HD-HOX, C2C2(Zn)DOF, and AP2/EREBP TFs or at least includes putative binding sites for these TFs (Kiran and Abdin, 2012; Fichman et al., 2015; Zarattini and Forlani, 2017). Some of the predicted regulators have been confirmed *via* physical binding to the promoter regions or regulation of proline biosynthesis genes' transcription level. For example, positive regulation of *P5CS1* during phosphate starvation involves the MYB-type transcription factors PHOSPHATE STARVATION RESPONSE 1 (PHR1) and PHR1-LIKE 1 (PHL1); moreover, proline accumulation due to phosphate starvation is controlled by PHR1 and PHL1 (Aleksza et al., 2017). *P5CS2* has been identified as a target of CONSTANS (CO) (Samach et al., 2000) and AtbHLH112, which was also reported to increase expression of *P5CS1* and decrease the expression of *P5CDH* and *PDH* genes (Liu et al., 2015). Reduction of *P5CDH* level upon stress is caused by the generation of an endogenous small interfering RNA *via* antisense overlapping of the 3' UTR region of *P5CDH* and *SIMILAR TO RCD ONE 5 (SRO5)* (Borsani et al., 2005). Group S1 and C bZIP TF family members were reported to regulate expression of *PDH1* by specific heterodimerization (Satoh et al., 2004; Weltmeier et al., 2006). Additionally, bZIP11 activates the expression of *PDH2* (Hanson et al., 2008), and bZIP63 acts as a transcriptional activator of *PDH1* expression (Veerabagu et al., 2014; Mair et al., 2015). The S1-group bZIP1 proteins bZIP11 and bZIP53, known as dimerization partners of bZIP63, were also reported to regulate *PDH* gene expression (Dietrich et al., 2011; Ma et al., 2011). Another TF that controls proline degradation is DROUGHT AND FREEZING RESPONSIVE GENE 1 (DFR1) which was demonstrated to interact with PDH1/2 and P5CDH and inhibit their activities (Ren et al., 2018).

The engineering of plants with a higher or more rapid proline accumulation enhances drought tolerance in several species (de Ronde et al., 2004; Yamada et al., 2005; Simon-Sarkadi et al., 2006). Genetic manipulation in proline metabolism is directed either towards promoting proline biosynthesis or the suppression of proline degradation. Also, removing a feedback inhibition of *P5CS1* by proline resulted in better plant tolerance to osmotic stress (Hong et al., 2000). The genetic manipulation of proline levels in soybean subjected to simultaneous drought

and heat stresses affects the levels of antioxidants (Kocsy et al., 2005). In tomato, the WRKY DNA-BINDING PROTEIN 81 (*SIWRKY81*) was identified as a repressor of proline biosynthesis. Under drought stress, proline biosynthesis was increased in *SIWRKY81*-silenced plants in comparison to non-silenced control (Ahammed et al., 2020). Overproduction of proline *via* the introduction of the *P5CS* gene of *Vigna aconitifolia* in transgenic citrus rootstock Carrizo citrange (*Citrus sinensis* Osb. x *Poncirus trifoliata* L. Raf.) leads to a higher photosynthetic rate and improved drought stress tolerance (Molinari et al., 2004). Evidence from our and other labs indicates a higher accumulation of proline in *JUNGBRUNNEN1* (*JUB1*) overexpressor plants under control and drought conditions in several species together with improvement of abiotic stress tolerance in these plants (Wu et al., 2012; Shahnejat-Bushehri et al., 2017; Tak et al., 2017; Alshareef et al., 2019). In chapter 1.4 I will discuss the function of *JUB1* in more detail. Hence, the identification of *JUB1* targets in proline metabolism could contribute to the elucidation of the mechanism through which *JUB1* overexpressor plants confer enhanced tolerance to drought stress.

### 1.2.2. Stomatal responses upon drought stress

When plants undergo water deficit, the decrease in the internal water potential leads to the closure of the stomata, reducing transpirational water loss. Stomata consist of the two guard cells around a pore, which are responsible for gas exchange. Usually, the stomatal movement is regulated by the light-dark cycle. However, under drought stress, stomatal closure occurs as a plant survival mechanism, sacrificing their productivity caused by a reduction in photosynthesis (Mansfield et al., 1990; Assmann, 1993).

The stomatal closure can occur *via* the hydro passive (or hydraulic) and active stomatal closure (ABA-mediated) pathways. ABA is one of the best-known signals that induce stomatal closure (McAinsh et al., 1990; Davies and Jones, 1991). ABA biosynthesis is promoted during drought stress *via* upregulation of NINE-CIS-EPOXYCAROTENOID DIOXYGENASE 3 (*NCED3*), a key enzyme of ABA biosynthesis (Qin and Zeevaart, 1999).

Several secondary messengers are also involved in stomatal closure mediated and generated by ABA, such as cytoplasmic pH, ROS ( $H_2O_2$ ), and NO.  $H_2O_2$  inhibits  $K^+$  channel activity, induces cytosolic alkalization in the guard cells, promotes NO signaling in response to ABA, and activates permeable  $Ca^{2+}$  channels (Zhang et al., 2001; Neill et al., 2002; Köhler et al., 2003; Song et al., 2014). Calcium, calcium channels, and sensors are known as ABA signaling components in guard cells upon drought. ABA upregulates  $Ca^{2+}$  level as a secondary messenger; in turn, the elevation of  $Ca^{2+}$  in the guard cell can also partially induce the ABA

response (Gilroy et al., 1992; Luan, 2002). Some reports indicate that  $\text{Ca}^{2+}$  is also required for  $\text{H}_2\text{O}_2$  and NO actions (Köhler et al., 2003; Wang and Song, 2008). During stomatal closure, accumulation of  $\text{Ca}^{2+}$  in the guard cell triggers anion efflux of malate<sup>2-</sup>,  $\text{Cl}^-$ , and  $\text{NO}_3^-$  via sustained (S-type) and rapid transient (R-type) channels. Membrane depolarization leads to efflux of  $\text{K}^+$  via  $\text{K}^+$  outwardly rectifying channels such as guard cell outwardly rectifying  $\text{K}^+$  channel (GORK), which causes stomatal closure by dropping guard cell turgor pressure and volume. The gluconeogenic conversion of malate into starch also leads to a decreased level of malate<sup>2-</sup>. Another event that occurs during stomatal closure is a release of  $\text{Ca}^{2+}$  via channels situated in both the plasma membrane and in the tonoplast, also leading to an increase of the  $\text{Ca}^{2+}$  (Kim et al., 2010; Daszkowska-Golec and Szarejko, 2013).

ABA,  $\text{Ca}^{2+}$ , and  $\text{H}_2\text{O}_2$  are the major point of convergence and divergence during signal transduction in the guard cell upon drought stress (Agurla and Raghavendra, 2016). Many reports indicate that enhanced drought tolerance in plants can be achieved by manipulating the points of convergence (ABA,  $\text{Ca}^{2+}$ ,  $\text{H}_2\text{O}_2$ ) or by introducing changes in stomatal development. For example, the LRR-RLK protein HSL3 was identified as a negative regulator of the drought tolerance through the control of  $\text{H}_2\text{O}_2$ -mediated stomatal closure in response to ABA signaling; thus, *hsl3* mutant was more tolerant than the wild type to moisture deficit (Liu et al., 2020). Another study demonstrated that glutathione (GCH) functions as a negative regulator of ABA signaling in the guard cells. GSH-deficient mutant showed enhanced  $\text{H}_2\text{O}_2$ -induced stomatal closure and a significant increase of ROS accumulation in whole leaves in response to ABA (Munemasa et al., 2013). Hormonal signaling also could be used to improve stomatal movement; for example, BR and ABA co-regulate stomatal movement through suppressing the expression of *BRASSINOSTEROID INSENSITIVE 1-ASSOCIATED RECEPTOR KINASE (HvBAK)* to release the interaction target OPEN STOMATA 1 (HvOST1), facilitating the activities of down-stream ion channels in ABA signaling, in drought-tolerant genotype XZ5 in barley (Chen et al., 2019).

Stomatal density and stomatal aperture might be potential tools for enhancing drought tolerance in plants (Elhaddad et al., 2014; Hepworth et al., 2015). Rice that has reduced stomatal density conserves water and has improved drought tolerance (Caine et al., 2019). The improved water-use efficiency was achieved in wheat by decreasing stomatal conductance and transpiration rate to maintain a higher photosynthetic rate (Li et al., 2017). Interestingly, exogenous application of proline could induce partial stomatal closure in *Vicia faba* (Sharma and Rai, 1989). Another example involves the manipulation of regulatory proteins; thus, DELLA proteins (named after a highly conserved DELLA amino acid motif) expression in guard cells

is sufficient to promote stomatal closure (Nir et al., 2017). CALCIUM DEPENDENT PROTEIN KINASE 21 (CPK21), a member of the calcium-dependent protein kinase, regulates stomatal movement under stress and *cpk21* mutant exhibits induced tolerance to osmotic and drought stress (Franz et al., 2011). Overexpression of MYB DOMAIN PROTEIN 15 (MYB15) in *Arabidopsis* also leads to improved drought tolerance. The overexpressor plant phenotype was more sensitive to ABA-induced stomatal closure in comparison to WT control (Ding et al., 2009).

Collectively, ABA, together with H<sub>2</sub>O<sub>2</sub> and Ca<sup>2+</sup> secondary messengers, are important points of convergence and divergence during signal transduction, and genetic manipulation with them plays an essential role in the regulation of stomatal movement upon drought stress leading to desired drought tolerance in plants.

### **1.3. Plant response to environmental stimuli *via* calcium signaling**

The ion Ca<sup>2+</sup> is one of the most versatile signals, involved in many aspects of plant biology, including biotic and abiotic stress responses, regulation of plant growth and development. Ca<sup>2+</sup> is an important divalent cation required for structural roles in the cell wall, membrane stability, and cell integrity. It is also required as a counter-cation for inorganic and organic anions in the vacuole and intracellular messenger in the cytosol response to the environmental stimuli (Tuteja and Mahajan, 2007; Hepler and Winship, 2010). Ca<sup>2+</sup> is important for plant reproduction through mediation and reorientation of pollen tube growth, regulation of directional growth of root hairs, and symbiosis of root hair cells and *Rhizobium* (Rudd and Franklin-Tong, 1999).

The cytosolic free calcium concentration is maintained at 100-200 nM, whereas in the apoplast and the vacuole the Ca<sup>2+</sup> concentration can reach 1-10 mM (Trewavas and Malhó, 1998). Mitochondria, the nucleus, and chloroplasts can generate calcium signals independently (Pauly et al., 2000; Xiong et al., 2006).

In general, during stress conditions, the signal transduction pathway starts with stress perception through membrane receptors followed by the generation of Ca<sup>2+</sup> and, in some cases, other secondary messengers leading to the formation of complexes and cascades that regulate gene expression and stress tolerance (Tuteja and Mahajan, 2007).

As a response to stimuli, cytosolic Ca<sup>2+</sup> concentration in plants rapidly elevates *via* an increased Ca<sup>2+</sup> influx through channels. It then quickly returns to the basal level by Ca<sup>2+</sup> efflux through pumps to extracellular spaces or intracellular compartments. Removing Ca<sup>2+</sup> is necessary to

avoid the toxic effects of high  $\text{Ca}^{2+}$  levels and maintenance of cytoplasmic metabolism (Evans et al., 2001).

$\text{Ca}^{2+}$  level has been found to increase in response to touch, light, gravity hormonal treatment, pathogens, and several abiotic stresses such as drought, cold, salt, and osmotic stress (Raggenbass, 1983; Lynch et al., 1989; Gehring et al., 1990; Knight et al., 1991; Knight et al., 1996, 1997; Yang et al., 1997).

A specific and controlled cell response for a given stimulus occurs through the spatial and temporal difference in  $\text{Ca}^{2+}$  spikes as well as the difference in the amplitude and frequency of  $\text{Ca}^{2+}$  oscillations and/or additional signaling events that occur accompanied by changes in cytosolic  $\text{Ca}^{2+}$  (Allen and Schroeder, 2001; Evans et al., 2001; Moore et al., 2002; Ng and McAinsh, 2003).  $\text{Ca}^{2+}$  influx from the plasma membrane and intracellular  $\text{Ca}^{2+}$  oscillation is a downstream event in ABA-induced stomatal closure (Kim et al., 2010).  $\text{Ca}^{2+}$  signals, in part, are generated, modified, propagated, and perceived through the action of proteins that bind  $\text{Ca}^{2+}$ , and an additional level of regulation in calcium signaling is achieved *via* the functional difference of calcium-binding proteins.

### **1.3.1. $\text{Ca}^{2+}$ signal transduction and decoding through calcium-binding proteins**

The decoding of  $\text{Ca}^{2+}$  signals occurs through  $\text{Ca}^{2+}$ -binding proteins that carry one or more  $\text{Ca}^{2+}$ -binding EF-hand motifs. In Arabidopsis, 250 proteins have a predicted  $\text{Ca}^{2+}$ -binding motif (Ding et al., 2009). There are also several proteins that bind  $\text{Ca}^{2+}$  but do not contain EF-hand motifs. These include phospholipase D, annexins, calreticulin, and Pistil-expressed  $\text{Ca}^{2+}$  binding protein (Tuteja and Mahajan, 2007). In plants,  $\text{Ca}^{2+}$  sensor proteins are calmodulins, calmodulin-like proteins (CMLs), calcineurin-B-like proteins (CBLs), calcium-dependent protein kinases (CDPKs), and calcium and calmodulin-dependent protein kinase (CCamK).

Calmodulin is an important calcium sensor in plants. These proteins are relatively small, around 17 kDa; they contain two globular domains, each harboring a pair of EF-hands, connected by a flexible helical region.  $\text{Ca}^{2+}$  binding to the EF-hands induces the exposure of hydrophobic surfaces that form high-affinity binding sites for downstream effectors (Ishida and Vogel, 2006). Since CaMs do not have any enzymatic activity on their own or no other functional domains,  $\text{Ca}^{2+}$  binding to them causes a conformational change in the protein structure, thereby modifying its interaction with various target proteins, leading to the transduction of  $\text{Ca}^{2+}$  signals (Kim et al., 2009). There are seven *CaM* genes in Arabidopsis (Zielinski, 1998; McCormack et al., 2005). Even though some CaM isoforms exhibit about 90% sequence

similarity, each CaM isoform has its individual function due to each gene's specific temporal and spatial expression patterns (Snedden and Fromm, 2001).

Calmodulin-like proteins similar to CaM possess only EF-hand calcium-binding motifs, but in contrast to them, they have a variable number of functional EF-hands (from 2 to 6). In *Arabidopsis*, 50 calmodulin-like proteins (CMLs) were identified. They share at least 16% overall amino acid identity with CaMs (Sistrunk et al., 1994; McCormack and Braam, 2003; McCormack et al., 2005). Like in CaMs, the binding of  $\text{Ca}^{2+}$  to CMLs induces their conformational change, leading to increased interaction affinity to downstream effectors and tuning their activity. CMLs are involved in various developmental processes and different stress responses (Batistič and Kudla, 2012; Kudla et al., 2018)

Calcineurin B-like proteins (CBLs) also possess four EF-hand domains that can bind at most four  $\text{Ca}^{2+}$  ions. These proteins are most similar to the regulatory B subunit of calcineurin (CNB) and neuronal calcium sensors (NCS) of animals (Kudla et al., 1999). CBLs specifically interact with group 3 SUCROSE NON-FERMENTING 1 (SNF1)-related serine/threonine kinases (SnRK3), also named CBL-interacting protein kinases (CIPKs) (Shi et al., 1999). The *Arabidopsis* genome encodes 10 CBL proteins and 26 CIPK proteins. CIPKs most likely represent targets of calcium signals sensed and transduced by CBL proteins (Kolukisaoglu et al., 2004; Batistič and Kudla, 2012; Zhang et al., 2014).

Calcium-dependent protein kinases also possess four EF-hand motifs for  $\text{Ca}^{2+}$  binding, a CaM-like, and a kinase domain that make them direct effectors upon activation by  $\text{Ca}^{2+}$  binding. In contrast, CDPK-related kinases (CRKs) can possess a degenerated calmodulin domain with non-functional EF-hands. They also can be active in the absence of  $\text{Ca}^{2+}$  but retained the ability and requirement to bind CaM in a  $\text{Ca}^{2+}$ -dependent manner that leads to full activation of the protein kinase. In *Arabidopsis* 34 CDPKs and 8 CRKs are identified (Furumoto et al., 1996; Hrabak et al., 2003). In all CDPKs, the kinase and calmodulin-like domains are separated by a junction domain, which physically interacts with the kinase domain and therefore functions as a pseudo-substrate inhibitor of kinase activity towards target substrates.  $\text{Ca}^{2+}$  binding leads to the conformational change and induces the release of the junction domain from the active site of the kinase domain followed by the intra-molecular autophosphorylation resulting in inactivation of the kinase (Batistič and Kudla, 2012; Liese and Romeis, 2013; Ranty et al., 2016)

Some plant species possess dual-regulated  $\text{Ca}^{2+}$ /CaM-dependent kinases (CCaMKs) that can bind both CaM and free  $\text{Ca}^{2+}$ . CCaMKs possess a serine/threonine kinase domain, an overlapping autoinhibitory/CaM-binding domain, and a  $\text{Ca}^{2+}$ -binding visinin-like EF-hand

domain (Patil et al., 1995). CCaMK activity requires both free  $\text{Ca}^{2+}$  and  $\text{Ca}^{2+}$  bound to CaM ( $\text{Ca}^{2+}/\text{CaM}$ ) with the EF-hand domain and CaM-binding (CaMB) domain acting as  $\text{Ca}^{2+}$ -triggered switch autophosphorylation-triggered molecular switch, respectively (Takezawa et al., 1996; Sathyanarayanan et al., 2000; Wang et al., 2015).

### 1.3.2. Calmodulins and their roles in the plant cell

In Arabidopsis, seven genes encode four calmodulin isoforms CaM1/4, CaM2/3/5, CaM6, CaM7. According to McCormack et al. (2005), the CaMs are expressed at all developmental stages, and the most similar expression patterns and clustering are observed for CaMs encoding the same isoform. Nevertheless, *CaM* genes, including genes of the same isoforms, are differentially expressed in response to numerous external stimuli. Some of the *CaMs* are known to be induced by touch (Braam and Davis, 1990), heat stress (Gong et al., 1997; Liu et al., 2003), cold stress (Chu et al., 2018), salt stress (Zhou et al., 2016), during senescence (Dai et al., 2018), and pathogen attack (Takabatake et al., 2007). *CaM1* and *CaM4* are upregulated in older leaves in comparison to younger leaves. Their expression is also induced during salt stress, while expression of the other CaM genes showed no obvious regular variation (Zhou et al., 2016; Dai et al., 2018). For example, *CaM7* regulates the expression of genes related to light responses. *CaM3* functions in cold-induced stress responses and in the induction of thermotolerance. The *CaM3* transcript is also induced by heat stress (Townley and Knight, 2002; Kushwaha et al., 2008; Zhang et al., 2009). CaMs are also known to be differentially expressed in different developmental stages and different tissues or cell types (Yang et al., 1998; Duval et al., 2002; Bergey et al., 2014).

CaMs regulate cell wall regeneration (Sun et al., 1995), growth of pollen tubes and pollen germination (Shang et al., 2005; Landoni et al., 2010), seedling development (Kushwaha et al., 2008), and abiotic stress responses (Zhang et al., 2009; Chu et al., 2018). Several studies also show that CaMs play a role in immune responses (Chiasson et al., 2005; Takabatake et al., 2007). CaMs are also critical for brassinosteroid biosynthesis and plant growth. Furthermore, they play a role in mediating auxin action (Yang and Poovaiah, 2000; Du and Poovaiah, 2005). It is known that CaMs do not have any enzymatic activity or ability to bind to DNA, except for CaM7, a unique member of the *CAM* gene family that directly binds to DNA. The reports indicate that CaM7 recognizes and binds to the Z-box and G-box motifs of light-regulated promoters and the promoter of the *ELONGATED HYPOCOTYL5 (HY5)* gene (Kushwaha et al., 2008; Abbas et al., 2014)



Generally, CaMs are considered to be localized in the cytosol. Nevertheless, different isoforms are also known to be additionally located in the nucleus, extracellular matrix, and peroxisomes (Ma et al., 1999; van der Luit et al., 1999; Yang and Poovaiah, 2002; Poutrain et al., 2011). Since CaMs have different subcellular localizations, this indicates one of the central roles of CaMs as a  $\text{Ca}^{2+}$  signal decoder in the cell. The increase of  $\text{Ca}^{2+}$  level by development cues and environmental stresses mediates plant responses by regulating transcriptional process in various ways, either by  $\text{Ca}^{2+}$  directly binding to the transcription factor or, most commonly, through a  $\text{Ca}^{2+}$ /CaM complex that binds to the transcription factor (Kim et al., 2009).

### **1.3.3. Role of the protein-protein interaction between calmodulins and other proteins**

The ability of CaM to bind different protein targets that share minimal amino acid sequence similarity in their binding sites is due to the flexible structure of the central  $\alpha$ -helical linker and the plasticity of hydrophobic surfaces that form binding interfaces (Ishida and Vogel, 2006). CaM interacts with its targets by hydrophobic interactions with long hydrophobic side chains in the amino acids of its target sites (Crivici and Ikura, 1995). The majority of known target sites of CaM are composed of a stretch of 12–30 contiguous amino acids with positively charged amphiphilic characteristics and a propensity to form an  $\alpha$ -helix upon binding to CaM. CaM recruitment motifs currently fall into two groups: motifs for  $\text{Ca}^{2+}$ -dependent binding, distinguished by their spacing of bulky hydrophobic and basic amino acids, and  $\text{Ca}^{2+}$ -independent binding through IQ motif. However, CaM-binding domains do not always have these features. The affinity of CaM for  $\text{Ca}^{2+}$  may be increased in the presence of targets, thereby providing a more sensitive signal response mechanism (Snedden and Fromm, 2001; Hoeflich and Ikura, 2002).

CaM targets in plants include transcription factors, protein kinases, protein phosphatases, channels, and pumps. Several TFs from the bHLH, bZIP, WRKY, NAC, and MYB families of transcription factors and calmodulin-binding transcription activators families (CAMTA) and CBP60 have been reported to bind CaMs. Some transcription factors have reduced DNA-binding capacity upon binding CaMs to their DNA-binding domain (Onions et al., 2000), while others show enhanced binding to their target *cis*-regulatory elements after CaM binding (Szymanski et al., 1996). The DNA binding activities of the same protein might be differentially regulated by different CaM isoforms (Yoo et al., 2005). A NAC transcription factor, CBNAC, was identified as a CaM-regulated transcriptional repressor in Arabidopsis. Using the GUS reporter system in Arabidopsis protoplasts, it was shown that interaction of

CBNAC with CaM promotes transcriptional repression through the CBNAC binding site (Kim et al., 2007).

Binding of CaM to WRKY group IId family members, including WRKY DNA-BINDING PROTEIN 7 (WRKY7), was demonstrated, and a binding motif was identified in Arabidopsis. The interaction occurs in a Ca<sup>2+</sup>-dependent manner. The WRKY7 - CaM interaction is believed to be important for the regulation of plant defense signaling; however, the biological relevance of this interaction was not studied yet (Park et al., 2005).

A CBP60s CaM binding protein family has eight members in Arabidopsis, and seven of them bind CaM. The *CBP60* genes are differentially expressed in response to biotic stresses and are involved in disease resistance against *Pseudomonas syringae* (Reddy et al., 2002; Wang et al., 2009).

Another separate and big group of proteins that all bind to CaMs is CAMTAs. CAMTAs function in diverse biological processes; for example, CAMTA1 is associated with auxin signaling and drought responses (Galon et al., 2010; Pandey et al., 2013), or CAMTA3 regulates biotic defense responses (Galon et al., 2008). CAMTA transcript levels are induced upon wounding (all CAMTAs), cold and heat treatment (CAMTA1 and CAMTA3-6), and salinity (CAMTA1-4 and CAMTA6) (Yang and Poovaiah, 2002)

Protein kinases and phosphatases are also often the targets of CaMs. MITOGEN-ACTIVATED PROTEIN KINASE 8 (MPK8) in Arabidopsis is activated by binding of CaMs in a Ca<sup>2+</sup>-dependent manner. MPK8 is activated through mechanical wounding and negatively regulates ROS accumulation in the wound signaling pathway (Takahashi et al., 2011). MITOGEN-ACTIVATED PROTEIN KINASE 1 (MPK1) also has enhanced phosphatase activity after binding to CaMs in a Ca<sup>2+</sup>-dependent manner (Lee et al., 2008). CaM3 interacts with a protein phosphatase PP7 that is involved in thermotolerance in Arabidopsis (Liu et al., 2007)

In Arabidopsis, several Ca<sup>2+</sup> pumps are CaM-regulated. CaMs target and activate AUTOINHIBITED CA(2+)-ATPASE (ACA9, ACA2, ACA4, and ACA8) Ca<sup>2+</sup>-ATPase (Hong et al., 1999; Bonza et al., 2000; Harper, 2001).

Cyclic nucleotide-gated non-selective cation channel proteins (CNGC) also bind to CaM in several different species. CNGC20 in Arabidopsis interacts with all known AtCaM isoforms and binds CaM in a Ca<sup>2+</sup>-dependent manner. Inactivation of the CNGCs results in a negative feedback loop *via* regulation of Ca<sup>2+</sup> influx into plant cells or across intracellular membranes (Ma, 2011; Fischer et al., 2013)

#### 1.4. JUB1 function in stress-associated networks

The NAC transcription factor JUB1 (ANAC042; AT2G43000) was identified as a central negative regulator of plant senescence in Arabidopsis. The expression profiles of senescence-associated genes in *JUB1* overexpressor plants support the extended longevity and delayed bolting phenotypes (Wu et al., 2012).

The developmental phenotype of *JUB1* overexpressors, which resembles the typical phenotype of gibberellin (GA)- and brassinosteroid-deficient mutants, can be explained by a direct negative regulation of the key genes *GIBBERELLIN 3-OXIDASE 1* (*GA3ox1*) and *DWARF 4* (*DWF4*) involved in GA and BR biosynthesis, respectively (Shahnejat-Bushehri et al., 2016). The inhibition of the two genes by JUB1 leads to reduced levels of GAs and BRs and, hence, the accumulation and activation of DELLA proteins. Moreover, JUB1 leads to an accumulation of DELLAs by direct transcriptional activation of two DELLA genes, namely *GIBBERELLIC ACID INSENSITIVE* (*GAI*) and *RGA-LIKE 1* (*RGL1*). JUB1 also directly represses the bHLH transcription factor *PHYTOCHROME INTERACTING FACTOR4* (*PIF4*) (Shahnejat-Bushehri et al., 2016), an essential regulator of photomorphogenic development that plays a role in the integration of multiple signals for the regulation of plant growth (Choi and Oh, 2016). In addition, PIF4 and BRASSINAZOLE-RESISTANT 1 (BZR1) act as direct upstream transcriptional repressors of *JUB1*, forming feedback loops in the JUB1 regulatory network (Shahnejat-Bushehri et al., 2016). When overexpressed in tomato (*Solanum lycopersicum*), *AtJUB1* regulates the tomato orthologs of *GA3ox1*, *DWF4*, *PIF4*, and *DELLA* genes and exhibits similar GA and BR deficiency phenotypes. These data indicate that the JUB1-mediated regulation of growth is conserved across species (Shahnejat-Bushehri et al., 2017).

In addition to growth regulation, overexpression of *JUB1* plays a role in response to biotic stress. The expression of *JUB1* is induced upon infection of plants with the (hemi)biotrophic pathogen *Pseudomonas syringae* pv. tomato DC3000 (*Pst* DC3000) and the necrotrophic fungus *Botrytis cinerea* (Shahnejat-Bushehri et al., 2016; Castillo et al., 2019). It is known that DELLA proteins can influence the disease outcome *via* modulation of the balance between the antagonistic interaction of jasmonic acid (JA) and salicylic acid (SA) signaling. JA-mediated signaling is associated with resistance to the necrotrophic pathogen, and SA-mediated signaling confers the resistance to (hemi)biotrophic pathogens. The reports indicate that the function of JUB1 during pathogen attack is mediated through the accumulation of DELLA proteins and the subsequent activation of JA signaling, leading to enhanced necrotrophic resistance and susceptibility to biotrophic resistance (Shahnejat-Bushehri et al., 2016; Castillo et al., 2019). The enhanced necrotrophic resistance can also be explained *via* induced biosynthesis of

camalexin, a phytoalexin that accumulates at pathogen infection areas, also regulated by *JUB1* overexpression (Saga et al., 2012). Recently, it was also reported that *JUB1* positively regulates the biosynthesis of another phytoalexin glyceollin, a known pathogen-inducible defense metabolite in soybean (Jahan et al., 2019). Interestingly, *JUB1* acts as a positive regulator of the biosynthesis of a number of phytoalexins. These data indicate a critical role of *JUB1* in the crosstalk between the regulation of plant growth and plant defense.

Overexpression of *JUB1* also enhances tolerance to various abiotic stresses, such as heat (Shahnejat-Bushehri et al., 2012; Wu et al., 2012), salinity (Wu et al., 2012; Tak et al., 2017; Alshareef et al., 2019), and drought (Ebrahimian-Motlagh et al., 2017; Tak et al., 2017; Thirumalaikumar et al., 2018). Moreover, enhanced tolerance to stresses upon overexpression of *JUB1* was reported for several different species: *Arabidopsis thaliana*, tomato, and banana (*Musa acuminata*) (Wu et al., 2012; Tak et al., 2017; Thirumalaikumar et al., 2018; Alshareef et al., 2019).

Homeodomain-leucine zipper transcription factor AtHB13 confers drought tolerance at least in part through direct transcriptional regulation of *JUB1*. Moreover, the expression of *JUB1* is induced by drought stress, and histochemical GUS staining revealed drought-induced *JUB1* promoter activity (Ebrahimian-Motlagh et al., 2017). In banana, *JUB1* overexpressors exhibit elevated expression of several genes belonging to the *CBF*, *WRKY*, and *LEA* families involved in responses to drought and salt stress (Tak et al., 2017). However, the molecular mechanism underlying the drought tolerance phenotype of *JUB1* overexpressors and its downstream targets that contribute to tolerance remain mostly unknown. Our group discovered that *JUB1* directly regulates the expression of *DEHYDRATION-RESPONSIVE ELEMENT BINDING PROTEIN 2 (DREB2A)*, which also activates many responsive TFs involved in drought and heat stress responses (Wu et al., 2012). In tomato, *SIJUB1* similarly controls the expression of the tomato orthologs *SIDREB1*, *SIDREB2*, and *SIDELLA* (Thirumalaikumar et al., 2018). Due to the fine-tuning of H<sub>2</sub>O<sub>2</sub> level partly through the *JUB1*–*DREB2A*–HsfA3–HsfA2 (HEAT SHOCK TRANSCRIPTION FACTOR A3 and A2) transcription factor cascade, *JUB1* overexpressors exhibit reduced intracellular ROS levels (Wu et al., 2012). A *JUB1* ortholog in apple, *MdNAC42*, positively regulates the accumulation of anthocyanins in red-fleshed fruits (Zhang et al., 2020). However, in *Arabidopsis*, the reduced level of anthocyanins in *JUB1* overexpression plants is consistent with their prolonged leaf longevity (Wu et al., 2012). It remains unknown if the abiotic stress tolerance phenotype of *JUB1* overexpressors solely depends on the direct induction of the *DREB2A* gene. It is also possible that the subsequent induction of other drought- and stress-related genes takes place, which then are able to reduce

the intracellular level of reactive oxygen species. Additionally, metabolite profiling also revealed elevated proline and trehalose levels in *JUB1* overexpressors in *Arabidopsis* (Wu et al., 2012). Similarly, other reports indicate a higher accumulation of proline in *JUB1* overexpressors under control and drought conditions in several species (Shahnejat-Bushehri et al., 2017; Tak et al., 2017; Alshareef et al., 2019). Nevertheless, the molecular mechanism by which JUB1 controls drought tolerance remains largely unknown.

Collectively, JUB1 is a central regulator of a complex cellular module and is involved in fine-tuning plant growth and stress responses. Hence, JUB1 provides a new anchor point for future studies of plant growth and its interaction with stress, which holds great promise for improving the tolerance of plants against abiotic stresses in general.

### **1.5. Aim of the thesis**

Our work addresses the importance of identifying the regulatory components and the mechanisms through which JUB1 controls tolerance to drought stress. Even though the drought tolerance phenotype of *JUB1-OX* plants has previously been reported, the regulatory mechanisms by which JUB1 controls the tolerance to drought remain unknown.

A higher level of proline and altered stomatal conductance in *JUB1* overexpressors might cause enhanced tolerance to drought stress. We also do not exclude the possibility that other mechanisms contribute to the enhanced drought resistance of plants overexpressing JUB1 like enhanced root growth, the accumulation of additional compatible solutes, or the contribution of particular chaperons.

Until today, none of the previous studies on JUB1's regulatory network focused on identifying proteins interacting with JUB1 and studying their roles. It is well known that protein-protein interactions can serve a regulatory role in either upstream or downstream levels *via* coordinating cellular signaling events and metabolic functions in the cell. Understanding the function of JUB1 in the proper biological context is impossible without taking into account other proteins involved in the same cellular processes.

The aim of the PhD work is to further investigate JUB1's regulatory network by:

- identifying the regulatory mechanisms through which JUB1 confers tolerance to drought;
- studying the control of proline biosynthesis genes as potential targets of JUB1;
- identifying proteins interacting with JUB1 and studying their roles.

## 2. MATERIALS AND METHODS

### 2.1. General methods

Standard molecular techniques were performed as described (Sambrook and Russell, 2001).

**Chemicals and reagents** were obtained from Invitrogen (Karlsruhe, Germany), Fluka (Buchs, Switzerland), Merk (Darmstadt, Germany), Roche (Mannheim, Germany), Sigma-Aldrich (Taufkirchen, Germany), Duchefa Biochemie (Haarlem, The Netherlands). Restriction enzymes were obtained from New England Biolabs (Frankfurt am Main, Germany) or Thermo Fisher Scientific (Darmstadt, Germany). Molecular biology kits were purchased from Qiagen (Hilden, Germany), Macherey-Nagel (Düren, Germany), New England Biolabs GmbH (Frankfurt am Main, Germany), Invitrogen (Karlsruhe, Germany), Ambion (Cambridgeshire, UK), Thermo Fisher Scientific, Chromotek GmbH (Planegg, Germany), Promega (Madison, USA), LI-COR Biosciences (Bad Homburg, Germany), Takara Bio (Shiga, Japan) and STRATEC Molecular (now Invitek Molecular, Berlin, Germany). All oligonucleotides (labeled and unlabeled) were obtained from Eurofins Genomics Germany GmbH (Ebersberg, Germany). Sequencing of different DNA fragments was performed by LGC Genomics (Berlin, Germany).

**Software and databases:** Arabidopsis Information Resource (TAIR; <http://www.Arabidopsis.org>) and Plaza 3.0 (<http://bioinformatics.psb.ugent.be/plaza/>; Proost et al., 2015) were used to obtain sequences. Sequence analysis was performed using online tools available at the National Center for Biotechnology Information (<http://www.ncbi.nlm.nih.gov/>) and SnapGene software version 4.2.11 (GSL Biotech LLC). The online tools of Genevestigator ([www.genevestigator.com](http://www.genevestigator.com); (Zimmermann et al., 2004), Electronic Plant browser from Bio-Array Resource for plant biology (ePlant BAR; <https://bar.utoronto.ca/eplant/>; Department of Cell & Systems Biology, University of Toronto), Subcellular localization database for Arabidopsis proteins (SUBA4; <https://suba.live/>; (Hooper et al., 2014); (Tanz et al., 2013), Calmodulin Target Database Binding Sites Search and Analysis (CTDB; <http://calcium.uhnres.utoronto.ca/ctdb/ctdb/home.html>; (Yap et al., 2000), and Calmodulation database and meta-analysis predictor (<http://cam.umassmed.edu/>; (Mruk et al., 2014) CRISPR-P v2.0 (<http://crispr.hzau.edu.cn/CRISPR2/>) were used for gene expression analysis of public databases and computational sequence analysis.

**Equipment:** ABI-PRISM 7900 HT sequence detection system (Applied Biosystems, USA), Odyssey Infrared Imaging System (LI-COR Biosciences, Germany), CLARIOstar microplate reader (BMG LABTECH, Germany), centrifuge 5427 R (Eppendorf, Germany) confocal scanning microscope Leica TCS-SP5/Leica TCS-SP8 (Leica, Germany), spectrophotometer Jasco V-730 (JASCO Deutschland GmbH, Germany), orbital shaker (Heidolph, Germany), differential interference contrast microscope BX51 (Olympus, Japan) SC-1 Leaf Porometer METER Environment Group, Inc. (Munich, Germany).

## 2.2. Plant materials and growth conditions

*Arabidopsis thaliana* (L.) Heynh. accession Col-0 was used in this study as a wild type (WT). Seeds were surface-sterilized with 70% (v/v) ethanol for 2 min, 20% (v/v) sodium hypochlorite for 20 min, and washed with sterile water 3 times. Then the seeds were germinated on Murashige-Skoog agar medium (Duchefa Biochemie), MES (Carl Roth), and 1% (w/v) sucrose, and the seedlings were grown under long-day (LD) condition (16-h light/8-h dark) at 22 °C. Plants were then transferred to a plant growing chamber with long-day conditions (LD, 16-h light, 120  $\mu\text{mol m}^{-2} \text{s}^{-1}$  20 °C/8-h dark, 16 °C, relative humidity of 60%/75%) or with a neutral day (ND, 12-h light, 120  $\mu\text{mol m}^{-2} \text{s}^{-1}$ /12-h dark, 22 °C, and relative humidity of 60%/75%). Leaf mesophyll protoplasts were isolated from four-week-old plants grown under 12-h light, 100  $\mu\text{mol m}^{-2} \text{s}^{-1}$  light intensity 22 °C/12-h dark 20 °C, and relative humidity of 60%. Five-week-old *Nicotiana benthamiana* plants grown under LD condition at 22 °C, light intensity 100  $\mu\text{mol m}^{-2} \text{s}^{-1}$ , and relative humidity of 75% were used for transient infiltration. The *jub1-kd*, *JUB1-OX*, *JUB1pro:GUS*, and *JUB1pro:JUB1-GFP* lines were described previously (Wu et al., 2012). The *cam1/cam4* double knockout mutant plants were generated in *Arabidopsis thaliana* Col-0 and the *35S:JUB1-GFP* background using the CRISPR-Cas9 approach. The *jub1 crispr* line was generated using the CRISPR-Cas9 system in Col-0 plants. *CaM1-OX* and *CaM4-OX* lines were obtained by transforming *35S:CaM1-RFP* or *35S:CaM4-RFP* construct in Col-0 plants. *JUB1-OX/CaM1-OX* and *JUB1-OX/CaM4-OX* lines were generated via co-superinfiltration of *Arabidopsis thaliana* *JUB1-OX* plants with *35S:Myc-CaM1* and *35S:Myc-CaM4* constructs. *bZIP63-OX* and *JUB1-OX/bZIP63-OX* double overexpressor plants were generated by transforming the *35S:bZIP63* construct into the *JUB1-OX* plants or Col-0 WT plants. *JUB1-OX/dreb2a-2* plants were obtained by transformation of the *35S:JUB1-GFP* (Wu et al., 2012) construct into the *dreb2a-2* mutant. *dreb2a-2* mutant seeds were kindly provided by Prof. Kazuko Yamaguchi-Shinozaki (Sakuma et al., 2006).

Seeds of R-GECO transgenic lines for Ca<sup>2+</sup> level measurements were kindly provided by Prof. Dr. Tina Romeis (Keinath et al., 2015).

*KST1:JUB1-GFP* lines were generated in Col-0 and *jub1-kd* background by transforming the *KST1:JUB1-GFP* construct into the *jub1-kd* mutant or WT Col-0 plants. Primer sequences for genotyping are given in **Supplemental Table S1**.

### 2.3. Plasmid construction and plant transformation

All PCR products utilized for cloning were amplified using Phusion high-fidelity DNA polymerase (New England Biolabs). To generate the constructs, cloning was performed by traditional cut-ligation method using restriction enzymes, In-Fusion Cloning (Takara Bio), or the GATEWAY system (Invitrogen). Amplicon accuracy was evaluated by DNA sequence analysis (LGC Genomics). Constructs were transformed into *Agrobacterium tumefaciens* GV3101 (pMP90) strain by electroporation. *Agrobacterium* positive clones confirmed by colony PCR were used to transform *Arabidopsis* plants by the floral deep method (Clough and Bent, 1998).

For *proKST1:JUB1-GFP*, a 648-bp long *KST1* promoter region was amplified by PCR from *Solanum tuberosum* Andegina genomic DNA. The CaMV 35S promoter in *JUB1-OX* (Wu et al., 2012) was replaced by the *KST1* promoter (Kelly et al., 2017) via In-Fusion Cloning using *SpeI* and *StuI* restriction sites in the pK7FWG2 (Karimi et al., 2002) destination vector.

For generating Yeast One-Hybrid-System (Y1H) bait constructs, the following promoter regions were PCR-amplified from *Arabidopsis* Col-0 genomic DNA: *pTUY1H-PDH2* – 369 bp, *pTUY1H-MYB2* – 283 bp, *pTUY1H-bZIP63* – 343 bp. The sequences of the used promoter regions are given in **Supplemental Figure S1**. The selected promoter regions were first cloned via primer-added *NruI* or *MluI* and *SacII* sites into pJET1.2/blunt (Invitrogen) and then transferred to the pTUY1H yeast transformation vector (with LEU2 as selection marker) (Castrillo et al., 2011) by restriction enzyme-mediated cloning.

For transactivation assay in *Arabidopsis* protoplasts, reporter construct *DREB2A:LUC* was cloned into RD29A:LUC (Kovtun et al., 2000) vector via In-Fusion Cloning using *NcoI* and *PstI* restriction sites. The *RD29A* promoter was exchanged with a 1-kb promoter region of *DREB2A* amplified by PCR from Col-0 genomic DNA. For effector constructs, full-length coding sequences of *JUB1* and *CaM4* were PCR-amplified from Col-0 cDNA and cloned via GATEWAY cloning following the manufacturer's protocol (Invitrogen) into donor vector pDONR-207 (Invitrogen) and subsequently into the destination vector p2GWF7 with a C-terminal fusion to eGFP (Karimi et al., 2002), or into the destination vector p2GWF7 where



the eGFP tag was exchanged with a Myc tag *via* In-Fusion Cloning using *SacII* and *NotI* restriction sites. RD29A:LUC, UBQ10:GUS, 35S:LUC (Kovtun et al., 2000; Boudsocq et al., 2010) vectors were kindly provided by Dr. Marie Boudsocq from the University of Paris-Saclay.

For transactivation assay in transiently transformed *Nicotiana benthamiana* leaves, reporter construct *DREB2A:LUC* was cloned into pGreenII 0800-LUC (Hellens et al., 2005) *via* restriction cloning using *NcoI* and *PstI* restriction sites to insert a 1-kb promoter region of *DREB2A*, amplified by PCR from Col-0 genomic DNA. As effector constructs BiFC2in1 constructs (described below) with *JUB1* and *CaM4* coding sequences, and only *JUB1* or *CaM4* CDS were used. For subcellular localization studies, the *JUB1* expression clone in the p2GWF7 vector was used. The full-length coding sequence of *CaM1* and *CaM4* previously obtained *via* the GATEWAY cloning system in pDONR-207 was introduced *via* LR recombination reaction into the destination vector p2GWF7. The eGFP tag was exchanged with an mRFP tag *via* In-Fusion Cloning using restriction sites *SacII* and *NotI*.

For BiFC analysis, all constructs were introduced *via* GATEWAY. Briefly, the full-length coding sequence of *JUB1*, *CaM1*, and *CaM4* and split *JUB1* region (*JUB1*<sub>Nterm</sub> 1-144 amino acid or *JUB1*<sub>Cterm</sub> region 136-275 amino acid) were PCR-amplified using Col-0 cDNA as template, and cloned into donor vector pDONR-207 *via* BP recombination. A subsequent LR recombination reaction resulted in expression clones in pUC-SPYNE and pUC-SPYCE (Walter et al., 2004). *JUB1* and split *JUB1* regions were tagged with nYFP and Myc at the C-terminus, respectively. In contrast, *CaM1*/*CaM4* were tagged with cYFP and HA at the C-terminus. For the BiFC2in1 cloning system, *JUB1*, split *JUB1* region (*JUB1*<sub>Nterm</sub> 1-144 amino acid or *JUB1*<sub>Cterm</sub> region 136-275 amino acid) were first PCR-amplified using Col-0 cDNA as template and cloned in donor vector pDONR221 P2-P3 (Invitrogen) *via* BP recombination reaction. *JUB1* and the *JUB1*<sub>Nterm</sub> region with substitution of Leu amino acid to Ala in position Leu<sup>121</sup> were generated by Twist Bioscience (San Francisco, USA), PCR-amplified from the Twist cloning vector (Twist Bioscience), and cloned in donor vector pDONR221 P2-P3 (Invitrogen) *via* BP recombination reaction. As a negative control for BiFC, the *ANAC063* (*AT3G55210*) coding sequence was PCR-amplified using Col-0 cDNA as template and cloned in donor vector pDONR221 P2-P3. *CaM1* and *CaM4* were first PCR-amplified using Col-0 cDNA as template and cloned in donor vector pDONR221 P1-P4 (Invitrogen) *via* BP recombination reaction. Entry clones pDONR221 P1-P4 and pDONR221 P2-P3 were introduced *via* LR recombination reaction into destination vector pBIFCt-2in1-CC (Grefen and Blatt, 2012).

For protein expression in *Escherichia coli* BL21 (DE3) CodonPlus-RP (Invitrogen), the CDS of *JUB1*, *CaM1*, and *CaM4* previously obtained via the GATEWAY cloning system pDONR-207, were introduced via LR recombination into destination vector pDEST24 (Invitrogen) to get JUB1-GST and pDEST17 to obtain CaM1-His and CaM4-His recombinant proteins.

For the generation of the *CaM1-OX* and *CaM4-OX* lines, the full-length coding sequences of *CaM1* and *CaM4* previously obtained via GATEWAY cloning system in pDONR-207 were introduced via LR recombination reaction into destination vector pGWB554 (Nakagawa et al., 2007).

For the generation of the *bZIP63-OX* and *bZIP63-OX/JUB1-OX* lines, the full-length coding sequences of *bZIP63* were PCR-amplified using Col-0 cDNA as template and cloned into donor vector pDONR-207 via BP recombination. Entry clone with *bZIP63* was then introduced into pGWB554 destination vector via LR recombination.

For the generation of the *JUB1-OX/CaM1-OX* and *JUB1-OX/CaM4-OX* lines, the full-length coding sequences of *CaM1* and *CaM4* were previously obtained via GATEWAY cloning in pDONR-207 and were introduced via LR recombination reaction into destination vector pGreen-Cmyc-GWinvers (obtained from Dr. Marie Boudsocq from the University of Paris-Saclay) Primer sequences used for cloning are given in **Supplemental Table S1**.

For the generation of the *jub1* *crispr* knockout mutants, two sgRNAs were selected with the help of the CRISPR-P software (<http://crispr.hzau.edu.cn/CRISPR2/>) and cloned into pJF1031 via primer-added *BsaI* sites (*JUB1*: sgRNA1-GCAGCGTCGGAGAAAAGGAG, sgRNA2-GCTGGTCTTAGAACAAGTGT). The pJF1031 vector was kindly provided by Dr. Joachim Forner from the MPI-MP (Ruf et al., 2019). For the generation of the *cam1/cam4* double knockout mutant, two pairs of sgRNAs were chosen with the help of the CRISPR-P software and cloned into pJF1031 via primer-added *BsaI* sites (*CaM1*: sgRNA1-GCTCCAAGACATGATCAACG, sgRNA2-AGTGGAAGAGATGATCCGTG; and *CaM4*: sgRNA1-GCTACAAGACATGATCAACG, sgRNA2-AGATGGTCAGATAAACTACG). Primer sequences used for the generation of knockout mutants are given in **Supplemental Table S2**.

## 2.4. Gene expression analysis

### 2.4.1. RNA isolation and cDNA synthesis

Total RNA was extracted from ~ 100 mg frozen seedlings or leaves using InviTrap Spin Plant RNA Mini Kit (STRATEC Molecular) or using Trizol reagent with subsequent RNA purification using Pure Link RNA Mini Kit (Invitrogen). DNase treatment (TURBO DNase

Kit; Ambion) was performed following the manufacturer's instructions to remove possible genomic DNA contamination. The absence of genomic DNA was verified by qRT-PCR using intron-specific primers that anneal to an intron of a control gene (*MADS AFFECTING FLOWERING 5*, *AT5G65080*). The quantity of RNA was determined using a NanoDrop ND1000 spectrophotometer (Thermo Fisher Scientific). The cDNA synthesis was accomplished with 2 µg of total RNA using Revert Aid First Strand cDNA Synthesis Kit (Thermo Fisher Scientific). The cDNA was diluted 1:2 with water for the qRT-PCR. The cDNA synthesis efficiency was evaluated by qRT-PCR amplification of transcripts from two housekeeping genes, *ACTIN2* (*AT3G18780*) and *GAPDH* (*AT1G13440*). Two sets of primers designed to amplify 5'- and 3'-end regions of the *GAPDH* transcript to check its integrity are given in **Supplemental Table S3**.

#### **2.4.2. Quantitative real-time PCR (qRT-PCR)**

The qRT-PCR experiments were conducted in three biological replicates using the ABI-PRISM 7900 HT sequence detection system (Applied Biosystems), and amplification products were visualized using SYBR Green (Life Technologies). The PCR reaction was carried out in 5 µL volume (2.5 µL SYBR Green mix; 2 µL primers and 0.5 µL cDNA). Data analysis was performed using SDS software version 2.4 (Applied Biosystems). Amplification curves were analyzed with a normalized reporter (Rn: the ratio of the fluorescence emission intensity of SYBR Green mix to the fluorescence signal of the passive reference dye) threshold of 0.2 to obtain the cycle threshold (Ct) values. In each PCR run, two to three technical replicates were used, and the mean of their Ct was subjected to relative gene expression analysis. The transcript level of each gene was normalized to *ACTIN2* (*AT3G18780*) as a reference gene. Gene expression data were normalized by subtracting the mean Ct value of the reference gene from the mean Ct value of the gene of interest ( $\Delta$ Ct). The Student's *t*-test was used for the determination of statistical significance. qRT-PCR primers for all genes were designed using the QuantPrime tool ([www.quantprime.de](http://www.quantprime.de); (Arvidsson et al., 2008)) and are given in **Supplemental Table S3**.

#### **2.5. Yeast one-hybrid screen**

The bait constructs in pTUY1H (Castrillo et al., 2011) (*LEU2* selection marker; *PDH2*, *MYB2*, or *bZIP63* promoter fragment upstream of the *HIS3* reporter) were transformed into the yeast strain Y187, mating type  $\alpha$ . The mating-based Y1H screen was done using JUB1 protein from a library of approximately 1,200 Arabidopsis TFs, established in vector pDEST22 (*TRP1*

selection marker) in yeast strain YM4271 (mating type a). Screening for interaction between JUB1 and the TF promoter fragments containing JUB1 BS (binding sites) was done on an SD medium lacking the essential amino acids Leu, Trp, and His in the presence of different concentrations of 3-amino-1,2,4-triazole (3AT) to exclude false-positive interactions.

## **2.6. Expression and purification of recombinant proteins in *E. coli***

Vectors with glutathione S-transferase (GST) and recombinant JUB1-GST, CaM1-His, and CaM4-His were heat-shock transformed into chemically competent in *E. coli* strain BL21 (DE3) CodonPlus-RP. Protein expression was induced using 1 mM isopropyl- $\beta$ -D-thiogalactoside (IPTG), and cells were harvested 4-6 hours after induction at 28 °C. Cells harvested from a 400-mL culture were lysed by sonication in 20 mL lysis buffer (50 mM Na<sub>2</sub>HPO<sub>4</sub>, 300 mM NaCl, 0.1 mM EDTA, 1 mM PMSF, 0.2% (v/v) Triton X-100 and 100 mg/l lysozyme). After centrifugation, 1 g of respective resin was added to the supernatant, and the mixture was rotated overnight at 4 °C.

His-tagged proteins were purified using Protino® Ni-IDA Resin (Macherey-Nagel, Düren, German), and GST-tagged proteins were purified using glutathione agarose (Sigma-Aldrich) following the manufacturer's protocol. Briefly, resin/protein mixture was transferred into the purification column and was washed with 10 mL LEW buffer (50 mM Na<sub>2</sub>HPO<sub>4</sub>, 300 mM NaCl pH 8,) for his-tagged proteins or PBS-T (10 mM phosphate buffer, pH 7.4, 150 mM NaCl containing, 1% Triton X-100) for GST-tagged protein. The proteins were eluted (10 mM reduced glutathione in 50 mM Tris-HCl, pH 9.0 for GST-, and 50 mM Na<sub>2</sub>HPO<sub>4</sub>, 300 mM NaCl, 250 mM imidazole, pH 8 for his-tagged proteins), and the aliquots of the elution fractions were analyzed by SDS-PAGE (sodium dodecyl sulfate-polyacrylamide gel electrophoresis) (Laemmli, 1970). Protein concentration was determined by Bradford assay (Bradford, 1976).

## **2.7. Electrophoretic mobility shift assay (EMSA)**

Recombinant JUB1-GST protein was prepared as described above. A 40 bp-long fragment of the promoter regions of the *bZIP63* gene, including the JUB1 binding site, was used to design complementary EMSA fragments. Oligonucleotides used for EMSA are given in **Supplemental Table S4**. Two fragments of DY682-labeled DNA oligonucleotides (forward: 5'-DY682 GGACCAACTCTGAGTGTAGCCGTTGAATAGTCCATTCATC-3'; reverse: 5'-DY682 GATGAATGGACTATTCAACGGCTACACTCAGAGTTGGTCC-3') and unlabeled oligonucleotides (with the same sequence) used as competitors were ordered from Genomics Germany. Annealing was performed for complementary pairs of labeled or non-labeled

oligonucleotides by heating each pair mixture to 100 °C, followed by slow cooling to room temperature. The binding reaction was performed for 20 min at room temperature using the Odyssey Infrared EMSA kit following the manufacturer's protocol (LI-COR Biosciences). Gel electrophoresis was performed using a 6% retardation gel (Invitrogen) and the DY682 signal was detected using the Odyssey Infrared Imaging System from LI-COR Biosciences.

## **2.8. Chromatin immunoprecipitation (ChIP) assay**

Rosette leaves of 4-week-old *JUB1-OX* (with JUB1-GFP fusion) plants grown under ND (12-h light, 120  $\mu\text{mol m}^{-2} \text{s}^{-1}$ /12-h dark, 22 °C, and relative humidity of 60%/75%) conditions were used for ChIP. All experiments were performed according to a published method (Kaufmann et al., 2010). Primers used to amplify *MYB2*, *PDH1*, and *bZIP63* promoter regions harboring the JUB1 binding site are given in **Supplemental Table S5**. Primers annealing to a transposable element gene, *TA3* (*AT1G37110*), lacking the JUB1 binding site, were used as a negative control. The chromatin extracts were isolated, and anti-GFP antibody beads (Chromotek) were used to immunoprecipitate protein-DNA complexes (Kaufmann et al., 2010). After reversion of the cross-linking, DNA was purified by QIAquick PCR Purification Kit (Qiagen) and analyzed by qPCR. Wild-type (Col-0) plants served as a negative control.

## **2.9. Yeast two-hybrid screen**

An initial screen was performed by Next Interactions (Richmond, USA) with bait JUB1 excluding the 16 N-terminal peptide sequence due to high self-activation levels, and an *Arabidopsis thaliana* cDNA library in the presence of 60 mM 3AT for *HIS3* reporter expression (low stringency, SD-L-T-H) and *HIS3* and *ADE2* reporter activation (high stringency, SD-L-T-H-A). The selection was done for three days. Most colonies were picked from HIS+ADE stringent selection plates on SD-L-T-H-A + 60 mM 3AT screening plates, and on SD-L-T-H + 60 mM 3AT screening plates. Prey cDNAs were amplified with colony PCR using a set of flanking primers. The resulting PCR products were then sequenced in the forward direction and searched against the *Arabidopsis* sequence using BlastN (nucleotide) and BlastX (protein) to find seventy-six and eighty hits, respectively.

## **2.10. Isolation and DNA transfection of mesophyll protoplasts**

Mesophyll protoplasts were obtained from 4-week-old soil-grown Col-0 or *JUB1-OX Arabidopsis thaliana* plants and transfected using the PEG-mediated protoplast transfection method as described (Yoo et al., 2007), with small modifications. Leaves were harvested 2

hours after the onset of the light phase and prepared for digestion in enzymatic solution (1.5% [w/v] Cellulase R-10 and 0.4% (w/v) Macerozyme R-10; both from Serva) using the Tape-Arabidopsis Sandwich method (Wu et al., 2009).

For transactivation assay, 100  $\mu\text{L}$  protoplasts at a density of  $4 \times 10^5$  cells/mL were transfected with 20  $\mu\text{g}$  total DNA. In the transactivation assay, *UBQ10:GUS* was co-transfected as an internal control for the normalization of transformation efficiency (Martinho et al., 2015). As a positive control, *35S:LUC* was used. The ratio of effectors and reporter DNA was 1:1. For the BiFC assay, 200  $\mu\text{L}$  protoplasts at a density of  $4 \times 10^5$  cells  $\text{mL}^{-1}$  were transfected with 36  $\mu\text{g}$  total DNA. For immunoblot analysis, 100  $\mu\text{L}$  protoplasts at a density of  $4 \times 10^5$   $\text{mL}^{-1}$  were transfected with 20  $\mu\text{g}$  total DNA. For subcellular localization assay, 100  $\mu\text{L}$  protoplasts at a density of  $4 \times 10^5$   $\text{mL}^{-1}$  were transfected with 20  $\mu\text{g}$  total DNA.

After transfection, protoplasts were transferred to the plant growth chamber in order to retain their diurnal cycle. After 20-24 hours, protoplasts were harvested and kept at  $-80$   $^{\circ}\text{C}$  until further analysis for reporter assay and immunoblot analysis, or used directly for the microscopic subcellular localization assay and BiFC.

### **2.11. Transient transformation of *Nicotiana benthamiana***

*N. benthamiana* leaves were transiently transformed by *A. tumefaciens* GV3101 strains carrying the generated expression vectors. Overnight grown culture of *A. tumefaciens* cells was collected at OD600 of 2.0 and resuspended in the infiltration buffer, containing 10 mM  $\text{MgCl}_2$ , 10 mM MES/KCl pH 5.6, and 200  $\mu\text{M}$  acetosyringone. Then, the strains were incubated on a shaker at 60 rpm at room temperature in the dark for three hours. The *N. benthamiana* leaf abaxial space was co-infiltrated with *Agrobacterium* expressing viral silencing suppressor P19 (1:1 dilution) using a needleless syringe, according to Grimsley et al. (1986). Transformed leaves were analyzed for fluorescence 72 hours after infiltration using a confocal microscope.

### **2.12. Transactivation assay**

Transactivation assay in Arabidopsis protoplasts was performed as described in Yoo et al. (2007) with small modifications. Briefly, after 20 hours after transfection, protoplasts were harvested and frozen in liquid nitrogen. Frozen protoplast cell pellets were then homogenized in 100  $\mu\text{L}$  protoplast lysis buffer (25 mM Tris-phosphate pH 7.8, 2 mM CDTA, 2 mM DTT, 10% [v/v] glycerol) to extract the proteins. Samples were briefly vortexed and centrifuged at 12,700 rpm for 1 min (centrifuge 5427 R, Eppendorf). LUC activity was measured with CLARIOstar microplate reader (BMG LABTECH, Ortenberg, Germany) using 30  $\mu\text{L}$  of the

lysate and 30  $\mu$ L LUC mix using Firefly Luciferase HT Assay Kit (GeneCopoeia, Heidelberg, Germany) following the kit user manual. For the GUS assay, 10  $\mu$ L of the lysate was incubated at 37 °C in 100  $\mu$ L of the GUS Buffer (10 mM Tris-HCl pH 8., 2 mM  $MgCl_2$ , 0.1 mM MUG). The reaction was stopped after 1 hour by adding 900  $\mu$ L of 200 mM  $Na_2CO_3$  to the sample. Fluorescence of 4-methyl umbelliferone (4-MU) was measured with CLARIOstar microplate reader (BMG LABTECH) using the following settings: emission 460 nm, excitation by 365 nm. Data were collected as ratios (firefly luciferase activity/GUS activity). Transactivation assay in transiently transformed *Nicotiana benthamiana* leaves was performed as described in Hellens et al. (2005). Briefly, *N. benthamiana* leaves were transiently transformed as described above with small modifications; 100  $\mu$ L of *Agrobacterium* transformed *DREB2A:LUC* fusion in pGreenII 0800-LUC was mixed with 900  $\mu$ L of a second *Agrobacterium* transformed effector construct (*JUB1-CaM4*, *JUB1-EV* or *EV-CaM4*). Tobacco leaves were harvested 3 days after infiltration. Approximately 2 cm leaf discs were harvested, frozen in liquid nitrogen, and ground in 500  $\mu$ L of Passive Lysis Buffer using Dual-Luciferase® Reporter Assay System kit (Promega). Five  $\mu$ L of a 1/50 dilution of this crude extract was assayed in 40  $\mu$ L of Luciferase Assay Buffer, and the chemiluminescence was measured. Forty  $\mu$ L of Stop and Glow™ buffer was then added, and a second chemiluminescence measurement was made. LUC activity was measured with CLARIOstar microplate reader (BMG LABTECH, Ortenberg, Germany) following the manufacturer's Dual-Luciferase® Reporter Assay System-kit protocol (Promega). Data were collected as ratios (firefly luciferase activity/renilla luciferase activity).

### **2.13. Immunoblot analysis**

Total proteins from Arabidopsis seedlings or *N. benthamiana* leaves were prepared by the phenol-based method (Cahoon et al., 1992). Tissue powder was homogenized in 500  $\mu$ L buffer containing 0.7 M sucrose, 0.5 M Tris-HCl (pH was adjusted with HCl to pH 9.4), 50 mM EDTA, 0.1 M potassium chloride, containing 2% (v/v) 2-mercaptoethanol. cOmplete Protease Inhibitor Cocktail (Roche; diluted to 1  $\times$  final concentration) was added before use. The homogenate was mixed with 500  $\mu$ L phenol and centrifuged at 12,700 rpm (centrifuge 5427 R, Eppendorf) for 10 min at 4 °C. The upper phenol phase was taken, and proteins were precipitated by the addition of 1 mL of 0.1 M ammonium acetate in methanol and overnight incubation at -20 °C. The protein pellet obtained following centrifugation at 12,700 rpm (centrifuge 5427 R, Eppendorf) for 10 min at 4 °C was washed sequentially with 1 mL of 0.1 M ammonium acetate in methanol. The protein pellets were dissolved in 1% (v/v) SDS. The

protein concentration was determined by the Bradford assay (Bradford, 1976). Frozen protoplast cell pellets were homogenized in 10  $\mu$ L of 4 $\times$ Laemmli sample buffer (Bio-Rad). Proteins were separated on denaturing 12%-15% Tris-Glycine polyacrylamide gels and electroblotted onto a nitrocellulose membrane (Sigma Aldrich). Rabbit anti-Myc polyclonal antibody (Abcam, ab9106, 1:1000), rabbit anti-HA polyclonal antibody (Abcam, ab9110, 1:4000) and rabbit anti-GFP (Invitrogen, A11122; 1:1000) were used as primary antibodies, and IRDye 800CW-conjugated goat anti-rabbit IgG (H+L) antibody was used as secondary antibody at 1:10 000 dilutions (LI-COR Biosciences; 926-32211). Image capture was done using the Odyssey Infrared Imaging System (LI-COR Biosciences). The membrane was stripped according to Burnette (1981) after immunodetection and then stained with Ponceau S (Sigma) for loading control.

#### **2.14. Microscopic analysis**

All fluorescence signals were imaged using a confocal scanning microscope Leica TCS-SP5 or Leica TCS-SP8 (Leica). The Argon laser was always set to 20% maximal intensity.

For the BiFC assay in transiently transformed Arabidopsis protoplasts, the excitation wavelength was set at 514 nm. The spectral detection was set between 524–600 nm to monitor the BiFC signal (YFP fluorescence) and 629–700 nm for chlorophyll fluorescence.

For the BiFC experiment in transiently transformed *N. benthamiana* leaves, the excitation wavelengths were 514 nm and 561 nm. The spectral detection of the RFP signal was set between 575–615 nm; of the YFP signal between 530–559 nm and 678–727 nm for the chlorophyll fluorescence. Laser DPSS 561 was active. Line sequential scanning mode was applied in dual-channel observation to avoid the possible bleed-through between two fluorophores. For quantification of the YFP/RFP relative fluorescence intensity ratio, the signal intensity measurement was done using Fiji imaging software (Schindelin et al., 2012). For the quantification of the nuclear signal intensity, only the nucleus was selected for measurement.

For the subcellular localization assay in the protoplast and the GFP and RFP signal detection in transgenic Arabidopsis lines, the excitation wavelength was 488 nm and/or 561 nm. For the RFP signal detection, laser DPSS 561 was active. To detect two fluorophores, the spectral detection was set between 492–538 nm to monitor the GFP signal, between 567–638 nm to monitor the RFP signal and 653–732 nm for the chlorophyll fluorescence. For the GFP or RFP signal detection in transgenic Arabidopsis lines, the spectral detection was set between 498–550 nm to monitor the GFP signal or between 575–615 nm to monitor the RFP signal and 650–700 nm for the chlorophyll fluorescence.



For the verification of YFP signal localization in BiFC in protoplast, Hoechst 33342 dye (Thermo Scientific) was used. Stock solution (10 mg/mL) was diluted 1:2000 in PBS buffer and added to the protoplast. After 10 min of incubation in the dark, protoplasts were imaged directly in the staining solution using the DAPI filter set in addition to previously described settings used in BiFC for transiently transformed Arabidopsis protoplasts.

For the measurement of  $\text{Ca}^{2+}$ , R-GECO1 was excited with 561 nm, and spectral detection was set between 580-640 nm, and for chlorophyll fluorescence spectral detection was set between 647–725 nm. Samples were mounted for bottom imaging without a cover glass. The magnification 40X and the water immersion objective were used.

Image analysis was performed with Fiji imaging software (Schindelin et al., 2012).

## **2.15. Treatments**

### **2.15.1. Drought treatment**

Drought stress tolerance of WT plants, *JUB1-OX*, *jub1-kd*, and *KST1:JUB1-GFP* transgenic lines were assessed for ND (12-h light,  $120 \mu\text{mol m}^{-2} \text{s}^{-1}$ /12-h dark, 22 °C, and relative humidity of 60%/75%) grown 5-6-week-old plants. They were grown in small pots filled with an identical amount of soil. Before subjecting plants to the drought, stress pots were fully saturated with water till the point soil could not uptake more water, and subsequently, drought stress was applied by withholding water from two to 20 days unless otherwise indicated.

Five-week-old WT, *JUB1-OX*, and *jub1-kd* plants were subjected to drought stress by withholding water for five and nine days. The plants were harvested and frozen in liquid nitrogen, and the material was used for further analysis. Eight-week-old WT, *JUB1-OX*, and *jub1-kd* plants were subjected to severe drought stress by withholding water for 20 days, followed by re-watering for six days, and survival rates were calculated as a ratio between plants that exhibit recovery and have green leaves or stem and the total number of plants. Five-week-old WT and *KST1pro:JUB1-GFP* plants were subjected to water withhold for two and three days, and then the stomatal conductance was measured.

### **2.15.2. Salt treatment**

The WT, *JUB1-OX*, *CaM4-OX*, and *JUB1-OX/CaM4-OX* seedlings were grown on half MS medium under long-day conditions and then transferred to liquid MS medium 12 hours before treatment with 150 mM  $\text{NaCl}_2$  or  $\text{H}_2\text{O}$  (mock-treated plants). Flasks with seedlings were placed under long-day conditions on an orbital shaker (Heidolph, UNIMAX 2010) with continuous

shaking at around 80 rpm. After 72 hours of treatment, photos of the plant phenotype were taken.

### **2.16. Determination of proline levels**

Proline concentrations were determined as described in (Bates et al., 1973). Arabidopsis rosettes were freeze-dried in liquid nitrogen and ground using Grinding mill MM301. Approximately 50 mg of plant material were homogenized at room temperature in 3% (w/v) sulfosalicylic acid ( $5 \mu\text{L mg}^{-1}$  fresh weight) and centrifuged at 12,000 rpm for 15 min at room temperature (centrifuge 5427 R, Eppendorf). The sample supernatant, 100  $\mu\text{L}$  3% (w/v) sulfosalicylic acid, 200  $\mu\text{L}$  glacial acetic acid and 200  $\mu\text{L}$  2.5% (w/v) acid ninhydrin solution were incubated for 60 min at 96 °C followed by extraction with toluene: The absorbance of the chromophore containing toluene was measured at 520 nm, using pure toluene as a blank. Proline concentration was normalized to the fresh or dry weight in the water withhold experiments.

### **2.17. Determination of Relative Water Content (RWC)**

Plant material (five to eight leaves per genotype) was weighed (fresh weight, FW), then put in a glass tube containing deionized water, and kept at 4 °C overnight to obtain the turgid weight (TW). Subsequently, the leaves were dried in an oven at 70 °C for at least 48 h, and the dry weight was measured (DW). RWC was calculated as  $\text{RWC (\%)} = [(FW - DW)/(TW - DW)] \times 100$ .

### **2.18. Measurement of chlorophyll content**

Chlorophyll was extracted by treating 50 mg of frozen plant tissue with 500  $\mu\text{L}$  80% (v/v) acetone. Samples were vortexed and centrifuged at 12,000 rpm for 90 sec at room temperature. Spectrophotometric absorbance reads were performed at both 663.6 and 646.6 nm by spectrophotometer Jasco V-730 (JASCO Deutschland, Germany). The total chlorophyll content data were processed and calculated using Spectra Manager software available from the spectrophotometer. The data were normalized to fresh weight

### **2.19. Measurement of $\text{Ca}^{2+}$ level in leaves**

Leaves of approximately eight-week-old *R-GECO* plants were cut and glued on microscope slides at least 12 hours before imaging. A thin layer of medical adhesive glue was applied on the microscope slide, and the middle part of the leaf was fixed on the slide, with the lower leaf

surface facing the glass slide, and covered with an appropriate amount of plant measuring buffer (PMB): 5 mM KCL, 50  $\mu$ M CaCl<sub>2</sub>, 10 mM MES-Tris pH 5.6. The samples were left at a phytochamber overnight before imaging. To calculate the background signal, WT leaves from plants growing with *R-GECO* plants were prepared as described above and imaged.

### **2.20. GUS staining assay**

Two-week-old *JUB1pro:GUS* seedlings after incubation in - 1,2 MPa water potential imposed by PEG8000 (Polyethylene Glycol 8000, Carl Roth) for two days were submerged in a staining solution of 50 mM sodium phosphate buffer pH 7.0 (no pH adjustment is required), 0.1% (v/v) Triton X-100, 0.1 mM potassium ferricyanide, 0.1 mM potassium ferrocyanide, 1 mM Na<sub>2</sub>EDTA pH 8.0, 20% (v/v) methanol, and 0.5 mg mL<sup>-1</sup> 5-bromo-4-chloro-3-indolyl- $\beta$ -D-glucuronic acid (X-gluc; Duchefa Biochemie) and incubated at 37 °C in the dark overnight. Chlorophyll was removed by submerging the samples in 70% (v/v) ethanol. GUS staining was visualized and recorded by using a differential interference contrast microscope (BX51, Olympus).

### **2.21. DAB staining assay**

To detect the level of hydrogen peroxide (H<sub>2</sub>O<sub>2</sub>) an *in situ* DAB staining method was employed (3, 3'-diaminobenzidine, tetrahydrochloride; Sigma-Aldrich) (Fryer et al., 2002). Brown color staining resulting from DAB oxidization by H<sub>2</sub>O<sub>2</sub> was used to determine H<sub>2</sub>O<sub>2</sub> content. DAB (1 mg/mL) solution was prepared in distilled water. Three-week-old Arabidopsis seedlings were immersed in 50-mL Falcon tubes containing DAB solution and incubated at room temperature overnight. As DAB is sensitive to light, Falcon tubes were covered with aluminum foil during the treatment. To avoid auto-oxidation, the DAB solution was freshly prepared. After DAB staining, to remove chlorophyll for better imaging of stain, plants were incubated in 100% ethanol at 60°C for 2 hours.

### **2.22. Stomatal conductance**

Five-week-old WT and *KST1pro:JUB1-GFP* plants at the control condition, two and three days after water withhold, as well as six-week-old WT, *JUB1-OX*, and *jub1-kd* plants grown under well-watered (daily watering) conditions and drought stress for five days were taken for the analysis. The measurement was conducted 3-4 hours after dawn using the SC-1 Leaf Porometer (METER Environment Group) At least 10 measurements per genotype were taken, up to three leaves from each plant were taken for the measurement.

### **2.23. Statistical analysis**

Statistical analyses were performed using GraphPad Prism (GraphPad Software, San Diego, CA). Experimental data were analyzed with Student's *t*-test at  $P < 0.05$ .

### 3. RESULTS

#### 3.1. Overexpression of *JUB1* results in resistance to severe drought stress

The drought tolerance phenotype in *JUB1-OXs* was already reported for Arabidopsis, tomato, and banana (Ebrahimian-Motlagh et al., 2017; Tak et al., 2017; Thirumalaikumar et al., 2018). None of the previous studies on *JUB1* drought tolerance phenotype was conducted with plants treated under severe drought conditions or scored the plant's survival rates after subsequent re-watering.

We performed a severe stress experiment with five-week-old *JUB1-OX*, WT, and *jub1-kd* plants dehydrated for 20 days. At this point, the RWC was extremely low ( $\approx 20\%$ ). No significant difference between the genotypes was detected (**Figure 3.1A**).

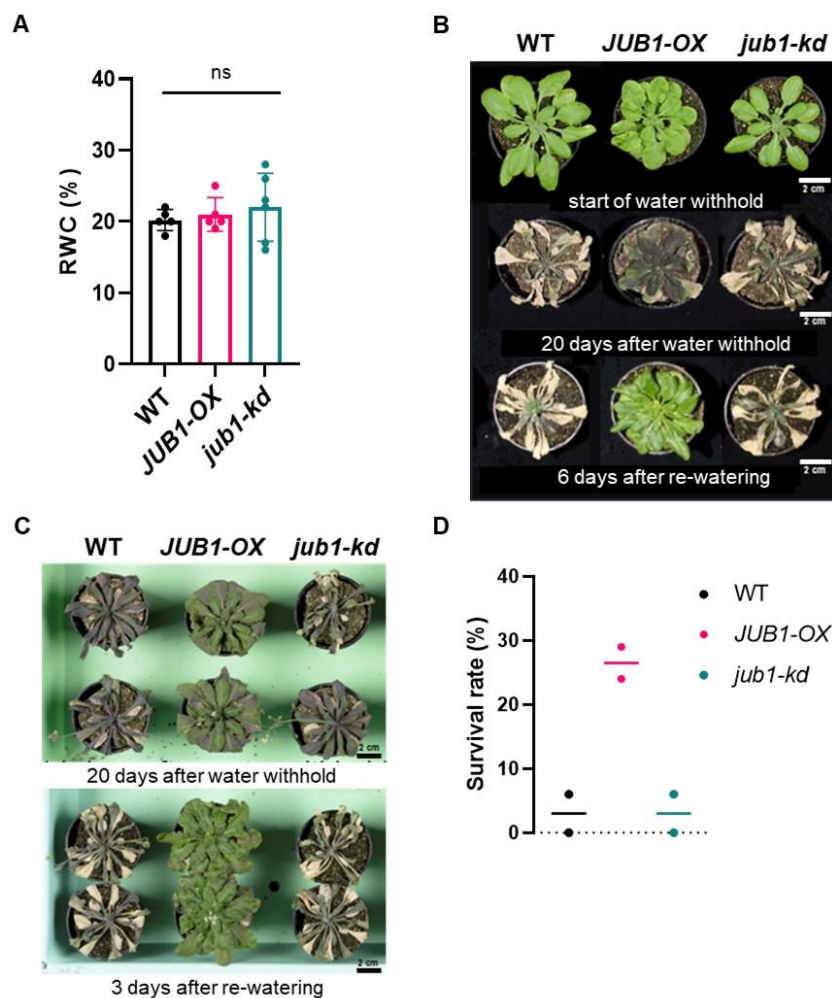


**Figure 3.1. *JUB1-OXs* plants are resistant to severe drought stress.** **A**, Relative water content (RWC) of leaves (%). Individual data points are shown with mean  $\pm$  s.d. for  $n = 5$  to 6 plants from one experiment. Ns, not significant. The experiment was repeated twice with similar results. **B**, Five-week-old *JUB1-OX*, WT, and *jub1-kd* plants at the start of water withhold, after 20 days of withholding water and six days after re-watering. Scale bar, 2 cm.

**C**, Seven-week-old WT, *JUB1-OX*, and *jub1-kd* plants were subjected to the drought stress by withholding water. Photos were taken after 14 days of water withhold and three days after re-watering. Scale bar, 2 cm. **D**, Survival rates (%) of WT, *JUB1-OX*, and *jub1-kd* plants after 20 days of withholding water and subsequent re-watering. Data points represent the percentage of plants counted as “survived” after re-watering for each genotype. The number of plants scored in each experiment is n = 7 to 35. The experiment was repeated twice with similar results.

Even though all plants were extremely dehydrated, *JUB1-OXs* plants recovered rapidly after re-watering. In contrast, WT and *jub1-kd* plants demonstrated their sensitivity to drought stress (**Figure 3.1B**). Moreover, after moderate drought stress *JUB1-OXs* showed rapid (already 3 days after re-watering) and complete recovery after re-watering distinct from the one observed for WT and *jub1-kd* plants (**Figure 3.1C**).

The increased survival rate of *JUB1-OXs* compared with the WT and *jub1-kd* in **Figure 3.1D** indicates that *JUB1-OX* mutants are resistant to severe drought stress (RWC  $\approx$  20%) and exhibit a better survival rate in comparison to the WT and *jub1-kd* plants.

### **3.2. Under control conditions, plants overexpressing *JUB1* accumulate a high level of proline**

Previous reports indicated a higher level of proline in plants overexpressing *JUB1* under ND control conditions (Wu et al., 2012; Thirumalaikumar et al., 2018). The metabolic profiles of Arabidopsis 35-day-old WT plants and *JUB1* overexpression lines under different promoters (*35S:JUB1* and *promRD29A:JUB1*) showed almost a two-fold change in the proline concentration between control and mutant plants. In the *promRD29A:JUB1* line *JUB1* is expressed under the control of the *RD29A* promoter, which shows induced activity in the presence of abiotic stress and only basal activity under control conditions (Wu et al., 2012). In tomato fruits, the proline concentration was 6- to 12-fold higher in *JUB-OXs* compared with WT plants (Shahnejat-Bushehri et al., 2017). However, it was not clear if the higher accumulation of proline in *JUB1-OXs* is related to any particular developmental stage. We measured proline concentration in 14-day-old seedlings grown on Murashige-Skoog agar medium containing 1% [w/v] sucrose under LD condition at 22 °C.

In 14-day-old seedlings of *JUB1-OXs* the proline concentration level was higher in comparison to the WT and *jub1-kd* plants (**Figure 3.2A**). When we measured proline concentration in 6-week-old plants, a significantly higher proline concentration was also detected for *JUB1-OX* compared with WT and *jub1-kd* (**Figure 3.2B**). No significant difference in proline levels was observed between WT and *jub1-kd*. This result can be explained by only a partial reduction of *JUB1* transcript level in *jub1-kd* mutants.

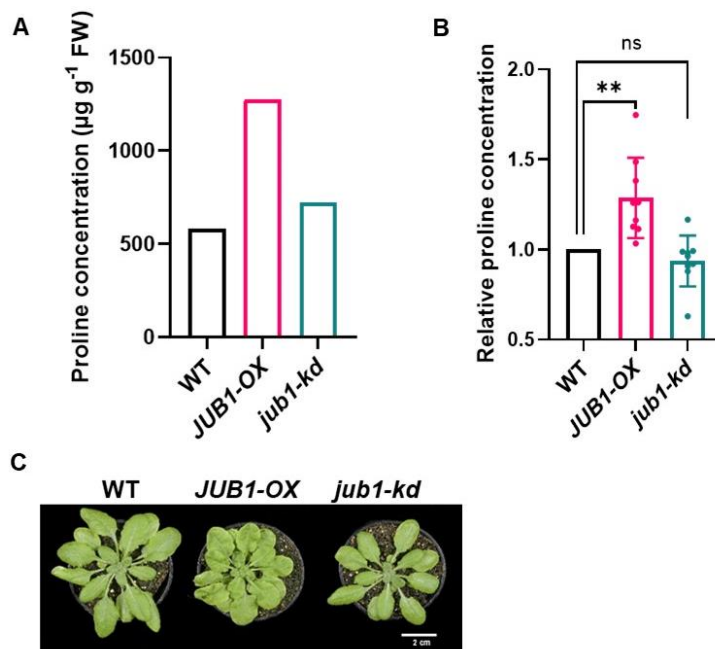


**Figure 3.2. Accumulation of proline under control conditions.** **A**, Proline concentration in 14-day-old seedlings of *JUB1-OX*, WT, and *jub1-kd* plants grown in half-strength solid MS medium. The pool of > 10 plants was harvested to do the measurements. The experiment was repeated twice with similar results. **B**, Relative proline concentration in six-week-old *JUB1-OX* and *jub1-kd* plants normalized to the WT. The WT is taken as a value of 1. The pool of three plants was harvested to do the measurements. Individual experiments are shown with mean  $\pm$  s.d. for  $n = 8$ . Asterisks represent statistically significant difference; Student's *t*-test (\*\* $p < 0.01$ ). n.s., not significant. **C**, The phenotype of six-week-old *JUB1-OX*, WT, and *jub1-kd* plants. Scale bar, 2 cm.

### 3.3. *JUB1-OXs* accumulate a high level of proline under drought conditions

A dramatic change in proline concentration upon water shortage is a known plant response to drought stress and was e.g. reported for *Arabidopsis*, *Oryza sativa*, *Pancreaticum maritimum*, *Ceratonia siliqua*, *Laurus nobilis*, *Myrtus communis*, and *Pinus halepensis* (Ibarra-Caballero et al., 1988; Szabados and Saviouré, 2010). Overexpression of *JUB1* in banana also leads to a higher proline level compared to the control plants under drought conditions. Moreover, transgenic banana lines could tolerate drought stress much better than the control plants (Tak et al., 2017).

To test whether overexpression of *JUB1* in *Arabidopsis* also leads to a higher level of proline under drought conditions, we subjected plants to drought stress by withholding water. After five days of drought stress, the decreased water potential symptoms in plants were only starting to occur, which was also supported by the RWC measurement (**Figure 3.3A,B**).

After 5 days of water withhold, we observed the tendency of increased proline concentration in *JUB1-OXs* mutants compared with the WT and *jub1-kd* plants (**Figure 3.3C-E**). Moreover,

*JUB1-OXs* exhibited a higher level of proline in comparison with WT and *jub1-kd* plants also after 9 days of water withhold (**Figure 3.3F**).

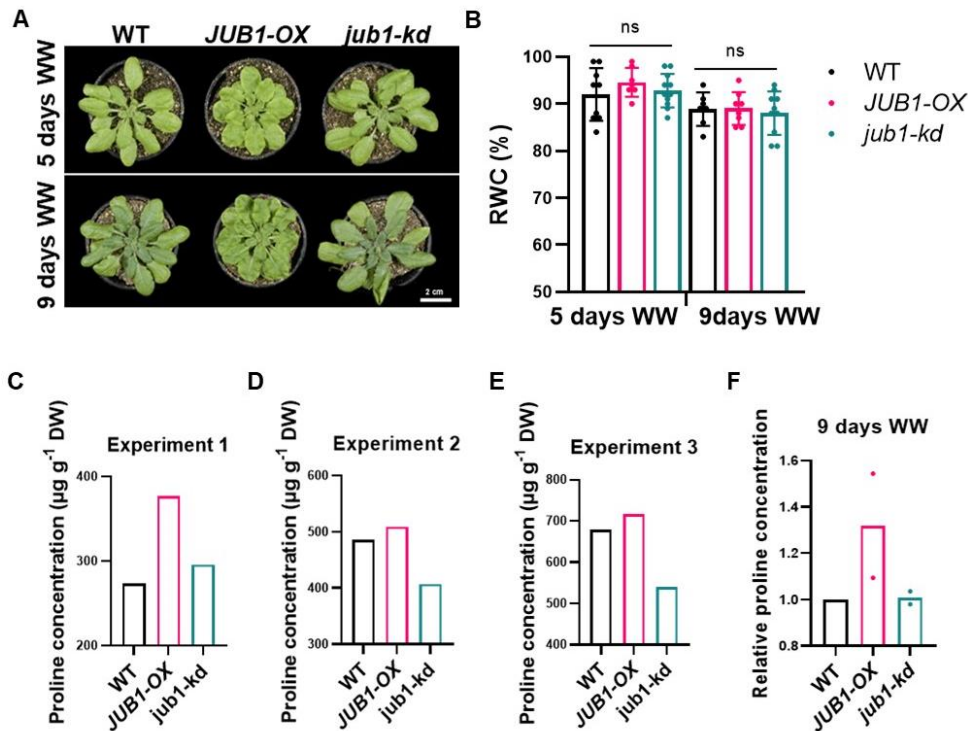


**Figure 3.3. Accumulation of proline under drought conditions.** **A**, Six-week-old *JUB1-OX*, WT, and *jub1-kd* plants after five and nine days of water withhold (WW). Scale bar, 2 cm. **B**, Relative water content (RWC) of leaves (%) in *JUB1-OX*, WT, and *jub1-kd* plants after five and nine days of water withhold (WW). Individual data points are shown with mean  $\pm$  s.d. for  $n = 7$  to 11 plants from one experiment. The experiment was repeated three times for five days water withhold and twice for nine days water with similar results. **C-E**, Proline concentration in six-week-old seedlings of *JUB1-OX*, WT, and *jub1-kd* plants after five days of water withhold normalized to the dry weight of the material. The pool of three plants was harvested to do the measurements. DW, dry weight. **F**, Relative proline concentration in six-week-old *JUB1-OX* and *jub1-kd* plants normalized to WT. The pool of three plants was harvested to do the measurements. Individual experiments are shown for  $n = 2$ .

### 3.4. Expression of proline metabolism genes is altered in *JUB1-OXs*

Microarray data previously obtained in our lab indicated that the expression profiles of some proline metabolism genes are altered in *JUB1-OX* plants. The *RD29A:JUB1*, *35S:JUB1*, and *JUB1-OE* lines are described in (Wu et al., 2012). The *PDH1* gene expression that is responsible for the rate-limiting step in proline degradation was downregulated in the *JUB1-OX* line and the estradiol inducible line *JUB1-IOE* (**Figure 3.4A**).

To study the expression profiles of proline metabolism genes under control and drought conditions, we performed a qRT-PCR analysis in *JUB1-OX*, *jub1-kd*, and WT seedlings (**Figure 3.4B-D**). Under control conditions, we observed a significant difference in the



transcript level for the genes that encode key proline enzymes like *P5CS1*, *PDH1*, and *PDH2* genes. In the case of *PDH1*, both *JUB1-OX* and *jub1-kd* lines show an opposite expression level under this condition. Under drought stress conditions that were imposed by water withhold for 5 days we also see a significant difference for *P5CS1* and *PDH2* genes. The downregulation or upregulation of the respective genes in *jub1-kd* could possibly also influence the levels of proline in this line. Also, the significantly lower transcript level of *PDH2* in *JUB1-OX* could contribute to the changes in proline degradation and be a reason for an increased level of proline in *JUB1-OX* also under drought conditions.

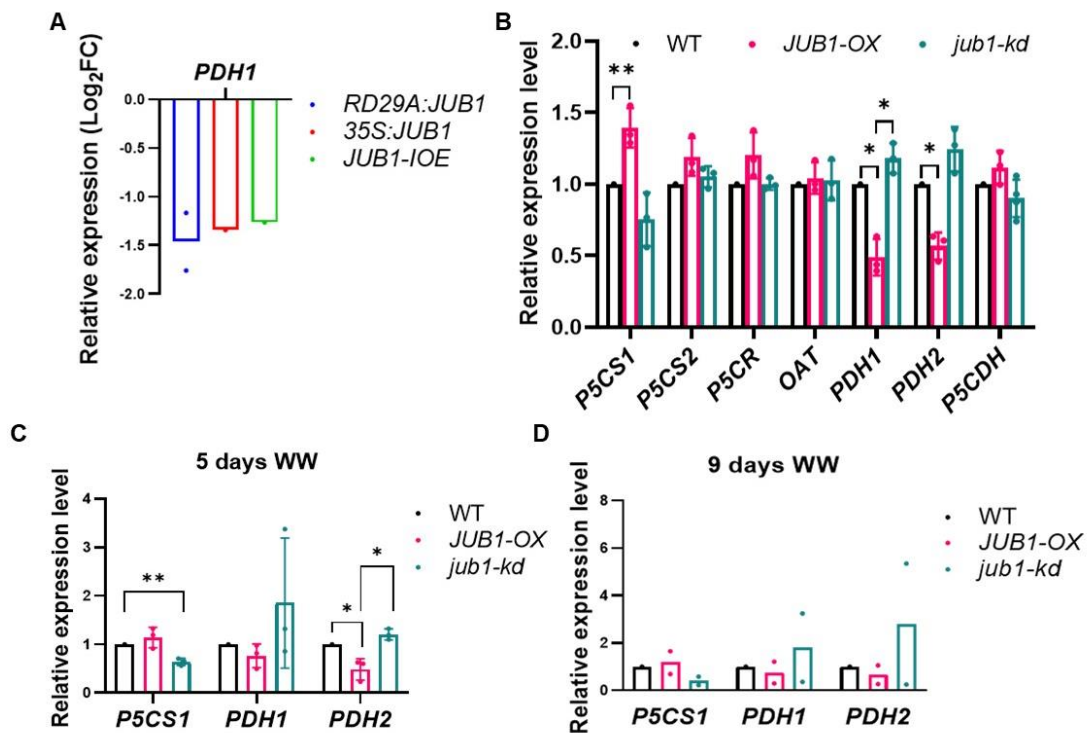


**Figure 3.4. Transcript levels of proline metabolism genes assessed using qRT-PCR. A,** Relative expression of *PDH1* in *RD29A:JUB1*, *35S:JUB1*, and *JUB1-OE* lines. Individual data points are shown for n = 1 to 2 pool of plants. **B,** Relative expression of proline metabolism genes under control conditions in six-week-old *JUB1-OX*, *jub1-kd*, and WT. The data was normalized to the WT. Individual data points are shown with mean  $\pm$  s.d. for n = 3 to 4. **C,** Relative expression of *P5CS1*, *PDH1*, *PDH2* after five days of water withhold (WW) in six-week-old *JUB1-OX*, *jub1-kd*, and WT. The data was normalized to the WT. Individual data points are shown with mean  $\pm$  s.d. for n = 3. **D,** Relative expression of *P5CS1*, *PDH1*, *PDH2* after nine days of water withhold (WW) in six-week-old *JUB1-OX*, *jub1-kd*, and WT. The data was normalized to WT. Individual data points are shown for n = 2. Primer sequences are given in **Supplemental Table S3**.

### 3.5. Identification of the putative downstream targets of JUB1 related to proline metabolism

To identify downstream targets transcriptionally regulated by JUB1, we first checked for JUB1 binding sites in the promoter regions of proline biosynthesis genes and other transcription factors reported to be involved in the regulation of proline metabolism. Looking at the promoter regions of *PDH2*, *MYB2*, and *bZIP63* genes, we identified the known JUB1 binding site “GCCGT” present in their sequence. Most of the binding site locations also corresponded to the area of the binding peak reported in the DNA affinity purification sequencing (DAP-seq) data (O’Malley et al., 2016). To study the possible protein-DNA interactions, we performed a yeast one-hybrid (Y1H) analysis using the promoter fragments of *PDH2*, *MYB2*, and *bZIP63* genes that contain the JUB1 binding site (**Figure 3.5A**). The yeast one-hybrid assay results indicate that JUB1 interacts with the promoters of *MYB2* and *bZIP63* which leads to the growth of yeast on selective medium (**Figure 3.5B**). One of the putative downstream targets of JUB1, proline degradation gene *PDH2*, showed a high autoactivation level, with strong growth of yeast cells on -L-H medium even at 80 mM 3-AT. In general, there is a high possibility of obtaining a false positive result if the autoactivation level was already high (Reece-Hoyes and Marian Walhout, 2012). Thus, for identifying a possible interaction between JUB1 and the promoter region of *PDH2*, we decided to use ChIP-qPCR as another method to study protein DNA interaction for this candidate (see below).

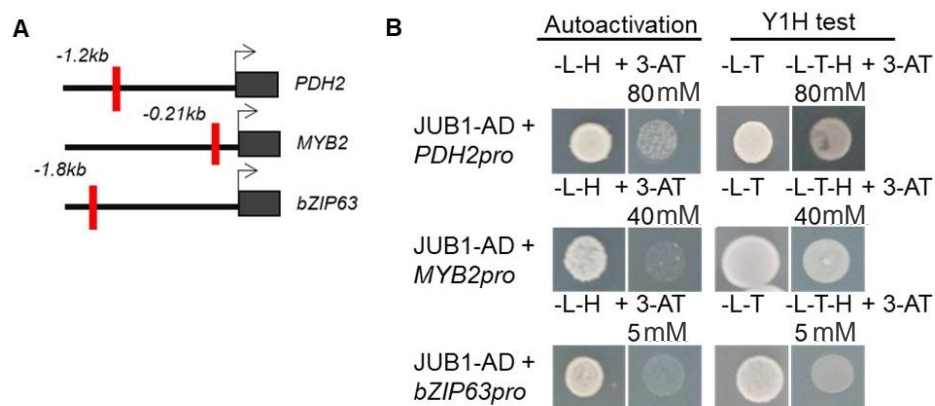


**Figure 3.5. JUB1 activates the promoters of *MYB2* and *bZIP63* in yeast.** **A**, JUB1 binding site in the promoter regions of *PDH2*, *MYB2*, *bZIP63* genes. The red box represents the position of the JUB1 binding site. **B**, Yeast-one-hybrid assay demonstrates the interaction between the promoter fragment of *MYB2*, *bZIP63* genes, and transcription factor JUB1. The promoter fragments containing a known JUB1 binding site up to 2 kb upstream of the translational start site (ATG). The size of the promoter fragments tested was: *PDH2* – 369 bp, *MYB2* – 283 bp, and *bZIP63* – 343 bp. The sequences of the used promoter regions are given in **Supplemental Figure S1**. Upon interaction of JUB1-GAL4AD fusion protein with the binding site, transcription of the yeast *HIS3* reporter gene is activated, and diploid yeast cells grow on SD

medium lacking the three essential amino acids Trp, Leu, and His (-T, -L, -H). 3-Amino-1,2,4-triazole (3-AT) is a competitive inhibitor of the product of the *HIS3* gene.

### 3.6. *bZIP63* is a downstream target of JUB1

Previously reported microarray data indicate that the expression of *bZIP63* is lower in *JUB1-OXs* lines than WT, similar to previously shown results for *PDH1*, which, in turn, is a target of *bZIP63* (Figure 3.6A). However, the relative expression level of the *bZIP63* gene under the control condition in the other experiment shows that *JUB1-OX* plants have higher expression levels of the *bZIP63* gene compared with WT plants (Figure 3.6B).

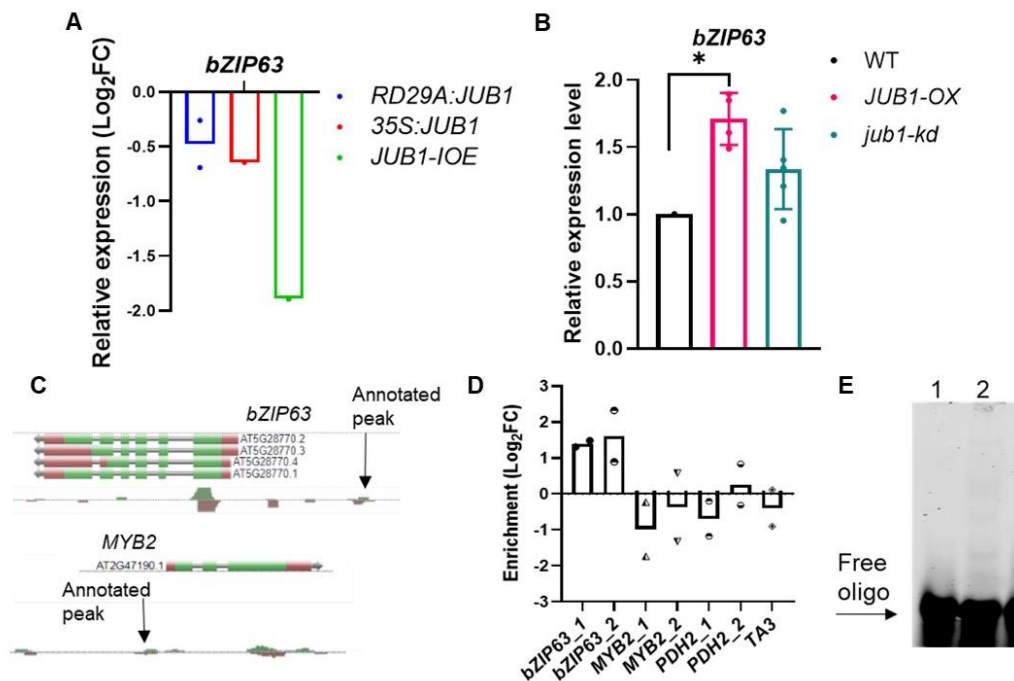


**Figure 3.6. *bZIP63* is a downstream target of JUB1.** **A**, Relative expression of *bZIP63* in *RD29A:JUB1*, *35S:JUB1*, and *JUB1-IOE* lines. Individual data points are shown with mean  $\pm$  s.d. for  $n = 1$  to 2. **B**, Relative expression of *bZIP63* under control conditions in six-week-old *JUB1-OX*, *jub1-kd*, and WT. The data was normalized to the WT. Individual data points are shown with mean  $\pm$  s.d. for  $n = 6$ . The primer sequence is given in **Supplemental Table S3**. **C**, The location of the JUB1 binding site on the *MYB2* and *bZIP63* promoter identified in the DAP-seq database. The location of the annotated peaks is shown with a black arrow and is taken from the DAP-seq website (O'Malley et al., 2016). **D**, ChIP-qPCR demonstrates the binding of JUB1-GFP to the *bZIP63* promoter. Four-week-old soil-grown *JUB1-OX* plants were harvested for ChIP. The Y-axis of ChIP-qPCR results shows enrichment of the *bZIP63* promoter region. Values were normalized to the values of *TA3* (*AT1G37110*), a transposable element gene lacking a JUB1 binding site, included as a negative control. Primer sequences are given in **Supplemental Table S5**. Individual data points are shown for  $n = 2$  from two experiments. FC, fold change. **E**, EMSA. Purified JUB1-GST does not bind to the JUB1 binding site within the *bZIP63* promoter. From left to right, 1<sup>st</sup> lane, labeled probe (5'-DY682-labeled double-stranded oligonucleotides); 2<sup>nd</sup> lane, labeled probe plus JUB1-GST protein. Oligonucleotides used for EMSA are given in **Supplemental Table S4**.

We have already confirmed that JUB1 interacts with the promoter region of *bZIP63* and *MYB2* in yeast (**Figure 3.5B**). Additionally, it was also reported that JUB1 binds to the *bZIP63* and *MYB2* promoters in the DAP-seq data (**Figure 3.6C**). In order to confirm the binding of JUB1 to the promoter region of *bZIP63*, *MYB2*, and *PDH2*, we performed a ChIP-qPCR experiment using *JUB1-OX* plants, where JUB1 was translationally fused to GFP (**Figure 3.6D**). Our ChIP-qPCR data indicate an enrichment only for *bZIP63* promoter regions. To confirm this result also using *in vitro* methods and to know if JUB1 binds physically and directly to the *bZIP63* promoter, we performed an EMSA. Surprisingly, we did not observe binding to the *bZIP63* probe by JUB1-GST fusion protein (**Figure 3.6E**). Taking into consideration previous data, we can conclude that JUB1 regulates *bZIP63*, but this regulation does not occur *via* direct physical binding of JUB1 to the promoter region of *bZIP63*. It is possible that JUB1 regulates *bZIP63* in a protein complex and is not necessarily itself bound to the promoter region of *bZIP63*.

### 3.7. JUB1 regulates accumulation of proline, possibly *via* *bZIP63*

It was previously reported that *bZIP63-OX* plants accumulate a lower proline concentration than WT plants (Mair et al., 2015). In order to analyze if the higher concentration of proline in the *JUB1-OX* plants is caused by the repression of proline degradation gene *PDH1* *via* *bZIP63*, we generated a *bZIP63-OX* line and a double overexpressor *bZIP63-OX/JUB1-OX* line, where *bZIP63* is translationally fused to RFP. The screening for transgenic *bZIP63-OX* lines was conducted using a confocal microscope. Indeed, the RFP signal was detected in *bZIP63-OX* (**Figure 3.7A**).

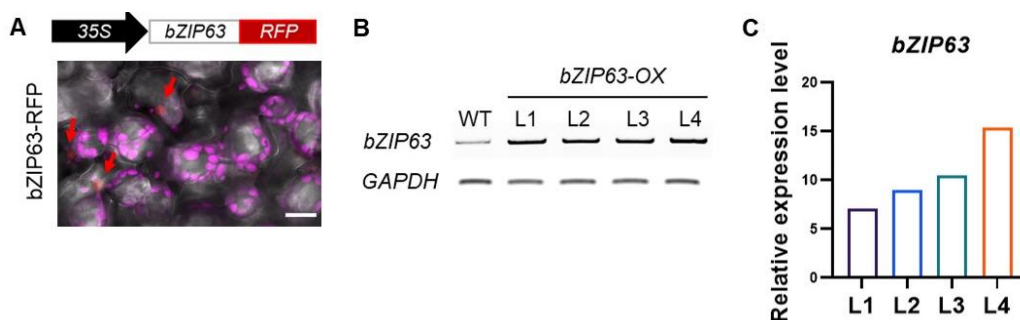


**Figure 3.7. Characterization of *bZIP63-OX* lines.** **A**, Scheme of the construct. Confocal microscope analysis showing *bZIP63-RFP* localization indicated with red arrowheads. Chlorophyll fluorescence is shown in magenta colour. Scale bar, 15  $\mu$ m. **B**, Expression levels of *bZIP63* in *bZIP63-OX* (L1-L4) mutant and WT analyzed by semi-quantitative RT-PCR. The housekeeping gene *GAPDH* (*AT1G13440*) was used as a control. Size of the PCR products for *bZIP63* – 945 bp, *GAPDH* – 217 bp. **C**, Relative expression of *bZIP63* in *bZIP63-OX* (L1-L4) mutant normalized to *bZIP63* expression in WT. Primer sequences are given in **Supplemental Table S3**.

The RFP signal was localized to the nucleus as expected for a transcription factor. We also confirmed the strongest lines by end-point PCR (**Figure 3.7B**), where all of the selected lines have a visibly stronger *bZIP63* band in comparison with WT, which indicates a higher level of *bZIP63* transcript in these lines, which was also then confirmed by qRT-PCR (**Figure 3.7C**). Next, we plan to select positive double overexpressor *bZIP63-OX/JUB1-OX* transgenic lines and test the proline concentration in these lines and their performance under drought stress conditions.

### 3.8. *JUB1-OXs* exhibit a lower stomatal conductance

The effect of water shortage on stomatal conductance is linked to other essential responses such as transpiration and photosynthetic rates. In addition to osmotic adjustment upon drought stress, plant protection mechanisms might also involve regulation of the stomatal aperture, leading to the preservation of high water potential in plants. In general, stomatal conductance is higher when stomata open wider and *vice versa* (Giménez et al., 2013). Our preliminary data suggested that *JUB1* might be involved in stomata regulation, as *JUB1-OX* plants exhibit a higher leaf temperature in comparison to WT plants (**Figure 3.8A**).

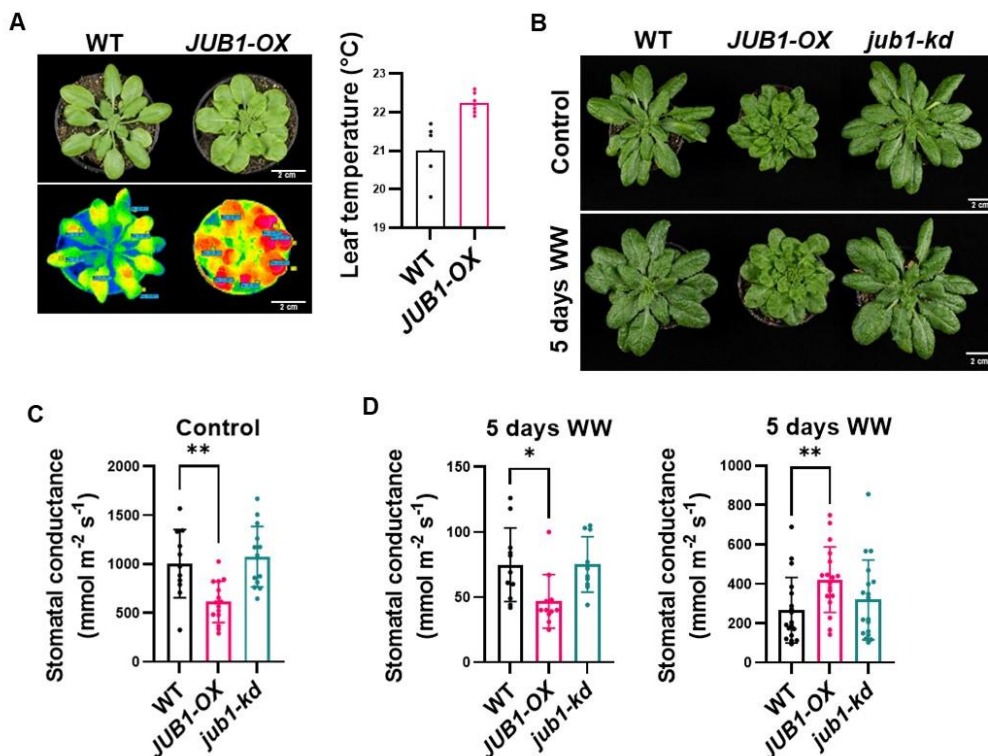


**Figure 3.8. Stomatal conductance in *JUB1-OX*, *jub1-kd*, and WT plants.** **A**, Left panel, a thermal image of six-week-old plants grown under control conditions. Right panel, the temperature points (°C) representing the leaf temperature in WT and *JUB1-OX* plants. **B**, Seven-week-old *JUB1-OX*, WT, and *jub1-kd* plants under control conditions and after 5 days of water withhold (WW). Scale bar, 2 cm. **C**, Stomatal conductance in seven-week-old plants



grown under control conditions. Individual data points are shown with mean  $\pm$  s.d. for  $n = 12$  to 15 leaves. The experiment was repeated three times with similar results. **D**, Stomatal conductance in seven-week-old plants subjected to water stress by withholding water for five days. Individual data points are shown with mean  $\pm$  s.d. for  $n = 10$  to 18 leaves. The experiment was repeated twice with opposite results for *JUB1-OXs* plants. In C-D, asterisks represent statistically significant difference; Student's *t*-test (\* $p < 0.05$ ; \*\* $p < 0.01$ ).

A higher leaf temperature can indicate changes in the stomatal conductance (Giménez et al., 2013; Schymanski et al., 2013; Urban et al., 2017). To study this hypothesis and examine whether or not a regulation of the stomata could contribute to the *JUB1* drought tolerance phenotype, we measured stomatal conductance in *JUB1-OX*, *jub1-kd*, and WT plants under control and drought conditions using a leaf porometer. The plant phenotype at the point of stomatal conductance measurement is shown in **Figure 3.8B**. Interestingly, stomatal conductance was significantly lower in *JUB1-OX* in comparison to WT and *jub1-kd* at control conditions (**Figure 3.8C**).

After 5 days of water withhold the stomatal conductance in *JUB1-OX*, *jub1-kd*, and WT plants showed high variation for the *JUB1-OX* plants. While in the first experiment, *JUB1-OX* plants had the lowest stomatal conductance, their stomatal conductance was the highest in the second experiment (**Figure 3.8D**). Due to the contradicting results in these two experiments, further investigation and repetition of the experiment are needed to investigate the changes in the stomatal conductance in *JUB1-OX*, *jub1-kd*, and WT plants also under drought conditions.

However, the altered stomatal conductance confirmed under control conditions in *JUB1-OX* might be explained either by a defective stomatal aperture or a defective stomatal development. Next to study this hypothesis we plan to look at the stomata of each genotype and measure the stomatal density and stomatal aperture.

### **3.9. Expression of *JUB1* under guard-cell specific promoter *KST1* does not alter drought tolerance**

In tomato, an exclusive overexpression of DELLAs in guard cells is sufficient to promote stomatal closure (Nir et al., 2017). Data from our lab indicate that *JUB1* activates *DELLA* genes and triggers *DELLA* accumulation in Arabidopsis (Shahnejat-Bushehri et al., 2016). We postulate that *JUB1* promotes drought tolerance at least partially by the accumulation of *DELLA* proteins in guard cells and by the regulation of stomatal closure. To test this hypothesis, we first checked if *JUB1* is expressed in the guard cells using publicly available data. In **Figure 3.9A**, microarray data indicates that *JUB1* is expressed in guard cells three

hours after treatment with ABA (Winter et al., 2007). Also, data from the Genevestigator database demonstrate that the expression level of *JUB1* in guard cells is similar to another transcription factor, *MYB61*, which has been reported to be expressed in guard cells and to regulate stomatal movement (Figure 3.9B).

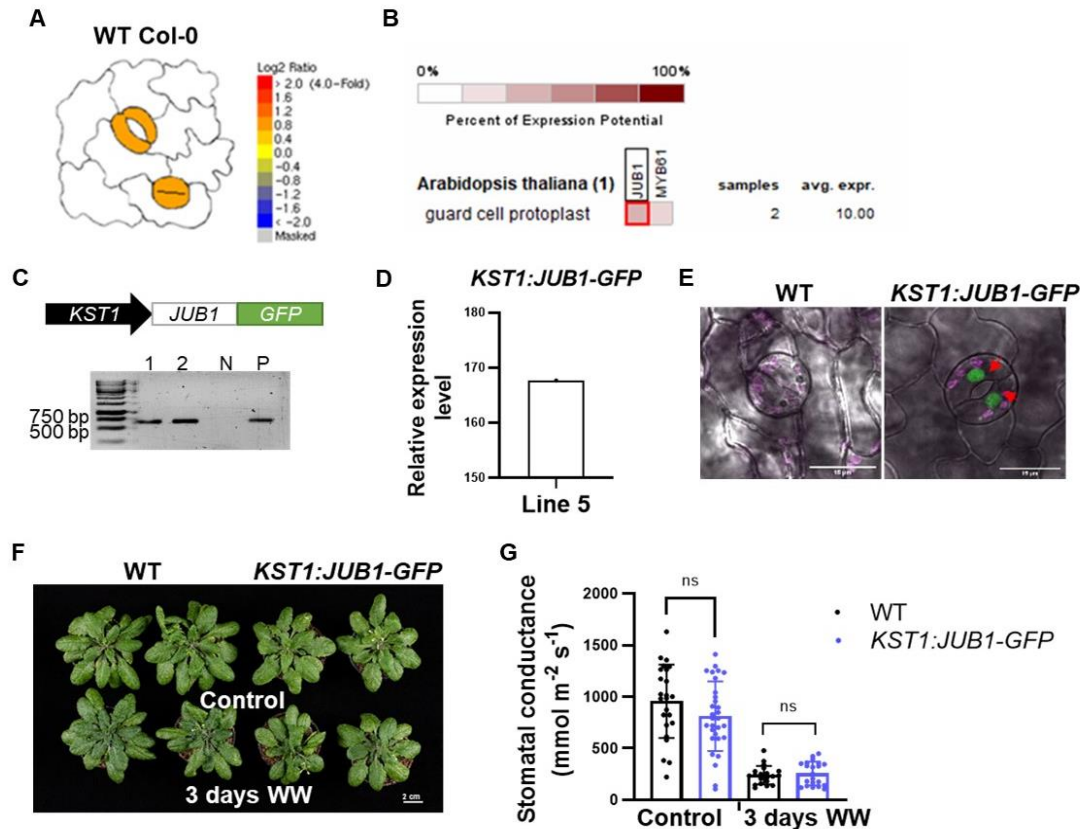


**Figure 3.9. Expression of *JUB1* under a guard-cell specific promoter.** **A**, The expression level of *JUB1* in the guard cells of 5-week-old *Arabidopsis thaliana* plants after treatment with 50  $\mu\text{M}$  ABA for 3 hours ( $n = 3$ ). Data retrieved from the Arabidopsis eFP Browser (Waese et al., 2017). **B**, Potential expression of *JUB1* and *MYB61* in guard cell protoplast of 5 to 6-week-old *Arabidopsis thaliana* from ABA-treated and control-treated plants ( $n = 2$ ). Data retrieved from Genevestigator (Zimmermann et al., 2004). **C**, A scheme of the *KST1pro:JUB1-GFP* construct. Agarose gel picture shows PCR genotyping for *KST1pro:JUB1-GFP* line. Line 1 and line 2 show transgenic *KST1pro:JUB1-GFP* lines with expected size 684 bp. N, negative control, *A. thaliana* Col-0 DNA. P, positive control, *Solanum tuberosum* DNA. Primer sequences are given in **Supplemental Table S1**. **D**, Relative expression level of *GFP* in five-week-old *KST1pro:JUB1-GFP* plants normalized to WT. Individual data point is shown for  $n = 1$ . The primer sequence is given in **Supplemental Table S3**. **E**, Confocal microscope analysis showing guard cells of WT and *KST1pro:JUB1-GFP* line. Arrows indicate *JUB1-GFP* localized in the guard cell in *KST1pro:JUB1-GFP* line. Scale bar, 15  $\mu\text{m}$ . **F**, Seven-week-old WT, and *KST1pro:JUB1-GFP* plants under control conditions and three days after water withhold. Scale bar, 2 cm. **G**, Stomatal conductance in seven-week-old WT and *KST1pro:JUB1-GFP* plants at the control condition and 3 days after water withhold. Stomatal conductance was measured using a leaf porometer 3-4 hours after dawn. Individual data points are shown with mean  $\pm$  s.d. for  $n = 21$  to 30 leaves. The experiment was repeated three times with similar results.

Next, we tested if the cell-specific expression of *JUB1* can affect drought tolerance. We overexpressed *JUB1* under the control of a partial segment of the potato (*Solanum tuberosum*) *KST1* promoter previously shown to confer expression in guard cells (Mueller-Roeber and Pical, 2002; Kelly et al., 2017). The T1 seedlings of *proKST1:JUB1-GFP* were genotyped using *KST1* primers (Figure 3.9C) and the qRT-PCR analysis was performed to detect the expression of *GFP* in the transgenic lines, to see the level of expression for only GFP-fused *JUB1*, without endogenous expression of *JUB1* (Figure 3.9D). A GFP signal in the nucleus of guard cells was confirmed using a confocal microscope (Figure 3.9E). Next, we subjected 5-week-old plants to water withhold for three days (Figure 3.9F). We did not observe any visible phenotypical difference between WT and *KST1:JUB1-GFP* plants at this stage after water withhold. Moreover, we did not detect any significant difference in stomatal conductance between these lines, neither under control nor under drought conditions (Figure 3.9G). These data indicate that overexpression of *JUB1* in guard cells is not sufficient to promote drought tolerance or alter stomatal conductance.

### 3.10. Abiotic stress tolerance phenotype of *JUB1* overexpressors might depend on the direct induction of *DREB2A*

Previously we identified that *JUB1* directly regulates the expression of *DREB2A*, which also activates many responsive TFs involved in drought and heat stress responses (Wu et al., 2012). However, if the drought tolerance phenotype of *JUB1-OX* solely depends on the direct induction of the *DREB2A* gene or/and on the subsequent induction of other drought- and stress-related genes that can reduce the intracellular level of reactive oxygen species, it is still a matter of investigation. To answer this question, we generated *JUB1-OX/dreb2a-2* plants (Figure 3.10A).

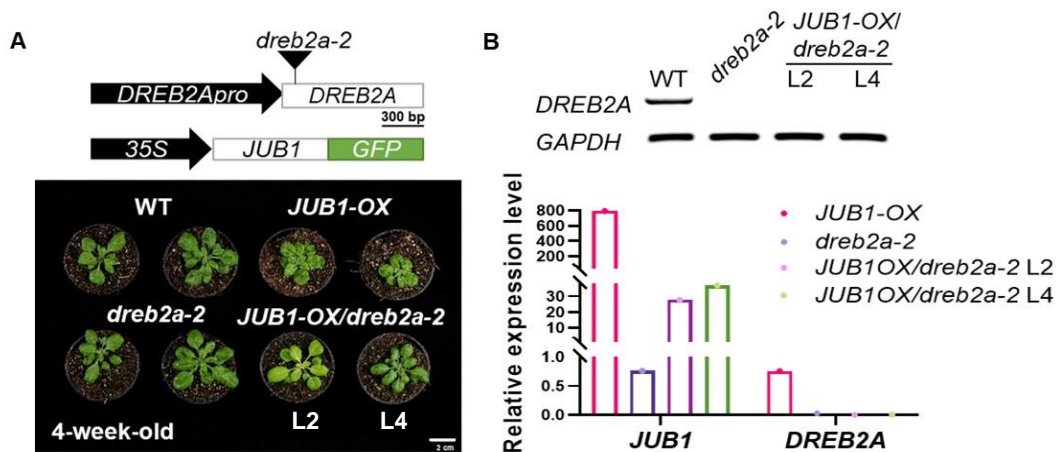


**Figure 3.10. Characterization of *JUB1-OX/dreb2a-2* line.** A, Upper panel, a scheme of the *Arabidopsis DREB2A* gene with the positions of the T-DNA insertions (not to scale). A scheme



of the *35S::JUB1-GFP* construct. Lower panel, four-week-old WT, *JUB1-OX*, and *JUB1-OX/dreb2a-2* (L2 – line 2 and L4 – line 4), and *dreb2a-2* plants under LD control conditions. Scale bar, 2 cm. **B**, Upper panel, Expression levels of *DREB2A* in *dreb2a-2* and *JUB1-OX/dreb2a-2* (L2 – line 2 and L4 – line 4) mutants and WT analyzed by semi-quantitative RT-PCR. The housekeeping gene *GAPDH* (*AT1G13440*) was used as a control. The size of the PCR product for *DREB2A* – 1008 bp, *GAPDH* – 217 bp. Lower panel, relative expression of *JUB1* and *DREB2A* in two-week-old WT, *JUB1-OX*, *dreb2a-2* and *JUB1-OX/dreb2a-2* (L2 – line 2 and L4 - line4) mutants normalized to expression in WT (n = 1). Primer sequences are given in **Supplemental Table S3**.

Next, a drought experiment using generated *JUB1-OX/dreb2a-2* (L2 - line2 and L4 - line4) lines and *JUB1-OX* plants was conducted (**Figure 3.11A**).



**Figure 3.11. Drought tolerance phenotype of *JUB1-OX/dreb2a-2* plants.** Phenotype of WT, *JUB1-OX*, *JUB1-OX/dreb2a-2* (L2 - line2 and L4 - line4) and *dreb2a-2* plants under control conditions at five and six weeks, and after withholding water (WW) for 7 days, 10 days and 14 days, and 4 days after subsequent re-watering (RW). Photoperiod: neutral day 12h/12h. Scale bar, 2 cm.

Our preliminary data indicate that *dreb2a-2* plants show susceptibility to drought stress. We observed stronger wilting symptoms in *dreb2a-2* plants compared to the WT after 10 days of water withhold. Nevertheless, *dreb2a-2* plants show recovery 4 days after re-watering, similar

to WT. The drought stress phenotype of *JUB1-OX/dreb2a-2* appears to be weaker than the phenotype observed in single *JUB1-OX* plants. Moreover, *JUB1-OX/dreb2a-2* also showed a weaker phenotype 4 days after re-watering in comparison to *JUB1-OX* plants.

### 3.11. Characterization of *jub1* *crispr* line

Until now, no *jub1* knockout plants were reported in the literature. To generate such lines, we employed CRISPR/Cas9-mediated genome editing, using an egg cell-specific promoter to drive the expression of the *Cas9* gene. sgRNAs employed in the genome editing construct were designed to introduce a deletion in the *JUB1* coding sequence. The lines obtained were genotyped by PCR using *JUB1* primers that anneal to the *JUB1* promoter close to the ATG site and the *JUB1* coding sequence near the stop codon. The PCR product was then subjected to Sanger sequencing to confirm the deletion in the *JUB1* gDNA in *jub1* *crispr* plants (**Figure 3.12A,B**). *JUB1* expression in positive lines was detected by end-point PCR, where the *JUB1* transcript in *jub1* *crispr* has a lower size band compared with the *JUB1* transcript in WT plants. The size of the obtained band in *jub1* *crispr* corresponds to the predicted size after deletion of the region between the two sgRNAs (**Figure 3.12C**). Homozygous *jub1* *crispr* knockout plants (T3 generation) showed no obvious difference in their developmental phenotype in terms of rosette area compared to WT at different developmental stages in plants grown under short-day conditions (**Figure 3.12D,E**).

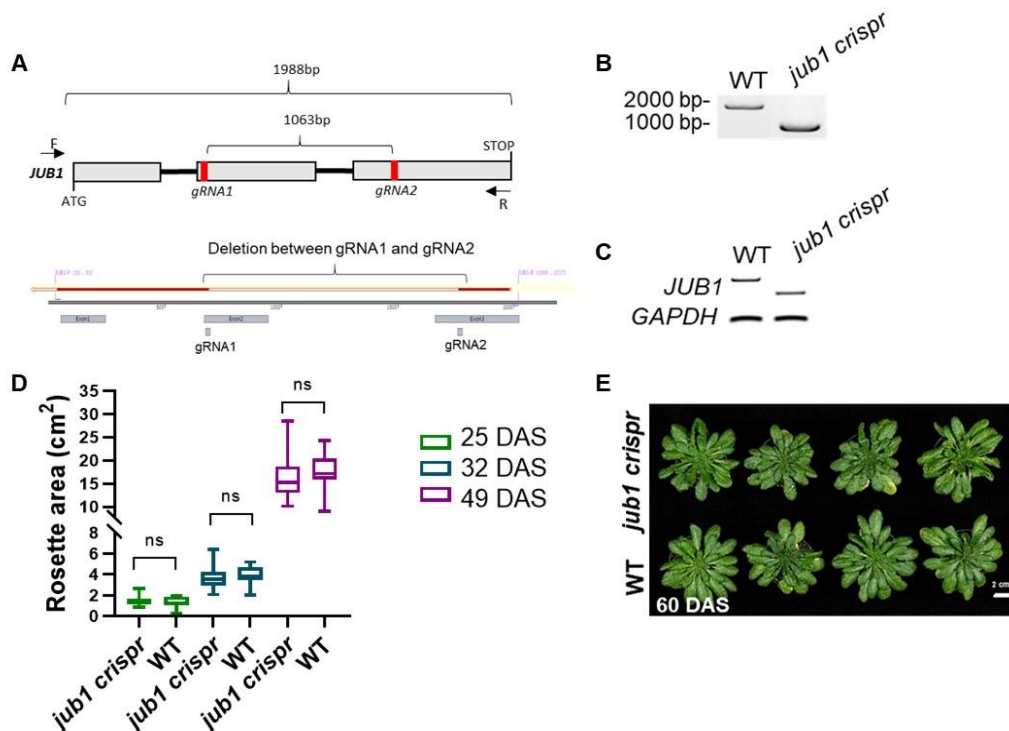


**Figure 3.12. Characterization of *jub1* *crispr* line.** **A**, Upper panel, schematic diagram of the sgRNAs location (red boxes) used for CRISPR/Cas9 genome-editing of the *JUB1* gene. ATG,

the start of the translation; F and R, primers used for genotyping transgenic lines. The primer binding sites are shown with arrows. Lower panel, the sequencing results of the *JUB1* gene. The aligned fragment of the *JUB1* gene in *jub1 crispr* plant is in red. **B**, Agarose gel picture showing PCR products obtained by genotyping for *jub1 crispr* plants. In WT, the *JUB1* fragment has an expected size of 1988 bp, and in transgenic *jub1 crispr* lines the expected size of the fragment is 925 bp. Primer sequences are given in **Supplemental Table S1**. **C**, Expression levels of *JUB1* in WT and *jub1 crispr* mutant analyzed by end-point PCR. The housekeeping gene *GAPDH* (*AT1G13440*) was used as control. Sizes of the PCR products are as follows: *JUB1* – 828 bp; *JUB1* in *jub1 crispr* – 443 bp; *GAPDH* – 217 bp. Primer sequences are given in **Supplemental Table S2**. **D**, Quantification of the rosette area in *jub1 crispr* and WT plants 25, 32, and 49 days after sowing (DAS). Data represent means  $\pm$  s.d. (n = 12-30). **E**, Eight-week-old *jub1 crispr* and WT plants grown under short-day conditions (SD). Scale bar, 2 cm.

### 3.12. Identification of proteins interacting with JUB1

None of the previous studies on JUB1's regulatory network focused on identifying proteins interacting with JUB1 and studying their roles. To identify possible protein-protein interactions, a yeast two-hybrid (Y2H) analysis was conducted by Next Interactions, Inc. The initial screen was performed with JUB1 protein as a bait, excluding its 16 amino acid-long N-terminal peptide which triggered a high self-activation level, and an *A. thaliana* cDNA library. We found 76 hits with BlastN (nucleotide) and 80 hits with BlastX (protein) databases. As JUB1 is a transcription factor and localized in the nucleus, we were particularly interested in identifying interaction partners that are also localized in the nucleus. We used a subcellular localization database for Arabidopsis proteins to determine the subcellular localization of the putative interactors (SUBA, <https://suba.live/>). Out of 79 proteins (one of the proteins was not presented in the database), 15 were predicted to be localized in the nucleus. It was previously reported that JUB1 is a transcription factor that confers tolerance to many stresses, such as salt, drought, and heat stresses (Wu et al., 2012; Tak et al., 2017; Thirumalaikumar et al., 2018; Alshareef et al., 2019). Among the 15 proteins predicted to be localized in the nucleus, CaM1 and CaM4 were also reported to regulate many plant stress responses, such as freezing tolerance, salt tolerance, and to play a role in the control of senescence. Since *CaM1.1* and *CaM4.1* encode the same protein present in both BlastN and BlastX lists and were reported to be involved in the response to the same stresses as JUB1, we decided to focus our further studies on these proteins.

### 3.13. Localization analysis of CaM1 and CaM4 proteins

A co-localization signal indicates the proximity of the two proteins of interest, suggesting interactions between them. Localization studies for CaM1 and CaM4 were previously reported

only for *Nicotiana benthamiana* using the transient infiltration method (Zhou et al., 2016; Chu et al., 2018). Considering *Arabidopsis* as a native host to express both proteins, we decided to perform a co-localization analysis in *Arabidopsis thaliana* protoplast. Col-0 protoplasts were co-transfected with *35S:JUB1-GFP* and *35S:CaM1-RFP* or *35S:CaM4-RFP*. GFP and RFP fluorescence signals were imaged 24 hours after protoplast transfection. We observed very specific coinciding GFP and RFP signals in the nucleus (**Figure 3.13A**). To demonstrate that the expression of *CaM1* and *CaM4* under their native promoters does not change the localization of the proteins, we co-transfected Col-0 protoplasts with *CaM1pro:CaM1-RFP* or *CaM4pro:CaM4-RFP* (**Figure 3.13B**).

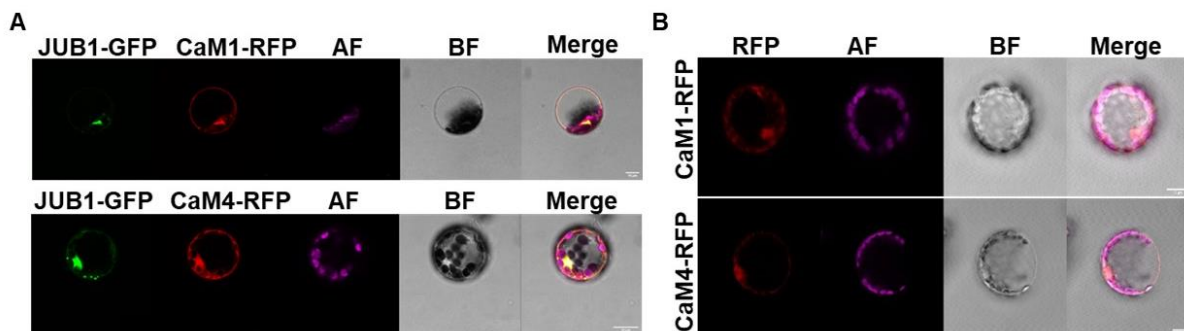


**Figure 3.13. Localization analysis of CaM1 and CaM4 proteins.** **A**, Confocal images of subcellular localization of JUB1-GFP and CaM1-RFP or CaM4-RFP in *Arabidopsis thaliana* protoplasts 24 hours after transfection. AF, chlorophyll autofluorescence; BF, bright field. Scale bar, 15  $\mu$ m. **B**, Confocal images of subcellular localization of CaM1pro:CaM1-RFP and CaM4pro:CaM4-RFP in *Arabidopsis thaliana* protoplasts 24 hours after transfection. AF, chlorophyll autofluorescence; BF, bright field. Scale bar, 15  $\mu$ m.

Similar to expression under constitutive promoter, under native promoter CaM1 and CaM4 proteins have nuclear and cytosolic subcellular localization in the *A. thaliana* protoplasts. Our data confirmed previous reports indicating that CaM1/CaM4 protein is localized in the nucleus and cytosol. These results suggest that JUB1 is co-localized with CaM1 and CaM4 proteins *in planta* in the nucleus but not in the cytosol of *Arabidopsis thaliana* protoplasts.

### 3.14. Expression analysis of *CaM1* and *CaM4* genes

Previous studies showed that *JUB1* is strongly induced during senescence and different abiotic stresses (Wu et al., 2012). In order to understand the biological role of the JUB1 and CaM4 protein interaction, we decided to determine the conditions when both genes are expressed.

Thus, an analysis of publicly available microarray data was conducted. *CaM1* and *CaM4* genes have similar expression levels in most of the tissues (**Supplemental Figure S2,S3**), with the exception that *CaM1* is highly expressed in pollen and *CaM4* is highly expressed in dry seeds



and during the last stages of embryo development. The data from the ePlant browser (<http://bar.utoronto.ca/eplant/>) also show that expression of *CaM1* and *CaM4* is increasing during natural aging, similar to *JUB1* expression (**Figure 3.14A**).

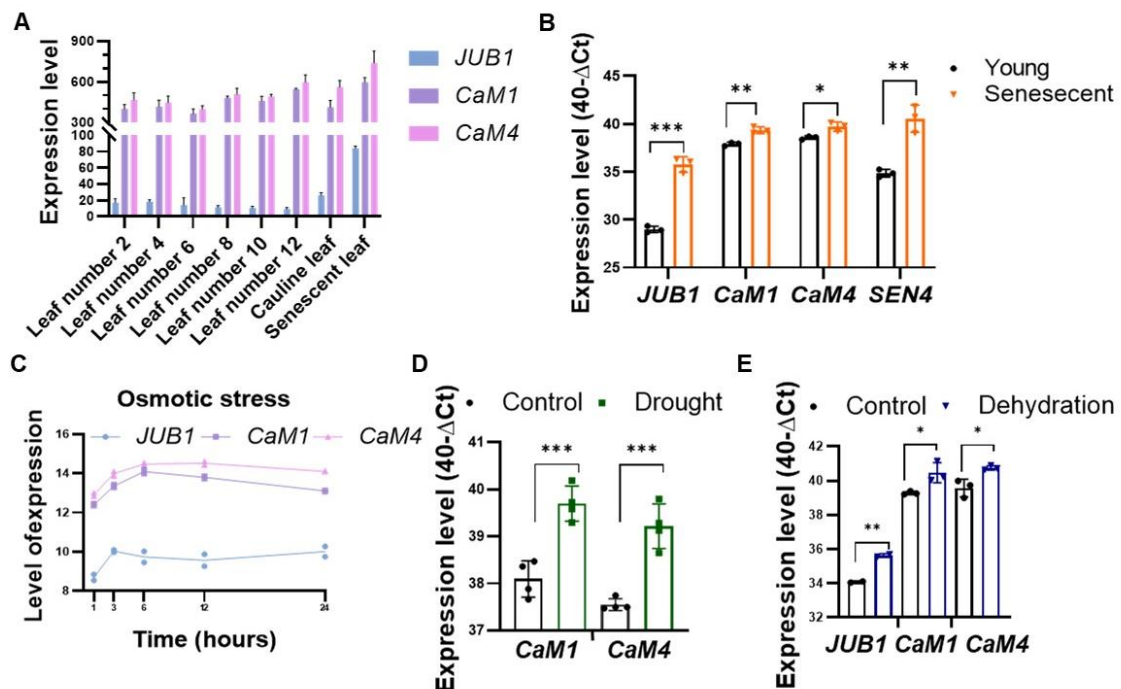


**Figure 3.14. Expression analysis of *CaM1* and *CaM4* genes.** **A**, Expression level of *JUB1*, *CaM1*, and *CaM4* in different leaves of *Arabidopsis thaliana*. Data generated by Affymetrix ATH1 arrays were normalized using the GCOS method, TGT value of 100. The data are shown with mean  $\pm$  s.d. for  $n = 3$ . Data were retrieved from the Arabidopsis eFP Browser (Waese et al., 2017). **B**, Expression level of *JUB1*, *CaM1*, and *CaM4* in young and senescent leaves of *Arabidopsis thaliana* in six-week-old WT plants; *SEN4* is used as a senescence-marker gene. Individual data points are shown with mean  $\pm$  s.d. for  $n = 3$ . **C**, Expression level of *JUB1*, *CaM1*, *CaM4* in 16 DAS Col-0 plants after 1, 3, 6, 12, and 24 hours after treatment with 300 mM mannitol added to the media. Individual data points are shown with mean  $\pm$  s.d. for  $n = 2$ . Data retrieved from Genevestigator. Experiment ID: AT-00120 (Zimmermann et al., 2004). **D**, Expression level of *JUB1*, *CaM1*, and *CaM4* genes in rosette leaves of four-week-old *Arabidopsis thaliana* plants under control condition and after nine days of water withhold. Individual data points are shown with mean  $\pm$  s.d. for  $n = 3$ . **E**, Expression level of *CaM1* and *CaM4* genes in rosette leaves of four-week-old *Arabidopsis thaliana* plants under control condition and after 3 hours of dehydration. Individual data points are shown with mean  $\pm$  s.d. for  $n = 3$ . In **B**, **D**, **E** asterisks represent statistically significant difference; Student's *t*-test (\* $p < 0.05$ ; \*\* $p < 0.01$ ; \*\*\* $p < 0.001$ ). Primer sequences are given in **Supplemental Table S3**.

To confirm the ePlant browser data, we conducted a similar experiment during natural plant aging (**Figure 3.14B**). The expression level of both *CaM1* and *CaM4* genes is induced during natural aging, as well as the expression level of *JUB1*. We also found that upon osmotic stress, the expression of all three genes is upregulated already 3 hours after the treatment and remains elevated 24 hours after the start of the treatment (**Figure 3.14C**).

Until now, no studies on the response of *CaM1* or *CaM4* to drought stress were reported. To test whether or not the transcript levels of *CaM1* and *CaM4* are induced by drought stress, we performed a qRT-PCR analysis using *CaM1* and *CaM4* primers (**Supplemental Table S2**). The expression levels of both *CaM1* and *CaM4* genes are induced upon drought stress compared to the control conditions (**Figure 3.14D**). We also observed increases in *CaM1*, *CaM4*, and *JUB1* expression 3 hours after dehydration stress (**Figure 3.14E**). These data indicate that *JUB1*, *CaM1*, and *CaM4* have increased expression levels, which overlap during natural senescence, and also during some other stresses.

### 3.15. JUB1 interacts with CaM1 and CaM4 proteins

To confirm the interaction between JUB1 and CAM proteins observed in yeast and to prove that the proteins co-localize and interact *in planta*, we conducted bimolecular fluorescence complementation (BiFC) assays in *Arabidopsis* protoplasts. The full-length CaM1 and CaM4 proteins were translationally fused to the cYFP part together with an HA-tag, while JUB1 was translationally fused to the nYFP part together with a Myc-tag. Col-0 protoplasts were co-transfected with *JUB1* and *CaM1* or *CaM4* constructs. Reconstitution of the YFP signal was observed in protoplasts 24 hours after transfection (**Figure 3.15A**).

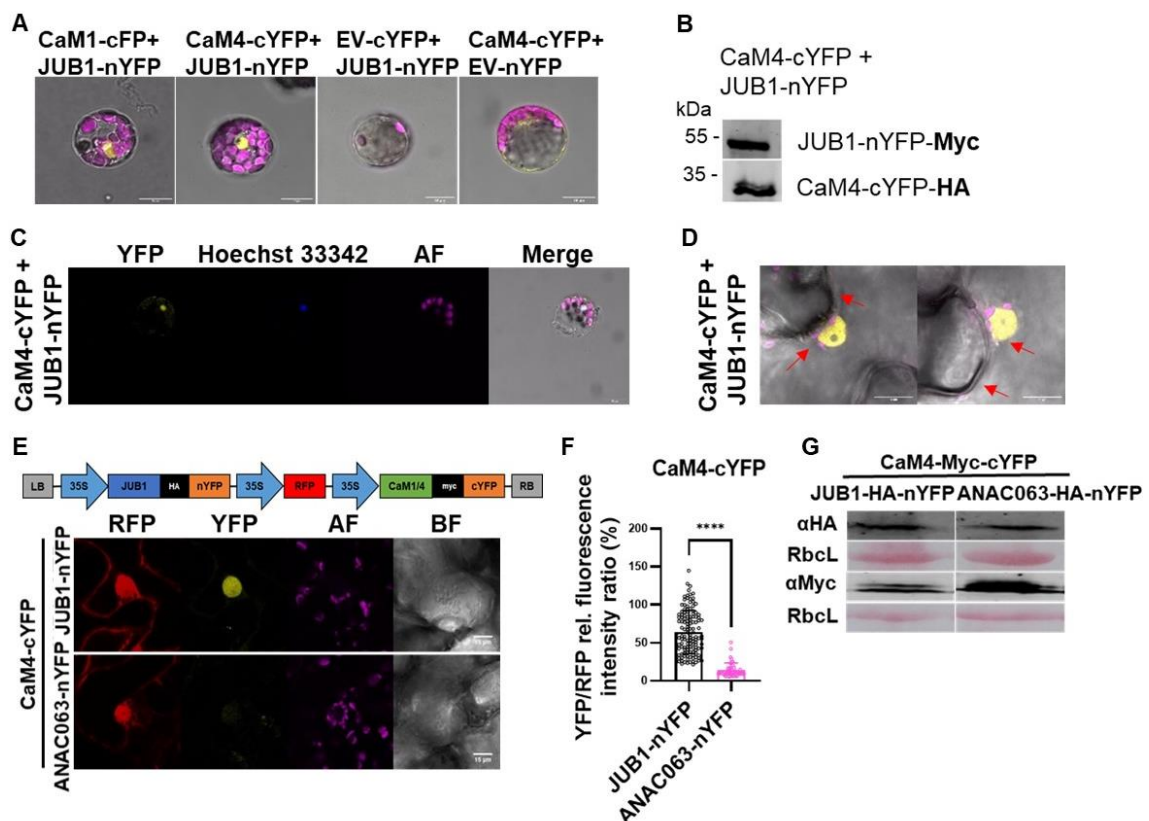


**Figure 3.15. CaM1 and CaM4 interact with JUB1.** A, Confocal images of BiFC in *Arabidopsis thaliana* protoplasts 24 hours after transfection. YFP fluorescence is reconstituted

when CaM1-cYFP or CaM4-cYFP are co-expressed with JUB1-nYFP. AF, chlorophyll autofluorescence. Scale bar, 15  $\mu$ m. **B**, Immunoblot analysis of protoplasts co-expressing JUB1 and CaM4 proteins in the BiFC assay, using  $\alpha$ Myc- and  $\alpha$ HA-antibodies. Expected molecular weights of JUB1-nYFP-Myc - 52 kDa and of CaM4-cYFP-HA - 29 kDa. **C**, Confocal images of *Arabidopsis thaliana* protoplasts expressing CaM4-cYFP and JUB1-nYFP, stained with nucleus staining dye (Hoechst 33342) 24 hours after transfection. AF, chlorophyll autofluorescence. Scale bar, 15  $\mu$ m. **D**, Image of a nucleus of a *Nicotiana benthamiana* epidermal cell. The picture shows the localization of the BiFC signal in the nucleus but not in the cytosol (shown with arrows). Scale bar, 15  $\mu$ m. **E**, Confocal images of BiFC signal in *Nicotiana benthamiana* leaves expressing CaM4-cYFP and JUB1-nYFP, or ANAC063-nYFP. ANAC063 was used as a negative control. Scale bar, 15  $\mu$ m. **F**, Quantification of the mean fluorescence ratioed against RFP from the nucleus of *Nicotiana benthamiana* with CaM4-cYFP and JUB1-nYFP or ANAC063-nYFP. Individual data points from three experiments are shown with mean  $\pm$  s.d. for  $n > 45$  and \*\*\*\* $P < 0.0001$  by Student's *t*-test. **G**, Immunoblot analysis of transformed *Nicotiana benthamiana* leaves co-expressing JUB1 or ANAC063 and CaM4 in the BiFC assay.  $\alpha$ Myc- and  $\alpha$ HA-antibodies were used as a primary antibodies; the expected molecular weights of JUB1-nYFP-Myc - 53 kDa; ANAC063-nYFP-Myc, and CaM4-cYFP-HA - 30 kDa. RbcL, ribulose-1,5-bisphosphate carboxylase/oxygenase large subunit (loading control). KDa, kilodalton. The membrane was stained with Ponceau S for loading control.

We also verified by western blot using  $\alpha$ Myc and  $\alpha$ HA antibodies that both proteins are expressed in protoplasts and have similar expression levels (**Figure 3.15B**). Since *CaM1.1* and *CaM4.1* encode proteins with identical amino acid sequences, all further experiments were performed with constructs involving the *CaM4* CDS, unless otherwise stated. To determine the subcellular localization of the YFP signal, we used the nuclei staining dye Hoechst 33342. Colocalization of the YFP fluorescence and Hoechst 33342 dye indicates that the two proteins colocalize in Arabidopsis protoplast nucleus (**Figure 3.15C**). We also verified by western blot using  $\alpha$ Myc- and  $\alpha$ HA-antibodies that both proteins are expressed in protoplasts and have similar expression levels. To supplement the BiFC data with a quantitative read-out of the fluorescence signal, we used the 2-in-12in1 cloning system (Grefen and Blatt, 2012). In that approach, both proteins are simultaneously cloned into a single vector which encodes a fluorescent marker for the expression control ratiometric analysis. In this system RFP is expressed under the control of the *35S* promoter and serves as a positive control for transiently transformed cells and for the quantitative analysis of the protein-protein interaction. The nYFP and cYFP parts together with a Myc-tag or an HA-tag, respectively, were translationally fused to the C-terminal parts of the JUB1 and CaM4 protein. To confirm that the interaction of JUB1 with CaM4 is specific, we tested another protein of the NAC transcription factor family (i.e., ANAC063) as a negative control for JUB1. The corresponding constructs were transiently infiltrated into the leaves of 5-week-old *Nicotiana benthamiana* plants and the reconstituted

YFP signal was visualized, together with RFP signal as an internal fluorescent marker, using a confocal microscope 72 hours after infiltration. In **Figure 3.15D**, *N. benthamiana* cells express internal RFP signals for both constructs in the nucleus and cytosol. The reconstitution of the YFP signal were observed only in cells infiltrated with the JUB1 CaM4 construct; Only a low background YFP signal was observed for the ANAC063-CaM4 construct used as a negative control. An image of the nucleus of tobacco cells shows that the YFP signal is localized to the nucleus with low intensity detected in the cytosol (**Figure 3.15E**). These data additionally indicate that the interaction between JUB1 and CaM4 proteins occurs in the nucleus. As seen in **Figure 3.15F**, relative fluorescence intensity ratio was quantified using the mean of fluorescence ratio YFP against RFP signal. We also verified by western blot using  $\alpha$ Myc- and  $\alpha$ HA-antibodies that the ANAC063-CaM4 construct was expressed after infiltration (**Figure 3.15G**). In summary, our data indicate that CaM4 does not interact with random NAC TF in a non-specific manner and that the association with JUB1 is specific.

### **3.16. Identification of CaM-binding sites in the JUB1 protein**

To determine putative CaM-binding sites in the JUB1 protein, we employed the Calmodulin Target Database (<http://calcium.uhnres.utoronto.ca/ctdb/ctdb/home.html>). The search for the potential calmodulin-binding sites predicted three sites (**Figure 3.16A**). The one with the highest normalized score is located within the DNA binding domain NAC sub-domain D of JUB1. It was previously reported that bulky hydrophobic amino acids at the first and last position of the binding sites are essential for binding of CaMs to their protein targets (La Verde et al., 2018). After assessing the motifs localized in the predicted binding site, we decided to substitute Leu at position 121 with Ala, and the second construct with substitutions in position L117 and L125 (**Figure 3.16B**). In this way, most of the motifs would be disrupted. We generated two JUB1 variants with mutations in their coding sequences that would lead to an amino acid substitution, such as JUB1 L121A, where L121 is substituted by Ala, and JUB1 L117A, L235A, where L117 and L125 are substituted by Ala. The data presented below were generated in the construct harboring mutation JUB1 L121A. To test whether the Leu substitution affects the JUB1-CaM4 interaction, we performed a quantitative BiFC analysis. Seventy-two hours after transient infiltration of *Nicotiana benthamiana* leaves, we observed a reconstituted YFP signal and an internal RFP signal in all protein pairs (JUB1-CaM4 and JUB1 L121A-CaM4) (**Figure 3.16C**). Quantification of the mean fluorescence ratioed YFP against RFP (**Figure 3.16D**) revealed no significant difference between mutated JUB1 protein compared to non-mutated JUB1 protein. We also performed western blot analysis with  $\alpha$ Myc-



and  $\alpha$ HA-antibodies to confirm that both proteins are expressed after the infiltration (**Figure 3.16E**). Surprisingly, the introduced mutation did not abolish or decrease the protein interaction.

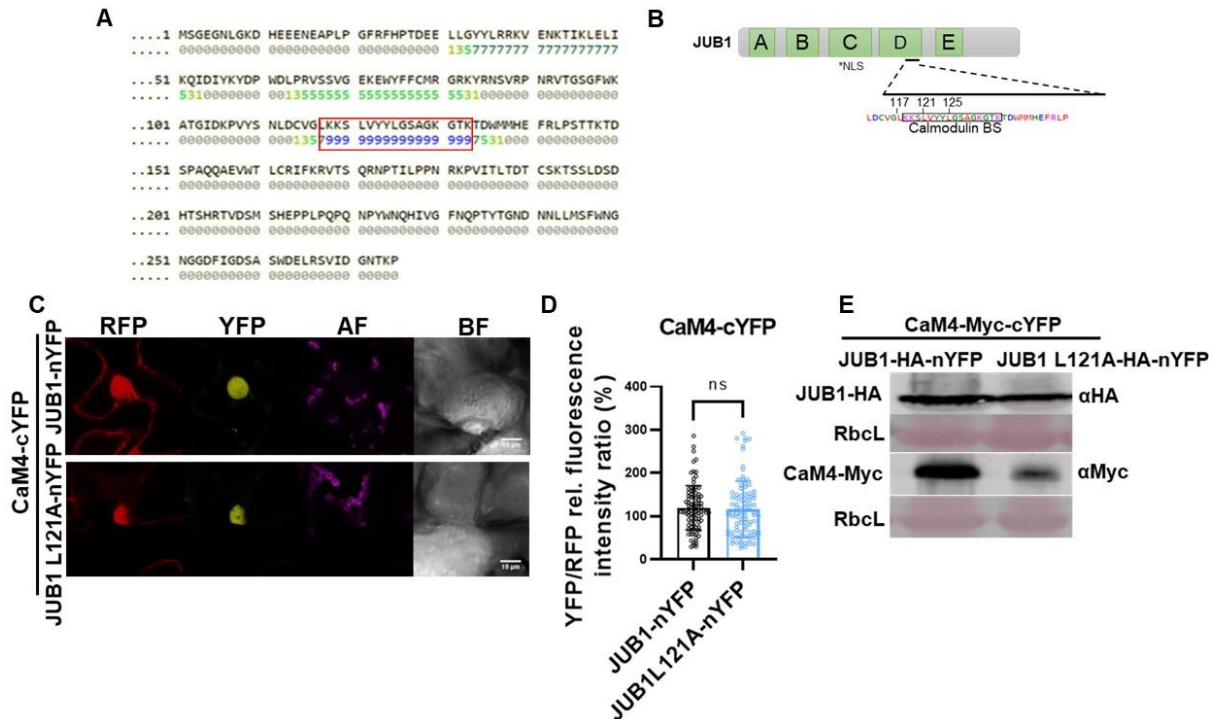


**Figure 3.16. Several CaM-binding sites present in the JUB1 protein.** **A**, JUB1 protein with identified potential CaM binding sites. The most likely binding site in a given sequence is highlighted as a series of 9s. The red box indicates the CaM binding site located in the DNA binding domain of the JUB1 protein. The numbers at the beginning of the sequence indicate the amino acid residue number. **B**, The scheme of the JUB1 protein with mutated amino acids in the calmodulin-binding site (BS). A, B, C, D, E, NAC sub-domains; BS, binding site; NLS, nuclear localization signal; 117, 121, 125, positions of mutated Leu amino acid. **C**, Confocal images of BiFC signal in *Nicotiana benthamiana* leaves 72 hours after infiltration with CaM4-cYFP and JUB1-nYFP or JUB1 L121A-nYFP. AF, chlorophyll autofluorescence; BF, bright field. Scale bar, 15  $\mu$ m. **D**, Quantification of the mean fluorescence ratioed against RFP in the nucleus of *Nicotiana benthamiana* with CaM4-cYFP and JUB1-nYFP or JUB1 L121A-nYFP. Individual data points from three experiments are shown with mean  $\pm$  s.d. for  $n > 90$ . **E**, Immunoblot analysis of transformed *Nicotiana benthamiana* leaves co-expressing CaM4 and mutated JUB1 in the BiFC assay.  $\alpha$ Myc- and  $\alpha$ HA-antibodies were used as a primary antibodies; the expected molecular weights of JUB1-nYFP-HA, JUB1 L121A-HA-nYFP - 53 kDa, and CaM4-Myc-cYFP - 30 kDa. RbcL, ribulose-1,5-bisphosphate carboxylase/oxygenase large subunit (loading control). KDa, kilodalton. The membrane was stained with Ponceau S for loading control.

To unravel whether the mutated (predicted) CaM binding site in JUB1 is functional, we decided to include split JUB1 protein constructs. Since the predicted calmodulin-binding site is located at the N-terminal part of the JUB1 protein, we generated constructs that have only the *JUB1*<sub>Nterm</sub> region (amino acids 1-144) or the *JUB1*<sub>Cterm</sub> region (amino acids 136-275) (**Figure 3.17A**).

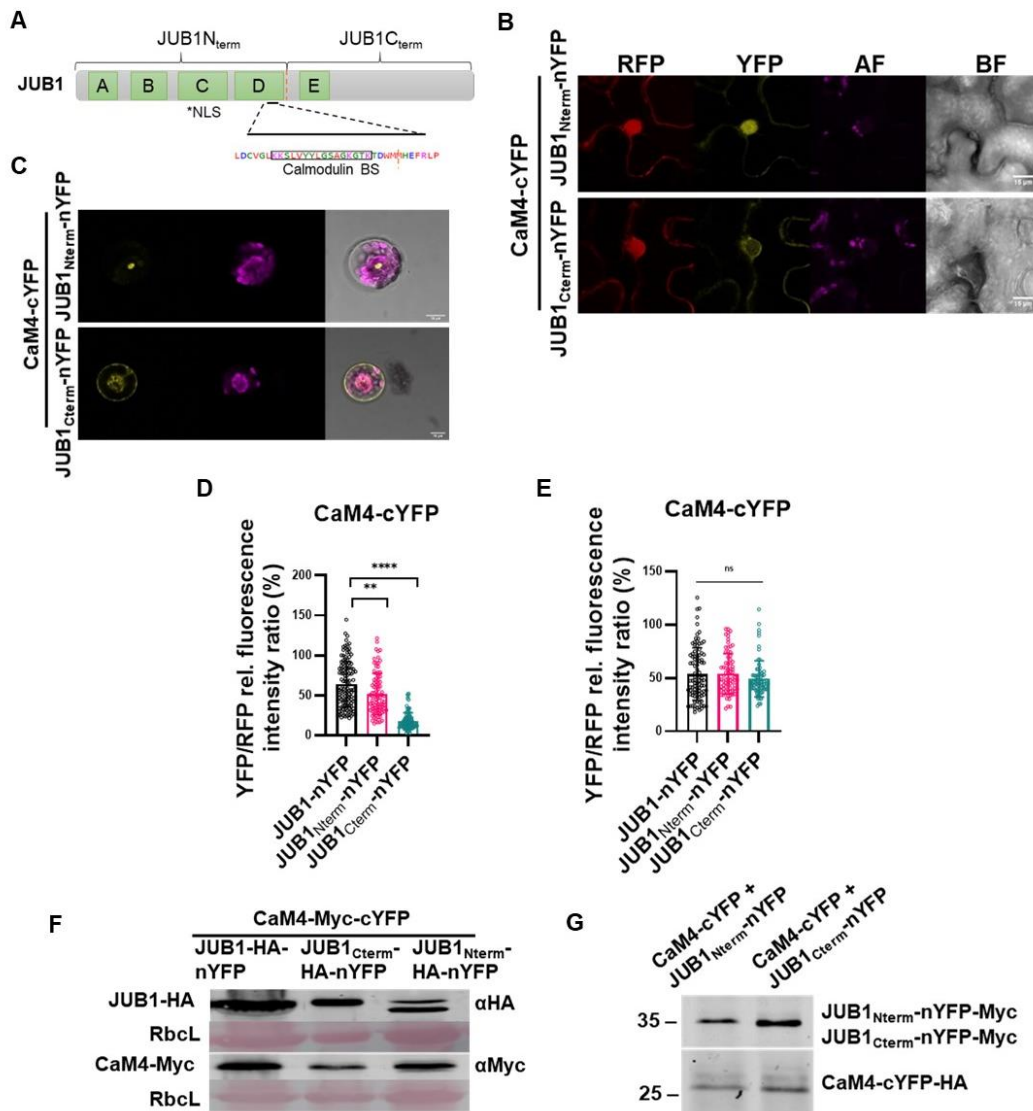


**Figure 3.17. JUB1 has calmodulin-binding sites in both the N- and C-terminal parts of the protein.** **A**, A scheme of the *JUB1* constructs that have only *JUB1*<sub>Nterm</sub> region (amino acids 1-144) or *JUB1*<sub>Cterm</sub> region (amino acids 136-275). A,B,C,D,E, NAC sub-domains; BS, binding site; NLS, nuclear localization signal. **B**, Confocal images of BiFC signal in *Nicotiana benthamiana* leaves 72 hours after infiltration, expressing CaM4-cYFP and *JUB1*<sub>Nterm</sub>-nYFP or *JUB1*<sub>Cterm</sub>-nYFP. AF, chlorophyll autofluorescence; BF, bright field. Scale bar, 15  $\mu$ m. **C**, Confocal images of BiFC signal in *Arabidopsis thaliana* protoplasts 24 hours after transfection. YFP fluorescence is reconstituted in the nucleus when CaM4-cYFP is co-expressed with *JUB1*<sub>Nterm</sub>-nYFP but not with *JUB1*<sub>Cterm</sub>-nYFP. AF, chlorophyll autofluorescence. Scale bar, 15  $\mu$ m. **D**, Quantification of the mean fluorescence ratioed against RFP calculated in the nucleus of *Nicotiana benthamiana* after infiltration with CaM4-cYFP and *JUB1*<sub>Nterm</sub>-nYFP or *JUB1*<sub>Cterm</sub>-nYFP. Individual data points from three experiments are shown with mean  $\pm$  s.d. for  $n > 95$  and  $**P < 0.01$   $****P < 0.0001$  by Student's *t*-test. **E**, Quantification of the mean fluorescence ratioed against RFP calculated in the nucleus and cytosol of *Nicotiana benthamiana* after infiltration with CaM4-cYFP and *JUB1*<sub>Nterm</sub>-nYFP or *JUB1*<sub>Cterm</sub>-nYFP. Individual data points from three experiments are shown with mean  $\pm$  s.d. for  $n > 95$ . NS, not significant. **F**, Immunoblot analysis of transformed *Nicotiana benthamiana* leaves co-expressing *JUB1* and CaM4 in the BiFC assay.  $\alpha$ Myc- and  $\alpha$ HA- antibodies were used as a primary antibodies; the expected molecular weights of *JUB1*<sub>Nterm</sub>-HA-nYFP– 38 kDa, *JUB1*<sub>Cterm</sub>-HA -nYFP– 37 kDa, and of CaM4-Myc-cYFP– 30 kDa. RbcL, ribulose-1,5-

bisphosphate carboxylase/oxygenase large subunit (loading control). kDa, kilodalton. The membrane was stained with Ponceau S for loading control. **G**, Immunoblot analysis of transfected protoplasts co-expressing JUB1 and CaM4 in the BiFC assay.  $\alpha$ Myc- and  $\alpha$ HA-antibodies were used as a primary antibodies; the expected molecular weights of JUB1<sub>Nterm</sub>-nYFP-Myc – 36 kDa, JUB1<sub>Cterm</sub>-nYFP-Myc – 35 kDa, and for CaM4-cYFP-HA – 29 kDa. kDa, kilodalton.

The JUB1<sub>Nterm</sub> or JUB1<sub>Cterm</sub> were translationally fused to nYFP+HA-tag, whereas CaM4 was fused to cYFP+Myc-tag. Seventy-two hours after transient infiltration of *Nicotiana benthamiana* leaves, we observed reconstituted YFP signal and internal RFP signal in the infiltrated leaf tissues for both protein pairs (JUB1<sub>Nterm</sub>-CaM4 and JUB1<sub>Cterm</sub>-CaM4) (**Figure 3.17B**).

Similar to the data obtained in the Arabidopsis protoplasts (**Figure 3.17C**), *N. benthamiana* cells transfected with the construct containing the JUB1<sub>Nterm</sub> region express YFP signal only in the nucleus while a YFP signal was only detected in the cytosol in cells equipped with the construct containing the JUB1<sub>Cterm</sub> region. Relative fluorescence was quantified using the intensity ratio between YFP and RFP signal localized exclusively to the nucleus (**Figure 3.17D**) and overall signal ratio that includes both cytosolic and nuclear signal (**Figure 3.17E**). The nuclear-based quantification of BiFC analysis indicates that the JUB1<sub>Nterm</sub> region of the JUB1 protein has a lower relative YFP/RFP fluorescence intensity ratio compared to the full-length JUB1 protein. However, the localization of the interaction still remains in the nucleus similar to the full-length JUB1 protein. Fluorescence intensity ratio measured only in the nucleus showed that the JUB1<sub>Cterm</sub> region has only a low background value equal to the negative control intensity ratio (**Figure 3.17D**). Quantification of the overall signal ratio that includes both cytosolic and nuclear signals revealed that the fluorescence intensity ratio of both split parts of the JUB1 protein and the full-length JUB1 protein have the same level of relative YFP/RFP fluorescence intensity ratio (**Figure 3.17F**). These data indicate that the JUB1<sub>Cterm</sub> region interacts with the CaM4 protein, but their interaction does not occur in the nucleus like the JUB1<sub>Nterm</sub> region. We also performed western blot analysis with  $\alpha$ Myc- and  $\alpha$ HA-antibodies using total protein extracts to confirm protein expression levels (**Figure 3.17F,G**). Both the JUB1<sub>Nterm</sub> and JUB1<sub>Cterm</sub> proteins were expressed in the infiltrated leaf tissues. Thus, both parts of the JUB1 protein can interact with CaM4. These data indicate that CaM4 has several binding sites in the JUB1 protein and at least one binding site is located within the C-terminal part of the protein. However, since the JUB1<sub>Cterm</sub> region does not include an NLS, the interaction is not localized to the nucleus, but rather to the cytosol.

To experimentally verify the exact CaM binding site or the possibility of multiple binding sites present in the N-terminal part of the JUB1 protein, we used a JUB1<sub>Nterm</sub>L121A construct, with amino acid substitutions in the JUB1<sub>Nterm</sub> region. After transient infiltration of *Nicotiana benthamiana* leaves with JUB1<sub>Nterm</sub>L121A constructs, we observed a clear decrease in YFP signal intensity in the infiltrated leaf tissues compared to the YFP signal intensity using non-mutated JUB1<sub>Nterm</sub> protein (**Figure 3.18A**).

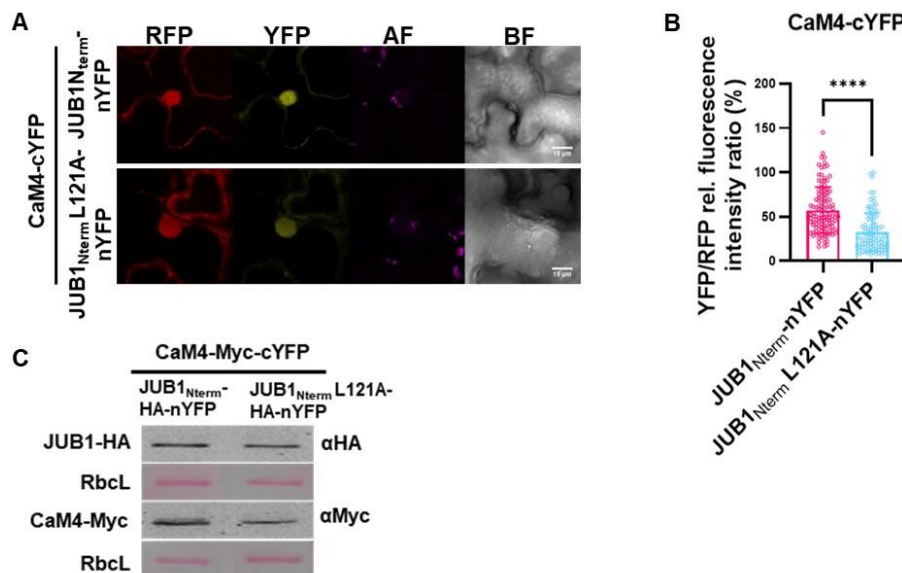


**Figure 3.18. Calmodulin-binding site in the JUB1 DNA-binding domain is functional. A,** Confocal images of BiFC signal in *Nicotiana benthamiana* leaves 72 hours after infiltration expressing CaM4-cYFP and JUB1<sub>Nterm</sub>-nYFP or JUB1<sub>Nterm</sub>L121A-nYFP. AF, chlorophyll autofluorescence; BF, bright field. Scale bar, 15  $\mu$ m. **B,** Quantification of the mean fluorescence ratioed against RFP coming from the nucleus of *Nicotiana benthamiana* after infiltration with CaM4-cYFP and JUB1<sub>Nterm</sub>-nYFP or JUB1<sub>Nterm</sub>L121A-nYFP. Individual data points from three experiments are shown with mean  $\pm$  s.d. for  $n > 90$  and \*\*\*\* $P < 0.0001$  by Student's *t*-test. **C,** Immunoblot analysis of transformed *Nicotiana benthamiana* leaves co-expressing JUB1 and CaM4 in the BiFC assay.  $\alpha$ Myc- and  $\alpha$ HA-antibodies were used as a primary antibodies; the expected molecular weights of JUB1<sub>Nterm</sub>-HA -nYFP and JUB1<sub>Nterm</sub>L121A-HA -nYFP– 38 kDa, and for CaM4-Myc-cYFP– 30 kDa. RbcL, ribulose-1,5-bisphosphate carboxylase/oxygenase large subunit (loading control). kDa, kilodalton. The membrane was stained with Ponceau S for loading control.

Quantification of the mean fluorescence ratioed against RFP measured only in the nucleus shows a significant difference in the relative intensity of JUB1<sub>Nterm</sub>L121A compared to the non-mutated JUB1<sub>Nterm</sub> region (**Figure 3.18B**). We also performed western blot analysis with  $\alpha$ Myc- and  $\alpha$ HA-antibodies to confirm that both proteins are expressed after infiltration (**Figure 3.18C**). However, the interaction was not abolished completely, as the relative intensity of JUB1<sub>Nterm</sub>L121A was still significantly higher than the value of the negative control. These data indicate that JUB1 harbors multiple CaM4 binding sites, both at the N- and

C-terminal part of the protein. Moreover, our data suggest that the interaction can be reduced by substituting Leu to Ala in the CaM binding site localized in the DNA binding domain NAC sub-domain D.

### 3.17. The role of Ca<sup>2+</sup> for JUB1-CaM4 protein interaction

It was previously reported that calmodulins may interact with other proteins in a calcium-dependent or calcium-independent manner (Poovaiah et al., 2013; Zeng et al., 2015; Ranty et al., 2016). We propose that the JUB1-CaM4 interaction may also be calcium-dependent since none of the IQ or IQ-like motifs to which CaM typically binds in the absence of calcium were identified in the JUB1 protein sequence using publicly available Calmodulation database and meta-analysis (predictor <http://cam.umassmed.edu/>; **Table 3.1**).

**Table 3.1. CaM-binding motifs present in the JUB1 protein**

Name of the motif	Times present in the JUB1 protein
1-10 Motif	13
1-12 Motif	13
1-14 Motif	19
1-16 Motif	12
1-5-10 Motif	3
1-5-8-14 Motif	1
1-8-14 Motif	3
IQ and IQ-like Motif	0

To confirm the JUB1 interaction with CaM4 *in planta*, co-immunoprecipitation was performed using the double over-expressor line, *JUB1-GFP-Myc-CaM4 (35S:JUB1-GFP/35S:Myc-CaM4)*. Three-week-old seedlings were harvested two days after treatment with 150 mM NaCl<sub>2</sub>. Proteins were extracted and immunoprecipitated with anti-GFP antibody beads, indicating that JUB1 interacts with CaM4 *in planta*. (**Figure 3.19A**). In the future, we plan to confirm this result and include *35S:GFP* line as a negative control.

These preliminary data suggest that JUB1 interacts with CaM4 under conditions where intracellular levels of Ca<sup>2+</sup> are increased.

The other observation made was a high standard deviation in the rBiFC using the JUB1 CaM4 construct variants. This result might be explained by a different calcium level present in the cells, leading to a different number of CaM4 that has bound calcium and could potentially interact with JUB1. To confirm our results *in planta*, we used a principle of rBiFC and combined it with the application of Ca<sup>2+</sup> blockers or Ca<sup>2+</sup>.



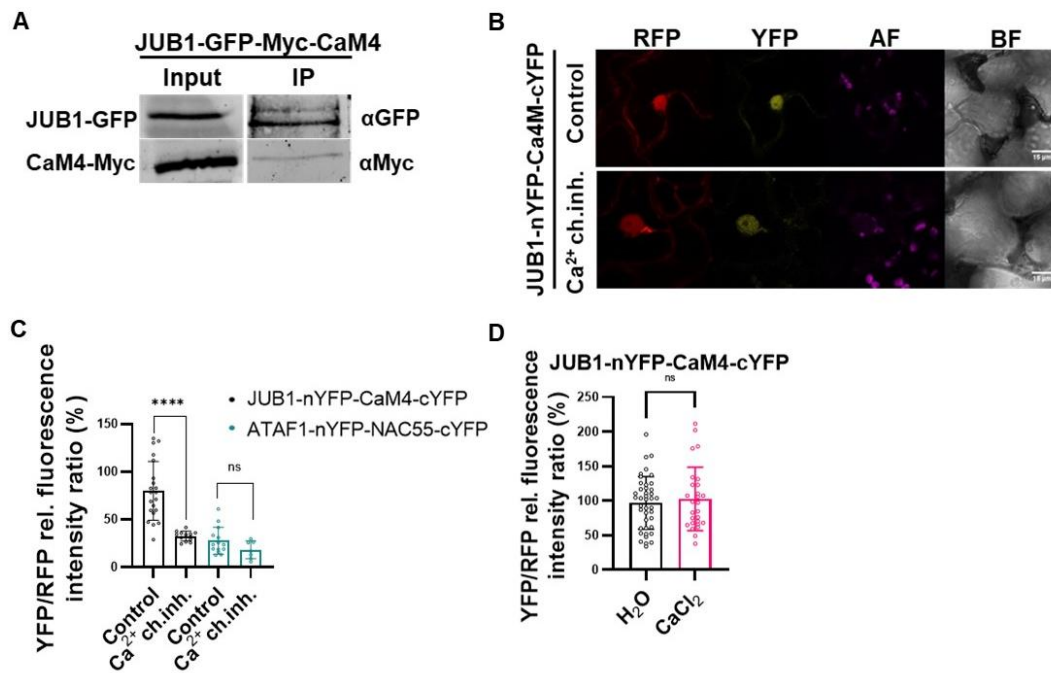


**Figure 3.19. Role of Ca<sup>2+</sup> in JUB1-CaM4 protein interaction.** **A**, Qualitative results of the Co-IP experiment in *JUB1-GFP-Myc-CaM4* line. Total protein extracts (input) and immunoprecipitates (IP) were immunoblotted with αGFP and αMyc antibodies. **B**, Confocal images of BiFC signal in *Nicotiana benthamiana* leaves expressing JUB1-nYFP-CaM4-cYFP after 48 hours (control) and after 2 hours of incubation with Ca<sup>2+</sup> channel inhibitors (20 mM EGTA, 10 mM CoCl<sub>2</sub>, and 1 mM LaCl<sub>3</sub>). AF, chlorophyll autofluorescence; BF, bright field. Scale bar, 15 μm. **C**, Quantification of the mean fluorescence ratioed against RFP coming from the nucleus of *Nicotiana benthamiana* after infiltration with JUB1-nYFP-CaM4-cYFP and ATAF1-nYFP/ANAC55-cYFP (used as a control). Individual data points are shown with mean ± s.d. for n = 7 to 20 and \*\*\*\**P* < 0.0001 by Student's *t*-test. **D**, Quantification of the mean fluorescence ratioed against RFP coming from the nucleus of *Nicotiana benthamiana* after infiltration with JUB1-nYFP-CaM4-cYFP after 2 hours of incubation with H<sub>2</sub>O or 10 mM CaCl<sub>2</sub>. Individual data points are shown with mean ± s.d. for n = 27 to 41. In A-D the experiment was repeated once.

The JUB1-nYFP-CaM4-cYFP and ATAF1-nYFP/ANAC55-cYFP (used as a control) were transiently infiltrated into 5-week-old *Nicotiana benthamiana* leaves, and after 48 hours, the reconstituted YFP signal was confirmed using a confocal microscope (labeled as control) (**Figure 13.9B**). The leaf discs were then incubated in the Ca<sup>2+</sup> channel inhibitor solution for 2 hours, and the YFP signal and internal RFP signal fluorescence were detected, and the relative fluorescence intensity ratio was measured (**Figure 3.19C**). However, the observation was made that the incubation of the leaf discs with Ca<sup>2+</sup> blocking decreases the internal RFP signal, which makes this assay not suitable for the purpose of the experiment. Next, we decided to incubate the leaf discs after infiltration with JUB1-nYFP-CaM4-cYFP in H<sub>2</sub>O or CaCl<sub>2</sub>.

The relative fluorescence intensity ratio measured in the nucleus shows no change upon treatment with CaCl<sub>2</sub> (**Figure 3.19D**) as it is possible that the preparation of the leaf discs and

the vacuum infiltration of  $\text{CaCl}_2$  could have already increased the level of intracellular free calcium level to the level that is sufficient for JUB1 and CaM4 to interact. That why for further study, we used a stable transformed Arabidopsis *BiFC2in1* line infiltrated with JUB1-nYFP-CaM4-cYFP. The screening for transgenic *BiFC2in1* lines was conducted using confocal microscopy. We also checked the expression level of *CaM4*, and *JUB1*, in these lines, which is lower than in one of the lines that was used for phenotyping and will be described in the next chapter (**Figure 3.20A**). As we did not observe any YFP signal in the control seedlings (data not shown), we decided to monitor the YFP and RFP signal in the mature plants looking at both young and senescent leaves (**Figure 3.20B**).

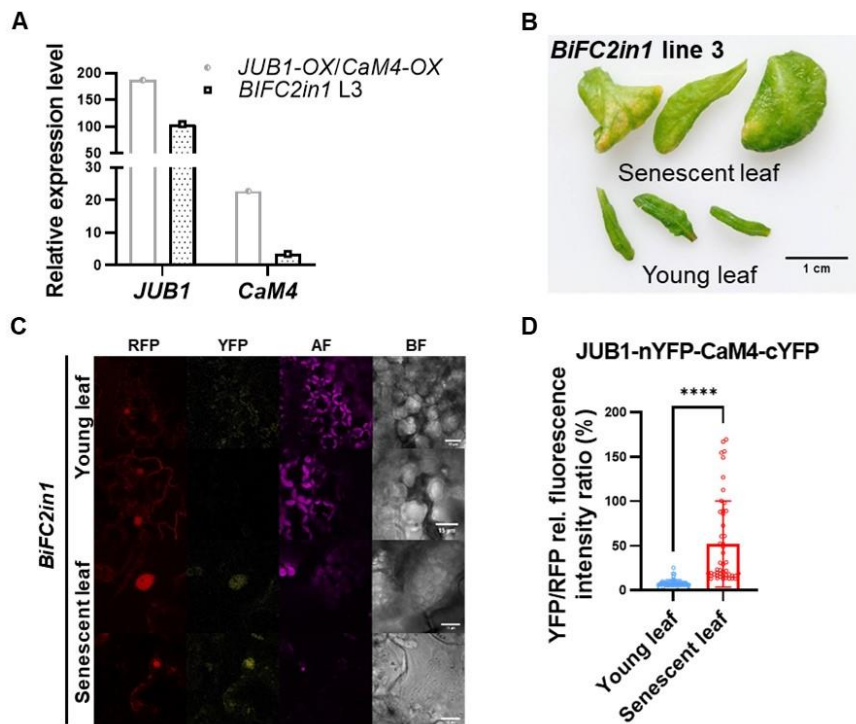


**Figure 3.20. JUB1-CaM4 protein interaction occurs in the senescent leaves.** **A**, Relative expression of *JUB1* and *CaM4* in eight-week-old *JUB1-OX/CaM4-OX* and *BiFC2in1* (L3 – line3) mutants normalized to expression in the WT. Primer sequences are given in **Supplemental Table S3**. **B**, Eight-week-old transgenic *BiFC2in1* line grown under control conditions. Young leaves and senescent leaves taken for the microscopy experiment are shown. Scale bar, 1 cm. **C**, Confocal images of young and old leaves of stable *BiFC2in1* line. AF, chlorophyll autofluorescence; BF, bright field. Scale bar, 15  $\mu\text{m}$ . **D**, Quantification of the mean fluorescence ratioed YFP against RFP in young and old leaves of stable *BiFC2in1* line. The experiment was repeated three times with similar results. Individual data points are shown with mean  $\pm$  s.d. for  $n = 50$  to  $55$  and \*\*\*\* $P < 0.0001$  by Student's *t*-test.

In the experiment, we included both young and senescent leaves. As expected, we observed no reconstitution of the YFP signal in the young green leaves. However, the YFP signal was detected in old leaves, indicating that JUB1 interacts with CaM4 in the senescent leaves but not at the young leaves (**Figure 3.20C**). Furthermore, the relative fluorescence intensity ratio

measured in the nucleus of both young and old leaves confirms the significant difference between different leaf stages made by confocal microscopy (**Figure 3.20D**).

Our data indicate that the interaction between CaM4 with JUB1 in senescent leaves occurs due to elevated  $\text{Ca}^{2+}$  levels that are induced at the senescent leaf stage. To show this, we used the previously reported *R-GECO* line and checked the  $\text{Ca}^{2+}$  level in young and senescent leaves (**Figure 3.21A,B**). The higher intensity of the signal in the senescent leaf compared with the young leaf confirms a higher  $\text{Ca}^{2+}$  level in the senescent leaf. The quantification of the fluorescence intensity of the R-GECO signal overall and only in the nucleus confirms a higher level of  $\text{Ca}^{2+}$  in the senescent leaves compared with young leaves (**Figure 3.21C,D**)

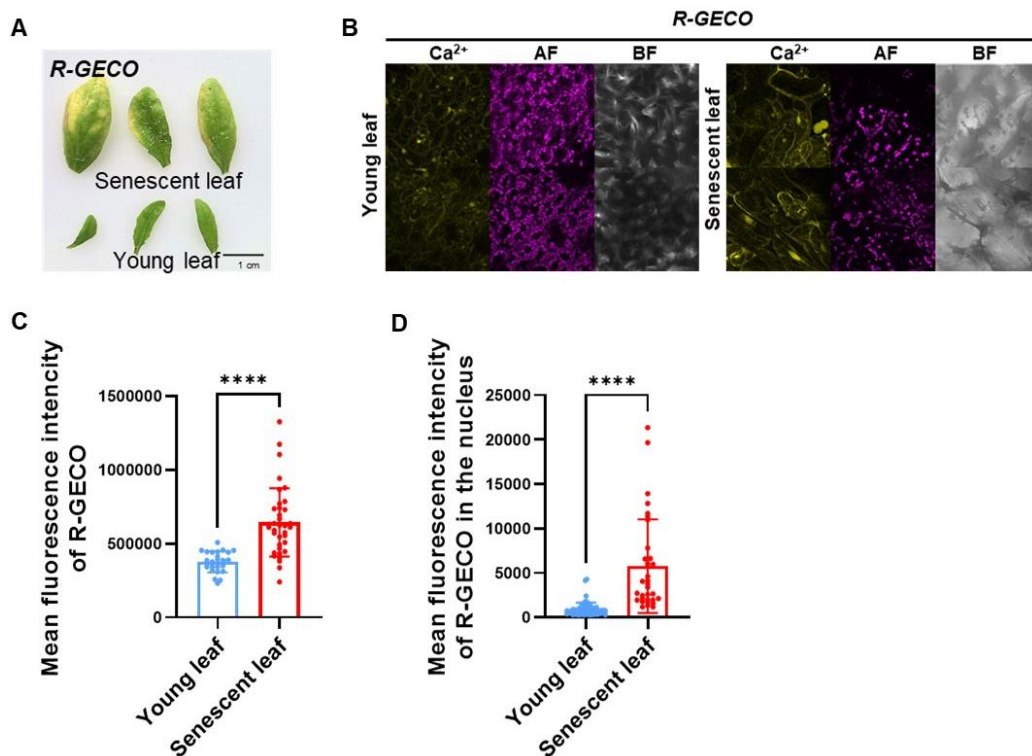


**Figure 3.21.  $\text{Ca}^{2+}$  level in young and senescent leaves.** **A**, Eight-week-old transgenic *R-GECO* line grown under control conditions. Young leaves and senescent leaves taken for the microscopy experiment are shown. Scale bar, 1 cm. **B**, Confocal images of young and senescent leaves in *R-GECO* line. AF, chlorophyll autofluorescence; BF, bright field. All pictures were taken using 40X magnification and zoom 2.5. **C**, Fluorescence intensity of R-GECO is calculated as an integrated density measurement for each image analyzed by Fiji. The experiment was repeated three times with similar results. Individual data points are shown with mean  $\pm$  s.d. for  $n = 25$  to 36 and  $****P < 0.0001$  by Student's *t*-test. **D**, Fluorescence intensity of R-GECO in the nucleus is calculated as an integrated density measurement only in the nucleus for each image analyzed by Fiji. The experiment was repeated three times with similar results. Individual data points are shown with mean  $\pm$  s.d. for  $n = 33$  to 60 and  $****P < 0.0001$  by Student's *t*-test.



These data indicate that the interaction between JUB1 and CaM4 is specific to older plants, particularly during senescence, and that the biological relevance of this interaction might be connected to its regulation.

### **3.18. Characterization of *JUB1-OX/CaM4-OX* and *CaM4-OX* lines**

To further investigate a possible role of CaM4/CaM1 interaction with JUB1, we generated *JUB1-OX/CaM1-OX*, *JUB1-OX/CaM4-OX*, and *JUB1-OX/CaM1-OX/CaM4-OX* plants and single overexpressor mutants of *CaM1-OX* and *CaM4-OX*. A scheme of the constructs is shown in **Figure 3.22A**.

The screening for transgenic *CaM1-OX* and *CaM4-OX* lines was conducted using confocal microscopy. The RFP signal alone was detected and localized to the nucleus and in the cytosol in *CaM1-OX* and *CaM4-OX* transgenic lines. We also confirmed the positive lines by qRT-PCR analysis to detect *CaM1* and *CaM4* gene expression (**Figure 3.22B**). The *JUB1-OX/CaM1-OX*, *JUB1-OX/CaM4-OX* lines were generated by transforming the *35S:Myc-CaM1* and *35S:Myc-CaM4* construct into the *JUB1-OX* mutant line. A scheme of the constructs is shown in **Figure 3.22C**. The screening for transgenic lines was performed *via* genotyping with a set of gene-specific and vector-specific primers that confirms which is able to detect the transgenic *Myc-CaM1* and *Myc-CaM4* transcripts and not the expression of endogenous *CaM1* and *CaM4*, and also detect the protein Myc-CaM1 and Myc-CaM4 protein fusions in selected positive lines with western blot analysis using  $\alpha$ Myc-antibodies.

The upper protein band corresponds to Myc-CaM1 and Myc-CaM4 proteins as this band is missing in the WT negative control lane (**Figure 3.22D**). We also conducted a qRT-PCR analysis to detect *JUB1*, *CaM1*, and *CaM4* gene expression to compare the level of overexpression of these genes in different lines (**Figure 3.22D**).

Next, we analyzed the growth phenotypes of *JUB1-OX/CaM1-OX* and *JUB1-OX/CaM4-OX* plants. Double overexpressor plants reveal smaller rosette areas, compact rosette shape, and shorter petioles than the WT plants and single overexpressor of *CaM1* or *CaM4* genes (**Figure 22F, 22G**). Our data show that overexpression of *CaM1* or *CaM4* in the *JUB1-OX* background mutant did not change the reported developmental phenotype of the *JUB1-OX* plants.

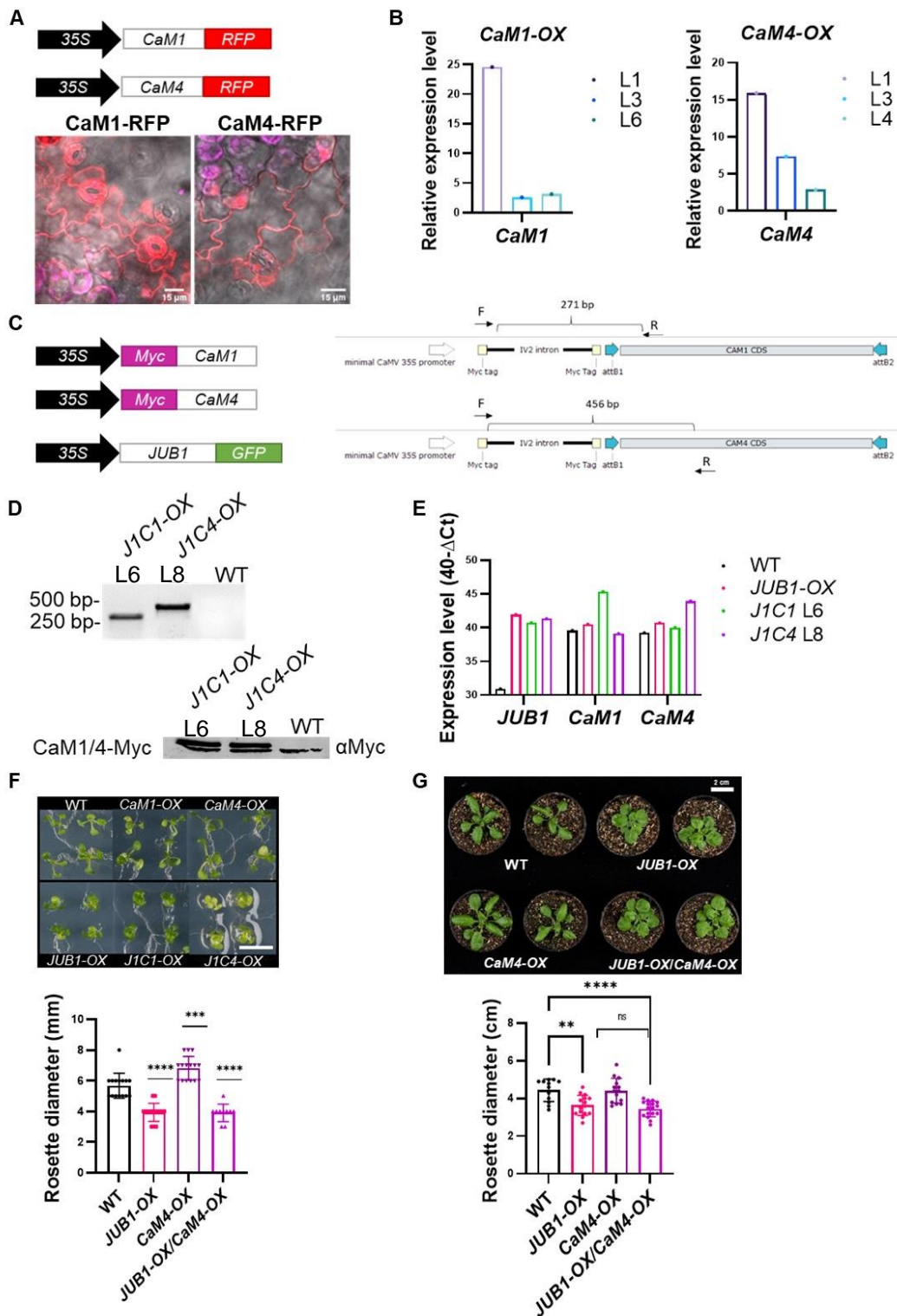


**Figure 3.22. Characterization of *JUB1-OX/CaM4-OX* and *CaM4-OX* lines.** **A**, Upper panel, scheme of the constructs *CaM1-RFP* and *CaM4-RFP* used to generate single overexpressor lines *CaM1-OX* and *CaM4-OX*. Lower panel, confocal microscope analysis showing *CaM1-RFP* and *CaM4-RFP* in *CaM1-OX* and *CaM4-OX* lines. Scale bar, 15  $\mu$ m. **B**, Relative expression of *CaM1* and *CaM4* in *CaM1-OX* (Lines: L1, L3, L6) and *CaM4-OX* (Lines: L1, L3, L4) mutants normalized to the expression in the WT. Primer sequences are given in **Supplemental Table S3**. **C**, Left panel, scheme of the constructs *Myc-CaM1*, *Myc-CaM4* used for generation of double overexpressor lines *JUB1-OX/CaM1-OX* and *JUB1-OX/CaM4-OX*.

Right panel, attB1, attB2, recombination sites for the GATEWAY BP reaction; IV2 intron, modified second intron of the potato *ST-LS1* gene; Myc tag, epitope tag; CDS, coding sequence; F, R, primers used for genotyping transgenic lines. The region for primer binding is shown with arrows. **D**, Upper panel, agarose gel picture shows PCR genotyping for *JUB1-OX/CaM1-OX* L6 in line 1 and *JUB1-OX/CaM4-OX* L8 in line 2 and WT. Expected size *JUB1-OX/CaM1-OX* L6 - 271 bp, *JUB1-OX/CaM4-OX* L8 - 456 bp. WT is used as a negative control. Primer sequences are given in **Supplemental Table S1**. Lower panel, immunoblot analysis in *JUB1-OX/CaM1-OX* L6 and *JUB1-OX/CaM4-OX* L8.  $\alpha$ Myc-antibodies were used as a primary antibodies, expected molecular weights of CaM1/CaM4 - 18 kDa. kDa, kilodalton. **E**, The expression level of *JUB1*, *CaM1*, and *CaM4* in 10-day-old seedlings of WT, *JUB1-OX*; *JUB1-OX/CaM1-OX* L6, and *JUB1-OX/CaM4-OX* L8 analyzed by qRT-PCR. Primer sequences are given in **Supplemental Table S3**. **F**, Upper panel, eight-day-old seedlings of WT, *JUB1-OX*, *CaM4-OX*, and *JUB1-OX/CaM4-OX* grown on half-strength MS media under long-day conditions. Lower panel, quantification of the rosette diameter. Data represent means  $\pm$  s.d. (n = 10-15), \*\*\**P* < 0.001, \*\*\*\**P* < 0.0001 by Student's *t*-test. Scale bar, 2 cm. **G**, Upper panel, four-week-old seedlings of WT, *JUB1-OX*, *CaM4-OX*, and *JUB1-OX/CaM4-OX* grown on soil under long-day conditions. Lower panel, quantification of the rosette diameter. Data represent means  $\pm$  s.d. (n = 12-17), \*\**P* < 0.01, \*\*\*\**P* < 0.0001 by Student's *t*-test. Scale bar, 2 cm.

### 3.19. CaM4 overcomes the JUB1 function upon senescence

Since *JUB1* and *CaM4* interact in a  $\text{Ca}^{2+}$ -dependent manner, we hypothesized that double overexpressor plants should have a distinct phenotype from *JUB1-OX* under conditions that induce an increase of intracellular calcium levels. As we previously showed that the interaction between *JUB1* and *CaM4* is specific to plants undergoing senescence, we performed further phenotypic analysis to observe the difference in the senescent phenotype of *JUB1-OX/CaM4-OX*, *CaM4-OX*, *JUB1-OX/CaM1-OX*, *CaM1-OX*, *JUB1-OX*, and WT plants. After growing seedlings on solid media for 1.5 weeks, we moved seedlings into liquid media and continued to grow them in a flask under continuous agitation for the next 2-2.5 weeks until the senescent phenotype was observed. For the *JUB1-OX* plants, we obtained similar results reported by Wu et al. (2012), where *JUB1-OX* plants remained green after 2 weeks of growth in these conditions. *CaM1-OX* plants showed an early senescent phenotype in comparison to the WT plants. *JUB1-OX/CaM1-OX* plants displayed a weaker phenotype and started to senesce earlier than the *JUB1-OX* plants, even though the lines have the same *JUB1* expression level. As the process of senescence involves the degradation of chlorophyll, the observed phenotype of *JUB1-OX/CaM1-OX* and *CaM1-OX* plants was also supported by chlorophyll content measurements under this condition (**Figure 3.23A**). The *JUB1-OX/CaM4-OX* plants, including the previously described *BiFC2in1* line and *CaM4-OX* line 1 and line 2 plants, similar to *JUB1-OX/CaM1-OX* and *CaM1-OX* plants, displayed a weaker phenotype during senescence compared with WT and *JUB1-OXs* (**Figure 3.23B**). The chlorophyll measurement in these

lines supports the observed phenotypes and indicates that even though the *JUB1* transcript abundance in *JUB1-OX/CaM4-OX* and *JUB1-OX* lines are similar, the *JUB1-OX/CaM4-OX* line is defined by an early senescence phenotype and lower chlorophyll content level compared with *JUB1-OX* (Figure 3.23C).

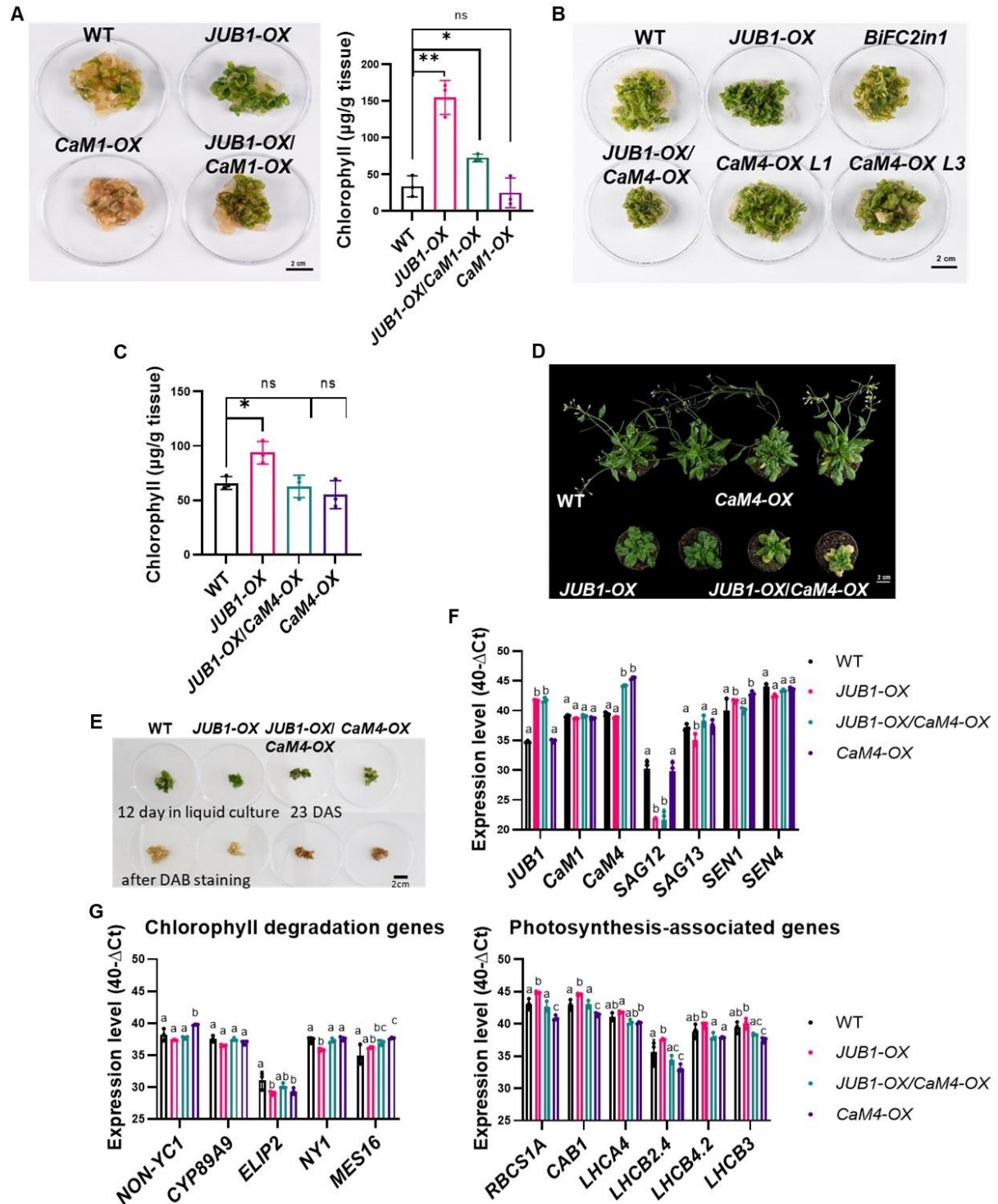


**Figure 3.23. CaM4 overcomes the JUB1 function.** A, Left panel, two-week-old WT, *JUB1-OX*, *CaM1-OX*, *JUB1-OX/CaM1-OX*, and *JUB1-OX/CaM4-OX* plants grown on half-strength MS medium under long-day conditions and then transferred to liquid media for another two

weeks. Scale bar, 2 cm. Right panel, chlorophyll level after 34 DAS in WT, *JUB1-OX*, *CaM1-OX*, *JUB1-OX/CaM1-OX* and *JUB1-OX/CaM4-OX* lines. Data represent means  $\pm$  s.d. (n = 3), \* $P < 0.05$ , \*\* $P < 0.01$  by Student's *t*-test. **B**, Three-week-old WT, *JUB1-OX*, *CaM4-OX*, *JUB1-OX/CaM4-OX*, and *BiFC2in1* plants grown on half-strength MS medium under long-day conditions and then transferred to liquid medium for another 11 days. Scale bar, 2 cm. **C**, Chlorophyll level in three-week-old WT, *JUB1-OX*, *CaM4-OX*, and *JUB1-OX/CaM4-OX* plants grown on half-strength MS medium under long-day conditions and then transferred to liquid medium for another 11 days. Data represent means  $\pm$  s.d. (n = 3), \* $P < 0.05$  by Student's *t*-test. **D**, Forty-five-day-old WT, *JUB1-OX*, *CaM4-OX*, and *JUB1-OX/CaM4-OX* plants grown on soil. Scale bar, 2 cm. **E**, DAB staining after 23 DAS in WT, *JUB1-OX*, *CaM4-OX*, and *JUB1-OX/CaM4-OX* grown on half-strength MS medium under long-day conditions and then transferred to liquid medium for another 12 days. Upper panel, plants before staining. Lower panel, plants after staining with DAB overnight. Scale bar, 2 cm. **F**, The expression level of *JUB1*, *CaM1*, *CaM4*, and senescence-associated genes after 23 DAS in WT, *JUB1-OX*, *CaM4-OX*, and *JUB1-OX/CaM4-OX* grown on half-strength MS medium under long-day conditions and then transferred to liquid medium for another 11 days. Individual data points are shown with mean  $\pm$  s.d. (n = 3). **G**, The expression level photosynthesis-associated genes and marker genes for chlorophyll breakdown after 23 DAS in WT, *JUB1-OX*, *CaM4-OX*, and *JUB1-OX/CaM4-OX* plants grown on half-strength MS medium under long-day conditions and then transferred to liquid medium for another 11 days. Individual data points are shown with mean  $\pm$  s.d. (n = 3). In **F,G** letters indicate significant differences among means ( $P < 0.05$ ; two-way ANOVA). Primer sequences are given in **Supplemental Table S3**.

We also detect an early senescence phenotype for soil-grown *JUB1-OX/CaM4-OX* and *CaM4-OX* plants already after 35-40 DAS (**Figure 3.23D**). The weaker phenotype in *JUB1-OX/CaM4-OX* double overexpressors, compared with single *JUB1-OX*, was also observed for the ROS accumulation levels, particularly for hydrogen peroxide, which was tested using DAB staining. A darker brown color in the *CaM4-OX* and *JUB1-OX/CaM4-OX* compared with WT and *JUB1-OX* indicates a higher level of ROS in the tissue (**Figure 3.23E**). The molecular data also indicate a significant difference in transcript level between tested genotypes for many of the genes that are markers for chlorophyll degradation or genes associated with chlorophyll degradation and senescence (**Figure 3.23F,G**).

These data indicate that CaM4 possibly overcomes the function of JUB1 upon leaf senescence. We hypothesize that CaM4 could possibly block the JUB1 DNA-binding domain, as we previously confirmed the location and functionality of the CaM-binding site in this region, which in turn could prevent JUB1 binding/regulation of its downstream targets upon senescence.

Using the transactivation assay in *A. thaliana* protoplasts and transiently infiltrated *Nicotiana benthamiana* leaves, we confirmed that *DREB2A*, one of the downstream targets of JUB1, exhibits altered promoter activity in the presence of JUB1 protein alone and when JUB1 is expressed together with CaM4 protein (**Figure 3.24A,B**). To identify other downstream targets



of JUB1 that are differentially expressed upon JUB1 interaction with CaM4, RNA-seq was performed using *JUB1-OX/CaM4-OX*, *CaM4-OX*, *JUB1-OX*, and WT plants after nine days of growing in liquid medium, as described previously (Figure 3.24C). The RNA-seq data are currently being analyzed.

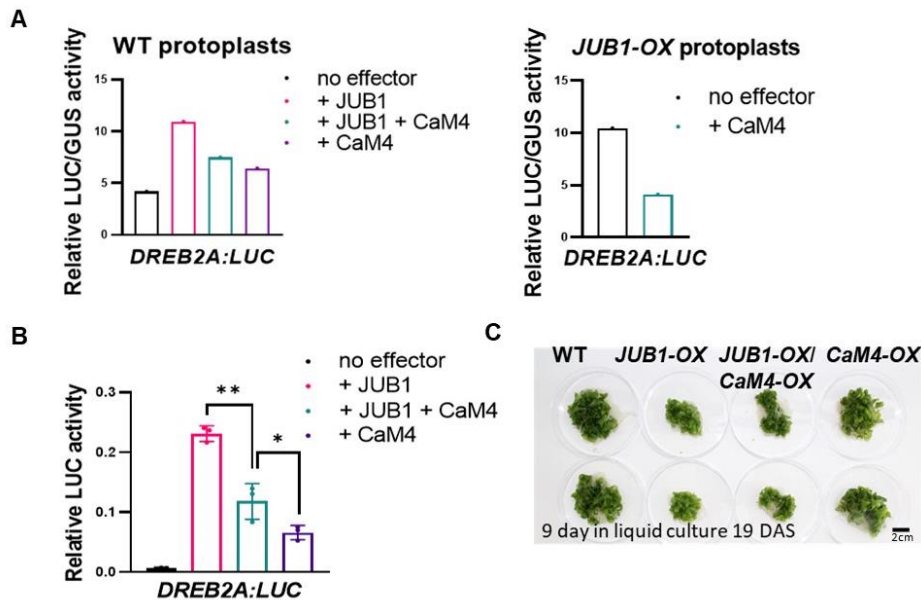


**Figure 3.24. CaM4 reduces JUB1 protein activity towards *DREB2A*.** **A**, Transactivation of *DREB2A* expression (from its 1.5 kb promoter) by JUB1 and CaM4 in WT Arabidopsis mesophyll cell protoplasts (left) (n = 1). The experiment was repeated once. Right panel, transactivation of *DREB2A* expression (from its 1.5 kb promoter) by JUB1 and CaM4 in *JUB1-OX* Arabidopsis mesophyll cell protoplasts (n = 1). The experiment was repeated twice with similar results. The *DREB2A:LUC* constructs harboring the *DREB2A* promoter upstream of the firefly luciferase open reading frame was cotransformed with the *UBQ10:GUS* plasmid, which was used for transformation efficiency normalization. **B**, Relative LUC activity from the transient expression analysis of *DREB2A* promoter, co-infiltrated with JUB1 and/or CaM4 in *Nicotiana benthamiana*. The data presented as a ratio between absolute LUC activity and absolute REN activity. **C**, The phenotype after 19 DAS of WT, *JUB1-OX*, *CaM4-OX*, and *JUB1-OX/CaM4-OX* grown on half-strength MS media under long-day conditions and then transferred to a liquid media for another 9 days harvested for RNA-seq. Error bars represent means  $\pm$  s.d. (n = 3); \*  $P < 0.5$ , \*\* $P < 0.01$  using Student's *t*-test. Scale bar, 2 cm. The experiment was repeated once.

These data indicate that JUB1 function upon senescence is compromised through the interaction with CaM4 protein that binds to the DNA-binding domain of JUB1 and in part prevents JUB1 from interaction with some of its downstream targets.

### 3.20. Characterization of *CaM1* and *CaM4* knockout mutants

It was previously reported that there is functional redundancy between *CaM1* and *CaM4* genes (Dai et al., 2018). Thus, to study the biological relevance of JUB1-CaM4 interaction under

these conditions, we generated *cam1/cam4* double knockout mutants in Arabidopsis Col-0 background using the CRISPR-Cas9 approach. To characterize *CaM1* and *CaM4* functions, we generated double knockout plants using two sgRNAs for each gene (sgRNA1, sgRNA2, sgRNA3, and sgRNA4) which were designed using the CRISPR-P 2.0 software (<http://crispr.hzau.edu.cn/CRISPR2/>) (**Figure 3.25A**). Several lines were genotyped, and positive lines were confirmed by qRT-PCR to assess *CaM1* and *CaM4* expression (**Figure 3.25B,C**). The developmental phenotype of *cam1/cam4* plants showed no clear phenotypical differences in terms of rosette area, senescence phenotype compared to the WT plants grown under short-day conditions (**Figure 3.25D**).

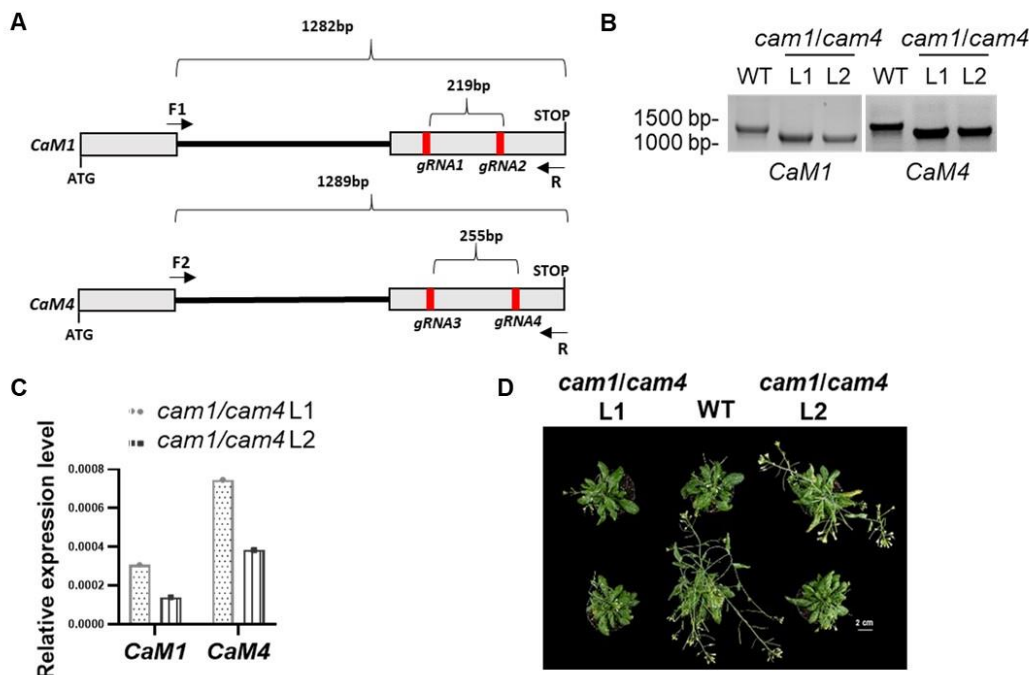


**Figure 3.25. Characterization of *CaM1* and *CaM4* knockout mutants.** **A**, Schematic diagram of the location of the sgRNAs (red boxes) used for CRISPR/Cas9 genome-editing of *CaM1* and *CaM4* gene. ATG, translational start codon; F and R, primers used for genotyping transgenic lines. The primer binding sites are shown with arrows. **B**, Agarose gel picture showing the PCR genotyping for *cam1/cam4* lines L1 and L2. In WT, *CaM1* and *CaM4* have an expected size of ~ 1200 bp, and in transgenic *cam1/cam4* lines *CaM1* and *CaM4* have an expected size of ~ 1000 bp. Primer sequences are given in **Supplemental Table S1**. **C**, Relative expression of *CaM1* and *CaM4* *cam1/cam4* L1 and L2 mutants normalized to expression in WT (WT=1). The *CaM1* and *CaM4* primers are localized within the deletion cite. Primer sequences are given in **Supplemental Table S3**. **D**, Seven-week-old *cam1/cam4* L1 and L2 mutants and WT grown under control conditions. Scale bar, 2 cm.

## 4. DISCUSSION

### 4.1. Role of the *JUB1-OXs* in drought stress tolerance

Our work addresses the importance of identifying the regulatory components as well as the mechanisms through which *JUB1* controls plant tolerance to drought stress. Currently, the molecular mechanism underlying this drought-tolerant phenotype is unknown, even though the drought tolerance phenotype in *JUB1-OXs* has already been reported (Ebrahimian-Motlagh et al., 2017). *HB13* was identified as a positive upstream regulator of *JUB1* in connection to drought stress tolerance. In *Arabidopsis* and tomato plants, drought tolerance in *JUB1-OXs* was linked to direct regulation of *DREB2A*, a key transcription factor controlling drought responses in *Arabidopsis* (Sakuma et al., 2006; Wu et al., 2012; Thirumalaikumar et al., 2018). However, no other data about other downstream targets of *JUB1* in connection to drought stress tolerance or data supporting the sole regulation of *DREB2A* by *JUB1* leading to such a strong drought-tolerant phenotype has been shown so far. Hence, the importance of including severe drought stress conditions and identification of the mechanism through which *JUB1* confers tolerance to drought cannot be underestimated. Confirmation of the drought resistance for plants with some degree of dwarfism is often assessed after scoring the survival rate after re-watering (Fàbregas et al., 2018). To include the correction on the phenotypical difference of the *JUB1-OXs*, we confirmed that all plants have the same RWC level, which was around 20%, before the start of the re-watering. For plants, 10-20% of RWC is estimated as a critical level of water deficiency prior to the cessation of photosynthesis which occurs at the mark below 45 % RWC (Di Blasi et al., 1998). Recovery after this and even lower RWC levels (<5%) was shown for resurrection plants like *Craterostigma pumilum* (Zia et al., 2016). *JUB1-OXs* plants exhibit a somewhat close phenotype to resurrecting plants. The plants recovered after extremely severe drought stress conditions whereby around 25 % of the plants survived after re-watering, while only about 5 % of the WT and *jub1-1* plants survived. Rapid recovery after re-watering during mild drought stress was also observed for *JUB1-OXs* (**Figure 3.1**). All this confirms a strong drought tolerance phenotype of *JUB1-OXs*, which in turn might be explained through different mechanisms (a higher accumulation of compatible osmolytes such as proline, regulation of the stomatal aperture/development, or scavenging of ROS *via* direct regulation of a stress-responsive TF *DREB2*) or changes in root system architecture, an increase in the root-to-shoot ratio, or a reduction in the cytokinin level in roots which also contribute to drought tolerance in *Arabidopsis*, soybean, and tobacco (Werner et al., 2010; Chen et al., 2021). It is not yet known if *JUB1-OXs* show enhanced root growth, changes in the root system architecture or



increase in the root-to-shoot ratio upon drought stress. This would also have an impact on a drought tolerance phenotype reported in plants overexpressing *JUB1*. Hence, the possible contribution of each drought tolerance mechanism to a drought-tolerant phenotype of *JUB1-OXs* requires further investigation.

#### **4.1.1. Regulation of proline accumulation by JUB1**

Increased resistance to drought stress in plants was often reported to be also correlated with increased proline content (Mona et al., 2017; Arteaga et al., 2020). Transgenic plants can confer drought tolerance *via* modulating proline biosynthesis or degradation by changing the transcription level of the respective genes that encode critical enzymes or proline transporters (An et al., 2013; Abdula et al., 2016; Li et al., 2018; Ahammed et al., 2020). It is not yet known if *JUB1* can regulate proline accumulation through direct binding to the promoter region of genes involved in proline metabolism or through regulation of the expression of TFs involved in proline metabolism. We performed a yeast one-hybrid screen to study the interaction of *JUB1* with promoter regions of proline metabolism genes and TFs known to be involved in the regulation of proline metabolism. *JUB1* has its binding site “GCCGT” present only in the promoter region of one of the proline degradation genes, *PDH2*. We also included *MYB2* and *bZIP63* as putative downstream targets of *JUB1* in connection to proline metabolism based on the reported data and the location of the *JUB1* binding site in their promoter region (Yoo et al., 2005; Veerabagu et al., 2014; Mair et al., 2015). The Y1H experiment confirmed both *MYB2* and *bZIP63* promoter regions are bound by *JUB1* in yeast (**Figure 3.5**). Next, binding of *JUB1* to DNA was confirmed by ChIP-qPCR under control conditions in *35S:JUB1-GFP* line, where *bZIP63* primers showed enrichment in the qPCR analysis, suggesting that *JUB1* immunoprecipitated together with *bZIP63* promoter region (**Figure 3.6**). Regulation of proline accumulation by *JUB1* might also occur without the direct binding to the promoters of proline metabolism genes. Based on our EMSA results, direct binding of *JUB1* to *bZIP63* was not observed (**Figure 3.6**). Next, to identify the contribution of proline accumulation towards enhanced drought tolerance, we super infiltrated *JUB1-OX* mutant plants with *35S:bZIP63-RFP* construct (**Figure 3.7**). In the next step, the drought stress experiment in these lines and *JUB1-OX*, *bZIP63-OX*, and WT plants, will be conducted to assess the phenotype of the double overexpressors under drought stress conditions.

#### **4.1.2. Regulation of stomatal conductance in *JUB1-OXs***

Changes in stomatal development can directly affect the drought tolerance of plants through the changes in their WUE, making stomata a key target for drought tolerance improvement in plants. For example, reduced stomatal density enhances drought tolerance in rice and maize (Caine et al., 2019; Xiang et al., 2021). The effect of lower stomatal conductance in *JUB1-OXs* under control and drought conditions might be due to lower stomatal aperture and/or density or altered stomatal development. It might also be correlated with the transpiration and photosynthetic rates (**Figure 3.8**). In *Loess plateau* photosynthetic rate is shown to be negatively correlated with stomatal density and positively with stomatal length. In Arabidopsis, increased stomatal density could both enhance the photosynthetic rate or have no effect on photosynthesis (Büsis et al., 2006; Tanaka et al., 2013; Vráblová et al., 2017; Yin et al., 2020). We would need to consider this in our studies and include the measurement of photosynthetic activity in *JUB1-OX* leaves in order to estimate the influence of the lower stomatal conductance on photosynthesis.

Nevertheless, it is important to investigate if the reduction in stomatal conductance observed in *JUB1-OX* is due to changes in the stomatal development or stomatal number. Both can also cause differences in the stomatal conductance, stomatal opening, and closure modulation. Recently, GABA was shown to be necessary for reduced stomatal opening and water loss due to transpiration. Thus, alteration of GABA levels or GABA signaling in the guard cell could affect drought stress tolerance (Xu et al., 2021). The positive role of ABA in stomatal closure is also well known (Leckie et al., 1998). ABA-induced stomatal closure has also been linked to changes in calcium levels (MacRobbie et al., 1992). BRs are also participating in co-regulation of stomatal movement together with ABA through suppression of *BR11-ASSOCIATED RECEPTOR KINASE 1 (HvBAK)* in barley (Chen et al., 2019).

Considering previously reported and recent data on JUB1 regulation of BR signaling and involvement of transduction of Ca<sup>2+</sup> signal through the interaction with CaM4, JUB1 might also contribute to the regulation of stomatal opening by altering Ca<sup>2+</sup> and BR signaling. In order to investigate the cause of lower stomatal conductance in *JUB1-OXs*, stomatal aperture and stomatal density, and stomatal conductance at the other developmental stages under both control and drought conditions need to be assessed.

#### **4.2. The effect of cell-specific overexpression of JUB1 on drought tolerance**

Cell-specific overexpression under promoters that drive expression of the gene in certain cell types allows the analysis of a normal function of the TF in the cell. At the same time, ectopic

expression of TF could result in artifacts due to the expression of the TF in all cell types regardless of the real TF endogenous expression profiles. Overexpression of the TF, even in one specific cell type, could already result in improved drought stress tolerance. For example, genetic engineering of target genes in stomata can enhance drought stress tolerance. Thus, overexpression of *PYL5* under the control of guard cell-specific promoter *pGCI* was shown to improve drought stress tolerance in Arabidopsis (Quan et al., 2018). In addition, the expression of another Arabidopsis gene, *ABF4*, in guard cells also enhanced drought tolerance in tomato and tobacco (Na and Metzger, 2017). In tomato, *DELLA*'s exclusive expression in guard cells is sufficient to promote stomatal closure (Nir et al., 2017). As *JUB1* activates *DELLA* genes and triggers *DELLA* accumulation in Arabidopsis, we hypothesized that *JUB1* could promote drought tolerance at least partially by accumulating *DELLA* proteins in the guard cells and by the regulation of stomatal closure. However, cell-specific overexpression of *JUB1* under the control of the *KST1* promoter does not seem to have a significant effect on drought tolerance. Ectopically expressing *JUB1* in guard cells had no visible effect on plant phenotype under drought or control conditions (**Figure 3.9**). The stomatal conductance measurement showed no significant difference between the WT and plants with *JUB1* expressed in guard cells (**Figure 3.9**). Overall, we conclude that the overexpression of *JUB1* solely in guard cells does not improve drought stress tolerance in Arabidopsis. It cannot be excluded that the expression of *JUB1* in guard cells could have an additive effect and combined with other genetic engineering of *JUB1* in these plants could have an effect on drought stress tolerance.

Overexpression of *JUB1* in the shoot apical meristem using a promoter that enhances expression of *JUB1* in the shoot apical meristem only under drought stress could also help assess the effect of cell-specific *JUB1* overexpression. It is known that an increased root-to-shoot ratio is also one of the traits of drought tolerance. As mentioned before, a possible change of the root development in *JUB1* overexpressor plants was not yet analyzed. However, microarray data indicate that *JUB1* is also expressed in different parts of the root (Winter et al., 2007; Wu et al., 2012).

#### **4.3. The effect of transcriptional control of *DREB2A* gene on drought tolerance of *JUB1-OXs***

Overexpression of *DREB2A* results in improved drought tolerance compared to WT plants. Also, *DREB2A* regulates many drought stress-inducible genes (Sakuma et al., 2006; Kant et al., 2008). It was previously reported that *JUB1* directly regulates the expression of stress-responsive transcription factor *DREB2A* in transactivation assays, ChIP-qPCR, and EMSA

(Wu et al., 2012). However, it is unknown if JUB1 requires only *DREB2A* or/and the subsequent induction of other drought- and stress-related genes that can reduce the intracellular level of reactive oxygen species to confer tolerance to drought. Until now, none of the reports showed a phenotype for *dreb2a* knockout mutant upon drought stress. However, as expected by the drought-tolerant phenotype in *DREB2A-OXs*, the *dreb2a* knockout mutant exhibits a drought-sensitive phenotype compared with WT plants (**Figure 3.11**).

Nevertheless, *dreb2a-2* plants showed recovery four days after re-watering, similar to WT. Thus, the drought stress phenotype of *JUB1-OX/dreb2a-2* appears to be weaker than the phenotype observed in single *JUB1-OX* plants. Moreover, *JUB1-OX/dreb2a-2* also showed a weaker phenotype four days after re-watering compared with *JUB1-OX* plants (**Figure 3.11**). This all could be explained by a lower *JUB1* transcript abundance in *JUB1-OX/dreb2a-2* lines. These lines do not show a typical *JUB1-OX*, which resembles a phenotype of GA and BR deficient mutants with shorter petioles and rounder leaf shape. As the expression level of *JUB1* in *JUB1-OX/dreb2a-2* lines is lower than in *JUB1-OX*, plants have a developmental phenotype similar to WT plants. For a more complete investigation into the phenotype of *JUB1-OX/dreb2a-2* plants under drought, another *JUB1-OX/dreb2a-2* line with an expression level of *JUB1* more similar to the expression level of *JUB1* in single *JUB1-OX* plants needs to be included. However, the preliminary data of *JUB1-OX/dreb2a-2* drought experiment, suggests that JUB1 confers drought tolerance not solely through transcriptional control of *DREB2A*.

#### **4.4. JUB1 confers tolerance to drought stress through the regulation of multiple components**

The mechanism through which JUB1 confers tolerance to drought stress is combinatorial. As we have previously shown, *JUB1-OX/dreb2a-2* are more tolerant to drought stress than *dreb2a* knockout mutant, meaning that the drought-tolerant phenotype of *JUB1-OX* does not depend only on the induction of *DREB2A* and the subsequent induction of its downstream drought-related genes. JUB1 possibly regulates the degradation of proline through indirect control of *bZIP63* (**Figure 3.6**). The interaction is believed to occur through another protein as JUB1 does not physically interact with *bZIP63* probe in EMSA, but does immunoprecipitate with *bZIP63* promoter region in ChIP-qPCR (**Figure 3.6**). We also observed higher expression in *JUB1-OX* of the *P5SC1* gene, a key gene in proline synthesis, which could have also resulted in indirect regulation of proline biosynthesis by JUB1 through the regulation of other genes or TF involved in the regulation of *P5SC1* expression (**Figure 3.4**). This hypothesis can be tested using JUB1 protein and *P5SC1* promoter in a transactivation assay. To identify the level of

contribution of proline accumulation to enhanced drought tolerance, *JUB1* mutant plants can be crossed with proline biosynthesis and degradation mutants *P5SC1* and *PDH1*, respectively, to assess the level of proline in these lines and their drought tolerance phenotype.

The lower stomatal conductance in *JUB1-OXs* also suggests a possible involvement of stomatal regulation to the drought-tolerant phenotype. However, so far, we only know that overexpression of *JUB1* under guard-cell specific promoter does not improve drought stress tolerance in Arabidopsis (**Figure 3.9**). Nevertheless, investigating the reasons for the lower stomatal conductance in *JUB1-OXs* can reveal a molecular mechanism of JUB1 action in the guard cells. Furthermore, as mentioned before, studying the stomatal density and stomatal aperture in this line will help understand where the alteration occurs in stomatal development or modulation of stomatal closure. Investigating how development and organ structure are altered in *JUB1-OXs* under drought stress with respect to root development and leaf structure will also contribute to a better understanding of JUB1 function and role in plants upon drought stress.

To study the total number of players involved in this mechanism, the investigation of other upstream, as well as downstream targets could give a better understanding of such a complex process. For that purpose, other target genes downstream of JUB1 can be identified using ChIP-seq and RNA-seq in *JUB1* transgenic lines under control and drought stress conditions. Furthermore, identifying the upstream regulators of *JUB1* can be performed using a transgenic Arabidopsis line expressing luciferase under the control of the *JUB1* promoter with subsequent mutagenesis of the seeds using EMS and screening for mutants that do not show induction of luciferase signal anymore. Such a line is generated and can be used for further EMS analysis. This approach will enable us to identify the affected genes that are upstream regulators of *JUB1* expression.

Collectively, JUB1 provides a new anchor point for future studies of plant growth and its interaction with stress, which holds great promise for improving the tolerance of plants against abiotic stresses in general (**Figure 4.1**)

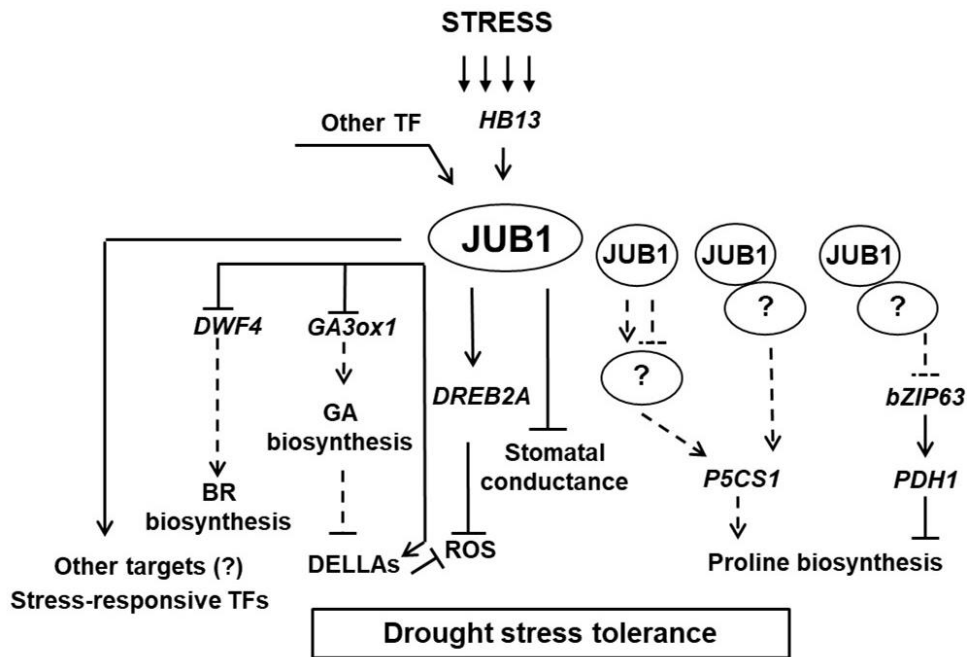


**Figure 4.1. Model of JUB1 action leading to drought stress tolerance.** When the stress occurs, *JUB1* is activated and expressed in part through regulation by *HB13* and another TF that has not been yet reported. *JUB1* acts as a positive regulator of *DREB2A* and a subsequent regulator of ROS level that contributes to drought stress tolerance. *JUB1* is also a negative regulator of BR and GA biosynthesis that acts through suppression of *DWF4*, *GA3ox1*, and promotion of *DELLAs*. *JUB1* is also involved in the regulation of stomatal conductance and proline biosynthesis. The activation of *P5CS1* could occur indirectly through protein-protein or protein-DNA interaction of *JUB1* with other not yet identified regulators or genes. Proline degradation is regulated through the bZIP63-PDH1 pathway. Proteins are shown with circles; dashed lines indicate the preliminary results or hypothesis; ? – unknown proteins or genes; arrows indicate positive regulation; blind end arrows indicate negative regulation.

#### 4.5. Interaction between JUB1 and CaM4

Most proteins do not operate alone but in complexes. It is well known that protein-protein interactions can serve a regulatory role *via* coordination of cellular signaling events as well as metabolic functions in the cell. Understanding protein function in the proper biological context is impossible without considering other proteins involved in the same cellular processes. None of the previous studies on the *JUB1* regulatory network focused on identifying proteins interacting with *JUB1* and studying their roles until today. It was unknown whether *JUB1* can form heterodimers with other TFs and regulate the expression of their target genes.

In this work, *JUB1* was identified as a novel calmodulin-binding protein in *Arabidopsis thaliana*.

Protein-protein interaction for *JUB1* and CaM1/4 proteins were confirmed in yeast and both *Arabidopsis* protoplasts and tobacco leaves using Y2H and BiFC assays (**Figure 3.15**).

According to the National Center for Biotechnology Information, there are three splice variants of *AtCaM1* (*CaM1.1*, *CaM1.2*, and *CaM1.3*) and two isoforms of *AtCaM4* (*CaM4.1* and *CaM4.2*). *CaM1.1* and *CaM4.1* encode proteins with identical amino acid sequences. *AtCaM1* and *AtCaM4* have similar expression patterns in most of the tissues, with the exception that *CaM1* which is highly expressed in pollen and *CaM4* which is highly expressed in dry seeds (Dai et al., 2018). The reason why multiple *CaM* genes encode for the same or similar proteins in plants is not fully understood. Nevertheless, evidence suggests that each of the *CaM* genes could have functional significance due to the different CaM expression, subcellular localization, or different activation of targeting proteins (Duval et al., 2002; Townley and Knight, 2002). Both CaM1 and CaM4 were previously shown to be localized in the nucleus and cytoplasm in tobacco. However, the proteins were expressed under the 35S promoter that might cause artifacts and makes it hard to conclude the natural localization pattern of the protein in the cell (Zhou et al., 2016; Chu et al., 2018). The expression of these proteins under native promoters confirmed that both CaM1 and CaM4 are indeed localized in the nucleus and cytosol (**Figure 3.13**). Expression of JUB1 as a TF is expected but also was confirmed in the nucleus. The co-localization of CaM1/4 and JUB1 in the nucleus fulfils one of the conditions observed for protein-protein interaction; In fact, proteins must exhibit exact localization to be able to interact with each other physically. Another condition for protein-protein interaction involves the protein being expressed under the same condition. This can be tested using a line that has both JUB1 and CaM1/4 expressed under native promoter and fused to some epitope tags making it able to identify proteins by Western blot using available antibodies for the tags, or in case the antibodies for JUB1 and CaM1/4 are available to check the protein levels in the WT plants. Unfortunately, there are no commercially available antibodies for JUB1 and CaM1/4. Due to this fact, JUB1 and CaM1/4 abundance were not quantified on a protein level. Of course, in some cases, induction and expression of the gene do not necessarily result in the same level of protein expression. That is why when analysing the data, we need to keep in mind that the data represents the condition under which *JUB1*, *CaM1*, and *CaM4* genes have increased expression levels. *CaM1* and *CaM4* genes already have high expression levels at the control condition. Nevertheless, the increase in the transcript expression was also observed after several stress conditions like drought and osmotic stress or during plant aging (**Figure 3.14**). The expression pattern of the *JUB1* gene has also increased transcript abundance under the same condition (**Figure 3.14**). The role of CaM has been implicated in response to many physiological processes like light, gravity, mechanical stress, phytohormones, pathogens, osmotic stress, heat shock, and chilling (Tuteja et al., 2007). Overexpression of *CaM1* or *CaM4*

leads to the early senescent phenotype in comparison to wild-type plants. Interestingly, the *cam4* single knock-out mutant does not exhibit any senescent phenotype compared with wild-type plants (Dai et al., 2018). These data indicate that there may be functional redundancy between *CaM1* and *CaM4*, which has to be considered when conducting further genetic studies using *cam1/cam4* lines in both WT and *JUB1-OX* backgrounds. Another anchor point is identifying the role of *CaM1* and *CaM4* in response to drought stress. Until now, no studies on *CaM1* and *CaM4* response to drought stress were reported. *In silico* analysis using publicly available microarray data shows that both genes are induced upon drought and osmotic stress. To test this hypothesis in more detail, drought stress studies in *cam1/cam4* need to be conducted.

Using BiFC assay in protoplasts and the nucleus staining dye Hoechst 33342, it was confirmed that JUB1 CaM4 interaction is localized in the nucleus, as the reconstitution of the YFP signal is co-which supports the co-localization data previously shown for both proteins (**Figure 3.15**). Moreover, the JUB1-CaM4 interaction was shown to be specific since CaM4 did not interact with another NAC transcription factor, ANAC063, which is supported by the quantitative BiFC assay in the *Nicotiana benthamiana* (**Figure 3.15**).

#### **4.6. Localization of active CaM4 binding sites in JUB1 protein**

Recently, the number of identified CaM target proteins has increased (Zhou et al., 2016; Koo et al., 2017; Chu et al., 2018). Since CaM has no catalytic activity of its own, it can only modulate other TFs through direct interaction or the control of kinase-mediated phosphorylation (Yang et al., 2003). Specific transcription factors of the basic helix-loop-helix family upon binding to CaM exhibit a decrease in their protein activity which results in the reduction of their DNA-binding properties (Onions et al., 2000). It was also shown that different CaM isoforms could even work in the antagonistic way where one enhances the DNA binding activity of AtMYB2, but another isoform inhibits it (Yoo et al., 2005). Within the WRKY transcription factor family, CaM could also interact with WRKY7 but only in the presence of calcium (Park et al., 2005).

The identification of the CaM binding site in the JUB1 protein sequence is also important to verify the interaction. The interaction between CaM7 and JAV1 is indeed mediated through *in silico* predicted binding sites; Amino acid substitution in that region led to a decrease or abolishment of the interaction (Yan et al., 2018). CaMs mainly bind targets through hydrophobic interactions with long hydrophobic side chains in the target sites. Bulky hydrophobic amino acids such as Leu, Trp, and others are known to be very important for all



CaM binding motifs (La Verde et al., 2018) which are also present in the JUB1 protein sequence. Thus, a mutation of Trp in the predicted CaM-binding site in PHYTOSULFOKIN RECEPTOR 1 (PSKR1) protein strongly reduced binding of CaM observed in BiFC (Hartmann et al., 2014). In some cases, to observe a complete abolishment of the CaM binding, it was enough to mutate one of four hydrophobic amino acids Val and Phe, mutated to other hydrophilic amino acids Arg or Lys (Wang et al., 2009). However, to detect these changes *in vitro*, a CaM-binding assay was used, which could have some limitations when comparing a change in protein-protein interaction *in vitro* with *in vivo* methods like BiFC.

Analysis of JUB1 protein sequence predicted only one CaM binding site with the highest normalized score (<http://calcium.uhnres.utoronto.ca/>). However, when we mutated Leu in position 121, this did not lead to any change in the protein-protein interaction and suggested that there could be more than one CaM binding site in JUB1 protein. Indeed, this hypothesis was confirmed using split versions of the JUB1 protein (the protein was divided roughly in half), and both parts were confirmed to interact with CaM4. However, since the JUB1<sub>Cterm</sub> region does not include nuclear localization signal, the split protein was not targeted to the nucleus, and the interaction between the JUB1<sub>Cterm</sub> region and CaM4 mainly was occurring in the nucleus. Thus, JUB1 has multiple functional CaM-binding sites on its protein sequence. Previously, multiple CaM-binding sites were reported for a CYCLIC NUCLEOTIDE-GATED CHANNEL12 (CNGC12) in Arabidopsis, also in both N and C termini (DeFalco et al., 2016). These data suggest a complex mode of JUB1 regulation by CaM, which could occur through binding at the different binding sites at specific conditions or developmental stages.

Since there is more than one binding site, we included only one part of the JUB1 protein, the JUB1<sub>Nterm</sub> region, for the mutation analysis of the CaM-binding site. We have shown that the substitution of the Leu 121 is indeed crucial for CaM4 JUB1 interaction, as we observed a strongly reduced binding of CaM4 to JUB1<sub>Nterm</sub>L121A. Thus, this indicates that the predicted CaM-binding site is one of the functional and active CaM-binding sites on JUB1 protein.

The relevance of the amino acid substitution for the interaction of JUB1 with CaM4 should be considered, together with the possible change in the activation of JUB1 direct downstream targets such as *DREB2A*. Additional experiments to test whether or not JUB1 L121A protein could still activate its downstream targets include transactivation assay and EMSA. We previously reported that JUB1 directly targets *DREB2A*, which functions as a positive regulator of a large number of abiotic stress-responsive genes involved in drought and heat stress responses, such as *HsfA3* and *RD29A* (Wu et al., 2012). The decrease in the promoter activity of *DREB2A* upon the addition of CaM4 as a second effector could be explained *via* an

interaction between proteins that occur in the DNA-binding domain of JUB1, leading to inhibition of the DNA-binding properties of JUB1. Due to this fact, the amino acid substitution in the CaM binding site would also mean the alteration of the DNA binding domain of JUB1, which could not only abolish the interaction between JUB1 and CaM4 but also abolish activation of JUB1 downstream targets such as *DREB2A*.

#### **4.7. Involvement of Ca<sup>2+</sup> in the regulation of the interaction between JUB1 and CaM4**

We speculate that JUB1 CaM4 interaction also could be calcium-dependent since none of the CaM binding motifs that were identified in the JUB1 protein sequence are calcium-independent. Moreover, since all buffers used for protoplast transfection include Ca<sup>2+</sup>, the interaction that we observe in the BiFC experiment also in *Nicotiana benthamiana* can be associated with the increased Ca<sup>2+</sup> level, as Ca<sup>2+</sup> increases upon infiltration with *Agrobacterium* as biotic stress (Atkinson et al., 1990). As the use of calcium channel blockers showed some limitations (especially in the transient system) that was connected to the reduction of the RFP signal in rBiFC assay, which makes the further YFP/RFP ratio calculation as a readout of the protein binding/interaction unreliable. To overcome this problem, the stable infiltration of Arabidopsis was performed using with a previously shown *BiFC2in1* construct (with JUB1-nYFP-Myc and CaM4-cYFP-HA). The ectopic expression of RFP served as a control for positive lines. As the YFP signal in this line will be detectable only in the case of the two protein are interacting with each. At the seedling stage, no YFP signal was detected, meaning the interaction does not happen at the early stage of the development. We detected the reconstitution of the YFP signal in the old, already senescent leaves; This observation corresponds with the expression profile of the *JUB1*, *CaM1*, and *CaM4* that are induced in the senescent leaves. During leaf development, Ca<sup>2+</sup>-mediated NO production is known to control *SAGs* expression and the production of SA and H<sub>2</sub>O<sub>2</sub>; this, in turn, acts as signals during the initiation of leaf senescence programs (Ma et al., 2010). In detached leaves of *Petroselinum crispum* an increase in cytosolic Ca<sup>2+</sup> concentration positively correlates with leaf senescence (Huang et al., 1997). Still, not much is known about the concentration of Ca<sup>2+</sup> during natural senescence. However, we hypothesized that during natural senescence, the concentration of Ca<sup>2+</sup> is increasing, transducing the signal further on CaM, which then binds to JUB1. This was confirmed using an *R-GECO* calcium sensor Arabidopsis line during imaging at the same condition as the *BiFC2in1* line.

Indeed, senescent leaves had a higher signal intensity, which also means higher Ca<sup>2+</sup> levels compared with young leaves. Whether or not the calcium level is elevated could also be

checked using live-cell calcium indicators, such as Fura-2 or Fluo-3 (Bush and Jones, 1990; Huang et al., 1997). To further test this hypothesis *in vitro*, pull-down assays will be performed, where JUB1-GST and CaM1-HIS/CaM4-HIS proteins would be incubated together in the presence of  $\text{Ca}^{2+}$  and  $\text{Ca}^{2+}$  chelator agent EGTA. After incubation with agarose beads to bind GST, the complex would be analyzed *via* immunoblotting. Alternatively, far western blot in the presence of  $\text{Ca}^{2+}$  or EGTA also could be performed. Further validation of the interaction *in planta* using co-immunoprecipitation assay can also be performed in seedlings and senescing plants. To this end, we have successfully generated *JUB1-GFP/CaM4-Myc* lines that have been confirmed to produce JUB1-GFP and CaM4-Myc protein fusions.

#### **4.8. The biological relevance of the JUB1 CaM4 interaction in connection to plant senescence**

Our results reveal the condition under which *JUB1* and *CaM4* genes are expressed and the condition under which two proteins interact. These interactions occur in senescent leaves, which we suspect is due to higher  $\text{Ca}^{2+}$  levels. Interestingly the phenotypic differences between single *JUB1-OX* and double *JUB1-OX/CaM4-OX* are also observed in connection to senescence through chlorophyll content and the difference in SAGs expression (**Figure 3.23**). Overexpression of *CaM4* leads to an early-senescence phenotype, which is opposite to the reported phenotype of *JUB1-OX* (Wu et al., 2012; Dai et al., 2018). These data indicate that the interaction between JUB1 and CaM4 is specific to the older plant age, particularly during senescence, and the biological relevance of this interaction might be connected to its regulation. The functional CaM-binding site was confirmed *via* introducing a mutation to the JUB1 protein sequence that led to the reduced binding of CaM observed in BiFC. As the binding site is located in the DNA-binding domain of JUB1, we suspect that the binding of JUB1 to its downstream targets might be disrupted by interaction with CaM4. As the interaction occurs during senescence, we suspect that the senescence-related downstream targets of JUB1 could be affected in this case. Under the condition of transactivation assay performed in Arabidopsis protoplasts and transiently infiltrated leaves of *Nicotiana benthamiana*, using two different sets of vectors for this, we observed a decrease in the promoter activity of the *DREB2A* gene when both CAM4 and JUB1 are expressed at the same time. That confirms the hypothesis that the interaction between JUB1 and CaM4 prevents JUB1 (at least to some extent) from binding and regulating some of its downstream targets. To identify more of the affected downstream targets, RNA-seq data derived from *JUB1-OX/CaM4-OX*, *CaM4-OX*, *JUB1-OX*, and WT, are currently being analyzed. These samples were harvested shortly before observing any difference in

senescence-related phenotype, and should reveal downstream targets of JUB1 that have altered expression in *JUB1-OX/CaM4-OX* compared with *JUB1-OX*. To further investigate how CaM binding affects the function of JUB1, a stable line with a mutated CaM site could be analyzed; However, due to the fact that JUB1 has multiple CaM-binding sites and the confirmation of the binding site only in the N<sub>term</sub> part of the protein was investigated, one has to either locate other CaM binding sites and mutate them, or also generate and analyze the *JUB1-OX* line that would have only JUB1<sub>Nterm</sub> part. Unfortunately, it is difficult to predict how the function of the TF will change if only half of the protein is expressed. As the *jub1 crispr* line has also been created in the scope of this thesis, this line can be further used to create the complementation lines to analyze the importance of CaM binding to JUB1. This approach has also been studied with *Arabidopsis thaliana* *SIGNAL RESPONSIVE 1* (*AtSR1*) when *AtSR1* with impaired CaM-binding ability was overexpressed in *atsr1* mutant plants. In this case, plant resistance to herbivore attack was not restored to WT level, suggesting that CaM binding was critical for the response to wound signaling (Qiu et al., 2012). A limitation to this study is that the mutation of the CaM-binding site of the DNA-binding domain of JUB1 could change JUB1 binding to its targets and affect the phenotype.

Collectively our data suggest a model of JUB1 CaM4 interaction that is dependent on the plant's age and the level of calcium in the cells (**Figure 4.2**). The fact that overexpression of *JUB1* both enhances drought tolerance and delays senescence in plants makes it an ideal candidate for improving drought tolerance and productivity in major crops. Thus, the findings of this PhD work can be used for further application in crops and may be of great importance for enhancing crop yield under current climate change conditions.

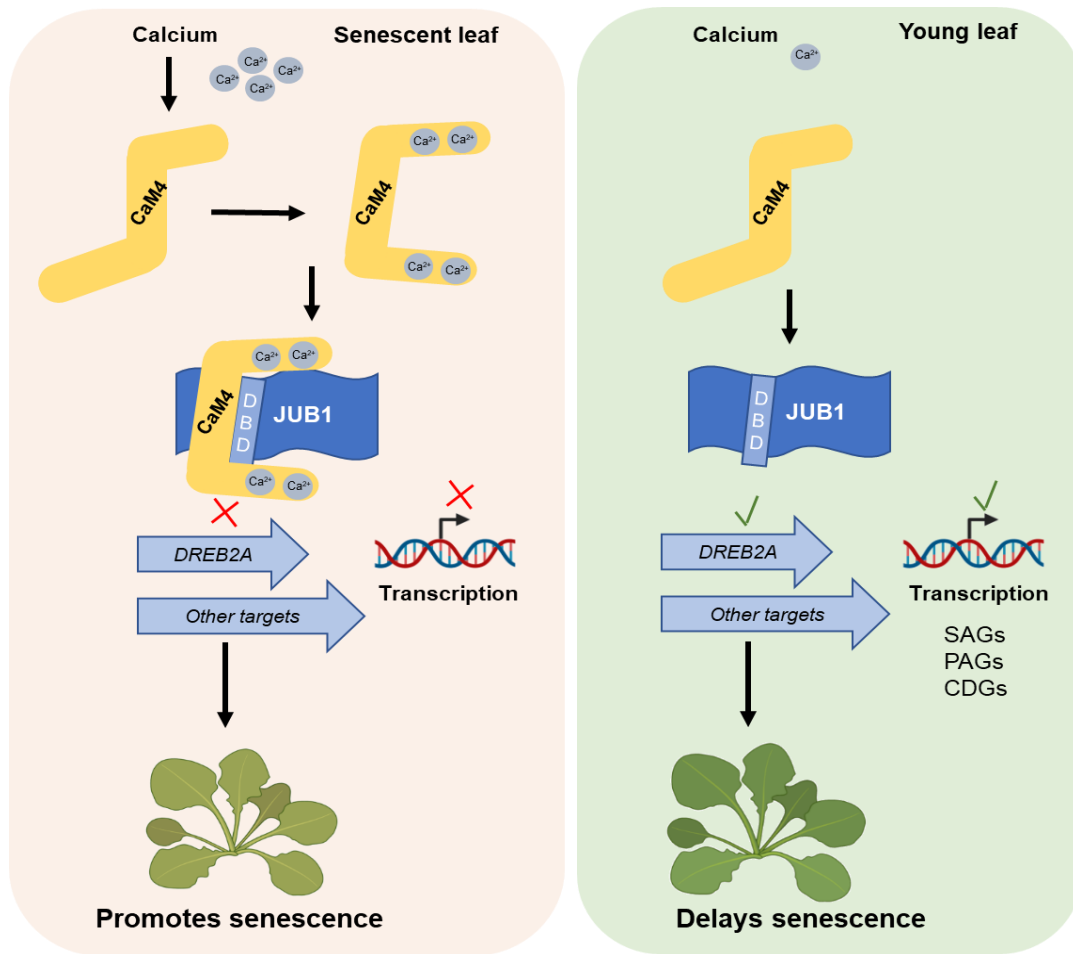


**Figure 4.2. Model of JUB1 CaM4 interaction.** When the intracellular concentration of Ca<sup>2+</sup> increases during leaf senescence, the Ca<sup>2+</sup> signal is transduced further to CaM4. The binding of Ca<sup>2+</sup> ions leads to changes in the conformation of CaM4, promoting its binding to JUB1 protein, where at least one of the binding occurs at the DBD region of the JUB1 protein. This binding prevents JUB1 from fully performing its previously reported function to delay senescence through transcriptional regulation of its downstream targets like *DREB2A* and other senescence-associated genes. DBD, DNA-binding domain; SAGs, senescence-associated genes; PAGs, photosynthesis-associated genes; CDGs, chlorophyll degradation genes. The image was created using BioRender.com

## 5. REFERENCES

- Abbas N, Maurya JP, Senapati D, Gangappa SN, Chattopadhyay S** (2014) Arabidopsis CAM7 and HY5 physically interact and directly bind to the HY5 promoter to regulate its expression and thereby promote photomorphogenesis. *Plant Cell* **26**: 1036-1052
- Abdula SE, Lee H-J, Ryu H, Kang KK, Nou I, Sorrells ME, Cho Y-G** (2016) Overexpression of *BrCIPK1* gene enhances abiotic stress tolerance by increasing proline biosynthesis in rice. *Plant Molecular Biology Reporter* **34**: 501-511
- Abrahám E, Rigó G, Székely G, Nagy R, Koncz C, Szabados L** (2003) Light-dependent induction of proline biosynthesis by abscisic acid and salt stress is inhibited by brassinosteroid in Arabidopsis. *Plant Molecular Biology* **51**: 363-372
- Agurla S, Raghavendra AS** (2016) Convergence and divergence of signaling events in guard cells during stomatal closure by plant hormones or microbial elicitors. *Frontiers in Plant Science* **7**: 1332-1332
- Ahammed GJ, Li X, Wan H, Zhou G, Cheng Y** (2020) SlWRKY81 reduces drought tolerance by attenuating proline biosynthesis in tomato. *Scientia Horticulturae* **270**: 109444
- Aharoni A, Dixit S, Jetter R, Thoenes E, van Arkel G, Pereira A** (2004) The SHINE clade of AP2 domain transcription factors activates wax biosynthesis, alters cuticle properties, and confers drought tolerance when overexpressed in Arabidopsis. *Plant Cell* **16**: 2463-2480
- Aleksza D, Horváth GV, Sándor G, Szabados L** (2017) Proline accumulation is regulated by transcription factors associated with phosphate starvation. *Plant Physiology* **175**: 555-567
- Allen GJ, Schroeder JI** (2001) Combining genetics and cell biology to crack the code of plant cell calcium signaling. *Science Signaling* **2001**: re13
- Alshareef NO, Wang JY, Ali S, Al-Babili S, Tester M, Schmöckel SM** (2019) Overexpression of the NAC transcription factor JUNGBRUNNEN1 (JUB1) increases salinity tolerance in tomato. *Plant Physiology and Biochemistry* **140**: 113-121
- Amini S, Ghobadi C, Yamchi A** (2015) Proline accumulation and osmotic stress: an overview of *P5CS* gene in plants. *Journal of Plant Molecular Breeding* **3**: 44-55
- An Y, Zhang M, Liu G, Han R, Liang Z** (2013) Proline accumulation in leaves of *Periploca sepium* via both biosynthesis up-regulation and transport during recovery from severe drought. *PLOS One* **8**: e69942
- Arteaga S, Yabor L, Díez MJ, Prohens J, Boscaiu M, Vicente O** (2020) The use of proline in screening for tolerance to drought and salinity in common bean (*Phaseolus vulgaris* L.) Genotypes. **10**: 817
- Arvidsson S, Kwasniewski M, Riaño-Pachón DM, Mueller-Roeber B** (2008) QuantPrime – a flexible tool for reliable high-throughput primer design for quantitative PCR. *BMC Bioinformatics* **9**: 465
- Assmann SM** (1993) Signal transduction in guard cells. *Annual Review of Cell Biology* **9**: 345-375
- Atkinson MM, Keppler LD, Orlandi EW, Baker CJ, Mischke CF** (1990) Involvement of plasma membrane calcium influx in bacterial induction of the K<sup>+</sup>/H<sup>+</sup> and hypersensitive responses in tobacco. *Plant Physiology* **92**: 215-221
- Balazadeh S, Wu A, Mueller-Roeber B** (2010) Salt-triggered expression of the ANAC092-dependent senescence regulon in *Arabidopsis thaliana*. *Plant Signaling & Behavior* **5**: 733-735

- Baltes NJ, Gil-Humanes J, Voytas DF** (2017) Genome engineering and agriculture: opportunities and challenges. *Progress in Molecular Biology and Translational Science* **149**: 1-26
- Basu S, Ramegowda V, Kumar A, Pereira A** (2016) Plant adaptation to drought stress. *F1000Research* **5**: F1000 Faculty Review-1554
- Bates LS, Waldren RP, Teare ID** (1973) Rapid determination of free proline for water-stress studies. *Plant and Soil* **39**: 205-207
- Batistič O, Kudla J** (2012) Analysis of calcium signaling pathways in plants. *Biochimica et Biophysica Acta (BBA) - General Subjects* **1820**: 1283-1293
- Baum G, Lev-Yadun S, Fridmann Y, Arazi T, Katsnelson H, Zik M, Fromm H** (1996) Calmodulin binding to glutamate decarboxylase is required for regulation of glutamate and GABA metabolism and normal development in plants. *EMBO Journal* **15**: 2988-2996
- Bergey DR, Kandel R, Tyree BK, Dutt M, Dhekney SA** (2014) The role of calmodulin and related proteins in plant cell function: an ever-thickening plot. *Springer Science Reviews* **2**: 145-159
- Bodner G, Nakhforoosh A, Kaul H-P** (2015) Management of crop water under drought: a review. *Agronomy for Sustainable Development* **35**: 401-442
- Bonza MC, Morandini P, Luoni L, Geisler M, Palmgren MG, De Michelis MI** (2000) *AtACA8* encodes a plasma membrane-localized calcium-ATPase of *Arabidopsis* with a calmodulin-binding domain at the N-terminus. *Plant Physiology* **123**: 1495
- Borsani O, Zhu J, Verslues PE, Sunkar R, Zhu J-K** (2005) Endogenous siRNAs derived from a pair of natural cis-antisense transcripts regulate salt tolerance in *Arabidopsis*. *Cell* **123**: 1279-1291
- Boudsoq M, Willmann MR, McCormack M, Lee H, Shan L, He P, Bush J, Cheng S-H, Sheen J** (2010) Differential innate immune signaling *via* Ca<sup>2+</sup> sensor protein kinases. *Nature* **464**: 418-422
- Braam J, Davis RW** (1990) Rain-, wind-, and touch-induced expression of calmodulin and calmodulin-related genes in *Arabidopsis*. *Cell* **60**: 357-364
- Bradford MM** (1976) A rapid and sensitive method for the quantitation of microgram quantities of protein utilizing the principle of protein-dye binding. *Analytical Biochemistry* **72**: 248-254
- Burnette WN** (1981) "Western Blotting": Electrophoretic transfer of proteins from sodium dodecyl sulfate-polyacrylamide gels to unmodified nitrocellulose and radiographic detection with antibody and radioiodinated protein A. *Analytical Biochemistry* **112**: 195-203
- Bush DS, Jones RL** (1990) Measuring intracellular Ca<sup>2+</sup> levels in plant cells using the fluorescent probes, Indo-1 and Fura-2: progress and prospects. *Plant Physiology* **93**: 841-845
- Büßis D, von Groll U, Fisahn J, Altmann T** (2006) Stomatal aperture can compensate altered stomatal density in *Arabidopsis thaliana* at growth light conditions. *Functional Plant Biology*. **33**: 1037-1043
- Butt HI, Yang Z, Chen E, Zhao G, Gong Q, Yang Z, Zhang X, Li F** (2017) Functional characterization of cotton GaMYB62L, a novel R2R3 TF in transgenic *Arabidopsis*. *PLOS One* **12**: e0170578
- Cahoon EB, Shanklin J, Ohlrogge JB** (1992) Expression of a coriander desaturase results in petroselinic acid production in transgenic tobacco. *Proceedings of the National Academy of Sciences of the United States of America* **89**: 11184-11188
- Caine RS, Yin X, Sloan J, Harrison EL, Mohammed U, Fulton T, Biswal AK, Dionora J, Chater CC, Coe RA, Bandyopadhyay A, Murchie EH, Swarup R, Quick WP, Gray**

- JE** (2019) Rice with reduced stomatal density conserves water and has improved drought tolerance under future climate conditions. *New Phytologist* **221**: 371-384
- Castillo N, Pastor V, Chávez Á, Arró M, Boronat A, Flors V, Ferrer A, Altabella T** (2019) Inactivation of UDP-Glucose sterol glucosyltransferases enhances Arabidopsis resistance to *Botrytis cinerea*. *Frontiers in Plant Science* **10**: 1162
- Castrillo G, Turck F, Leveugle M, Lecharny A, Carbonero P, Coupland G, Paz-Ares J, Oñate-Sánchez L** (2011) Speeding cis-trans regulation discovery by phylogenomic analyses coupled with screenings of an arrayed library of Arabidopsis transcription factors. *PLOS One* **6**: e21524
- Chen G, Wang Y, Wang X, Yang Q, Quan X, Zeng J, Dai F, Zeng F, Wu F, Zhang G, Chen Z-H** (2019) Leaf epidermis transcriptome reveals drought-induced hormonal signaling for stomatal regulation in wild barley. *Plant Growth Regulation* **87**: 39-54
- Chen Z, Fang X, Yuan X, Zhang Y, Li H, Zhou Y, Cui X** (2021) Overexpression of transcription factor *GmTGA15* enhances drought tolerance in transgenic soybean hairy roots and Arabidopsis plants. *Agronomy* **11**: 170
- Chernyad'ev II** (2005) Effect of water stress on the photosynthetic apparatus of plants and the protective role of cytokinins: a review. *Applied Biochemistry and Microbiology* **41**: 115-128
- Chiasson D, Ekengren SK, Martin GB, Dobney SL, Snedden WA** (2005) Calmodulin-like proteins from Arabidopsis and tomato are involved in host defense against *Pseudomonas syringae* pv. tomato. *Plant Molecular Biology* **58**: 887-897
- Choi H, Oh E** (2016) PIF4 Integrates multiple environmental and hormonal signals for plant growth regulation in Arabidopsis. *Molecules and Cells* **39**: 587-593
- Chu M, Li J, Zhang J, Shen S, Li C, Gao Y, Zhang S** (2018) AtCaM4 interacts with a Sec14-like protein, PATL1, to regulate freezing tolerance in Arabidopsis in a CBF-independent manner. *Journal of Experimental Botany* **69**: 5241-5253
- Crivici A, Ikura M** (1995) Molecular and structural basis of target recognition by calmodulin. *Annual Review of Biophysics and Biomolecular Structure* **24**: 85-116
- Dai C, Lee Y, Lee IC, Nam HG, Kwak JM** (2018) Calmodulin 1 regulates senescence and ABA response in Arabidopsis. *Frontiers in Plant Science* **9**: 803
- Daneshmand F, Arvin MJ, Kalantari KM** (2009) Physiological responses to NaCl stress in three wild species of potato *in vitro*. *Acta Physiologiae Plantarum* **32**: 91
- Daszkowska-Golec A, Szarejko I** (2013) Open or close the gate - stomata action under the control of phytohormones in drought stress conditions. *Frontiers in Plant Science* **4**: 138-138
- Davies WJ, Jones HG** (1991) Physiology and biochemistry of abscisic acid. *Journal of Experimental Botany* **42**: 7-17
- de Ronde JA, Laurie RN, Caetano T, Greyling MM, Kerepesi I** (2004) Comparative study between transgenic and non-transgenic soybean lines proved transgenic lines to be more drought tolerant. *Euphytica* **138**: 123-132
- DeFalco TA, Marshall CB, Munro K, Kang H-G, Moeder W, Ikura M, Snedden WA, Yoshioka K** (2016) Multiple calmodulin-binding sites positively and negatively regulate Arabidopsis CYCLIC NUCLEOTIDE-GATED CHANNEL12. *Plant Cell* **28**: 1738-1751
- Deuschle K, Funck D, Forlani G, Stransky H, Biehl A, Leister D, van der Graaff E, Kunze R, Frommer WB** (2004) The role of [Delta]1-pyrroline-5-carboxylate dehydrogenase in proline degradation. *Plant Cell* **16**: 3413-3425
- Di Blasi S, Puliga S, Losi L, Vazzana C** (1998) *S. stapfianus* and *E. curvula* cv. *Consol in vivo* photosynthesis, PSII activity and ABA content during dehydration. *Plant Growth Regulation* **25**: 97-104



- Dietrich K, Weltmeier F, Ehlert A, Weiste C, Stahl M, Harter K, Dröge-Laser W** (2011) Heterodimers of the transcription factors bZIP1 and bZIP53 reprogram amino acid metabolism during low energy stress. *Plant Cell* **23**: 381
- Ding Z, Li S, An X, Liu X, Qin H, Wang D** (2009) Transgenic expression of MYB15 confers enhanced sensitivity to abscisic acid and improved drought tolerance in *Arabidopsis thaliana*. *Journal of Genetics and Genomics* **36**: 17-29
- Du L, Poovaiah BW** (2005) Ca<sup>2+</sup>/calmodulin is critical for brassinosteroid biosynthesis and plant growth. *Nature* **437**: 741-745
- Duval FD, Renard M, Jaquinod M, Biou V, Montrichard F, Macherel D** (2002) Differential expression and functional analysis of three calmodulin isoforms in germinating pea (*Pisum sativum* L.) seeds. *Plant Journal* **32**: 481-493
- Ebrahimian-Motlagh S, Ribone PA, Thirumalaikumar VP, Allu AD, Chan RL, Mueller-Roeber B, Balazadeh S** (2017) JUNGBRUNNEN1 confers drought tolerance downstream of the HD-Zip I transcription factor AtHB13. *Frontiers in Plant Science* **8**: 2118-2118
- Elhaddad NS, Hunt L, Sloan J, Gray JE** (2014) Light-induced stomatal opening is affected by the guard cell protein kinase APK1b. *PLOS One* **9**: e97161-e97161
- Evans NH, McAinsh MR, Hetherington AM** (2001) Calcium oscillations in higher plants. *Current Opinion in Plant Biology* **4**: 415-420
- Fàbregas N, Lozano-Elena F, Blasco-Escámez D, Tohge T, Martínez-Andújar C, Albacete A, Osorio S, Bustamante M, Riechmann JL, Nomura T, Yokota T, Conesa A, Alfocea FP, Fernie AR, Caño-Delgado AI** (2018) Overexpression of the vascular brassinosteroid receptor BRL3 confers drought resistance without penalizing plant growth. *Nature Communications* **9**: 4680
- Fabro G, Kovács I, Pavet V, Szabados L, Alvarez ME** (2004) Proline accumulation and AtP5CS2 gene activation are induced by plant-pathogen incompatible interactions in *Arabidopsis*. *Molecular Plant-Microbe Interactions* **17**: 343-350
- Farooq M, Wahid A, Kobayashi N, Fujita D, Basra SMA** (2009) Plant drought stress: effects, mechanisms and management. *Agronomy for Sustainable Development* **29**: 185-212
- Ferguson JN** (2019) Climate change and abiotic stress mechanisms in plants. *Emerging Topics in Life Sciences* **3**: 165-181
- Fichman Y, Gerdes SY, Kovács H, Szabados L, Zilberstein A, Csonka LN** (2015) Evolution of proline biosynthesis: enzymology, bioinformatics, genetics, and transcriptional regulation. *Biological reviews of the Cambridge Philosophical Society* **90**: 1065-1099
- Fischer C, Kugler A, Hoth S, Dietrich P** (2013) An IQ domain mediates the interaction with calmodulin in a plant cyclic nucleotide-gated channel. *Plant & Cell Physiology* **54**: 573-584
- Franz S, Ehlert B, Liese A, Kurth J, Cazalé AC, Romeis T** (2011) Calcium-dependent protein kinase CPK21 functions in abiotic stress response in *Arabidopsis thaliana*. *Molecular Plant* **4**: 83-96
- Fryer MJ, Oxborough K, Mullineaux PM, Baker NR** (2002) Imaging of photo-oxidative stress responses in leaves. *Journal of Experimental Botany* **53**: 1249-1254
- Funck D, Eckard S, Müller G** (2010) Non-redundant functions of two proline dehydrogenase isoforms in *Arabidopsis*. *BMC Plant Biology* **10**: 70-70
- Funck D, Stadelhofer B, Koch W** (2008) Ornithine- $\delta$ -aminotransferase is essential for Arginine Catabolism but not for Proline Biosynthesis. *BMC Plant Biology* **8**: 40
- Furumoto T, Ogawa N, Hata S, Izui K** (1996) Plant calcium-dependent protein kinase-related kinases (CRKs) do not require calcium for their activities. *FEBS Letters* **396**: 147-151

- Galon Y, Aloni R, Nachmias D, Snir O, Feldmesser E, Scrase-Field S, Boyce JM, Bouché N, Knight MR, Fromm H** (2010) Calmodulin-binding transcription activator 1 mediates auxin signaling and responds to stresses in *Arabidopsis*. *Planta* **232**: 165-178
- Galon Y, Nave R, Boyce JM, Nachmias D, Knight MR, Fromm H** (2008) Calmodulin-binding transcription activator (CAMTA) 3 mediates biotic defense responses in *Arabidopsis*. *FEBS Letters* **582**: 943-948
- Garapati P, Xue G-P, Munné-Bosch S, Balazadeh S** (2015) Transcription factor ATAF1 in *Arabidopsis* promotes senescence by direct regulation of key chloroplast maintenance and senescence transcriptional cascades. *Plant Physiology* **168**: 1122
- Gehring CA, Williams DA, Cody SH, Parish RW** (1990) Phototropism and geotropism in maize coleoptiles are spatially correlated with increases in cytosolic free calcium. *Nature* **345**: 528-530
- Giberti S, Funck D, Forlani G** (2014)  $\Delta$ 1-pyrroline-5-carboxylate reductase from *Arabidopsis thaliana*: stimulation or inhibition by chloride ions and feedback regulation by proline depend on whether NADPH or NADH acts as co-substrate. *New Phytologist* **202**: 911-919
- Gilroy S, Fricker MD, Read ND, Trewavas AJ** (1992) The role of  $Ca^{2+}$  and ABA in the regulation of stomatal aperture. In: CM Karssen, LC van Loon, D Vreugdenhil, eds, *Progress in Plant Growth Regulation: Proceedings of the 14th International Conference on Plant Growth Substances*, Amsterdam, 21–26 July, 1991. Springer Netherlands, Dordrecht, pp 105-115
- Giménez C, Gallardo M, Thompson RB** (2013) Plant–water relations. in: reference module in earth systems and environmental sciences. Elsevier
- Gong M, Li Y-J, Dai X, Tian M, Li Z-G** (1997) Involvement of calcium and calmodulin in the acquisition of heat-shock induced thermotolerance in maize seedlings. *Journal of Plant Physiology* **150**: 615-621
- Grefen C, Blatt MR** (2012) A 2in1 cloning system enables ratiometric bimolecular fluorescence complementation (rBiFC). *BioTechniques* **53**: 311-314
- Grimsley N, Hohn B, Hohn T, Walden R** (1986) “Agroinfection,” an alternative route for viral infection of plants by using the Ti plasmid. *Proceedings of the National Academy of Sciences* **83**: 3282
- Groppa MD, Benavides MP** (2008) Polyamines and abiotic stress: recent advances. *Amino Acids* **34**: 35-45
- Guo L, Yang H, Zhang X, Yang S** (2013) Lipid Transfer Protein 3 as a target of MYB96 mediates freezing and drought stress in *Arabidopsis*. *Journal of Experimental Botany* **64**: 1755-1767
- Guo X, Zhang L, Wang X, Zhang M, Xi Y, Wang A, Zhu J** (2019) Overexpression of *Saussurea involucreata* dehydrin gene *SiDHN* promotes cold and drought tolerance in transgenic tomato plants. *PLOS One* **14**: e0225090
- Hall MC, Lowry DB, Willis JH** (2010) Is local adaptation in *Mimulus guttatus* caused by trade-offs at individual loci? *Molecular Ecology* **19**: 2739-2753
- Hanson J, Hanssen M, Wiese A, Hendriks MMWB, Smeekens S** (2008) The sucrose regulated transcription factor bZIP11 affects amino acid metabolism by regulating the expression of *ASPARAGINE SYNTHETASE1* and *PROLINE DEHYDROGENASE2*. *Plant Journal* **53**: 935-949
- Harper JF** (2001) Dissecting calcium oscillators in plant cells. *Trends in Plant Science* **6**: 395-397
- Hartmann J, Fischer C, Dietrich P, Sauter M** (2014) Kinase activity and calmodulin binding are essential for growth signaling by the phytosulfokine receptor PSKR1. *Plant Journal* **78**: 192-202

- He M, He C-Q, Ding N-Z** (2018) Abiotic stresses: general defenses of land plants and chances for engineering multistress tolerance. *Frontiers in Plant Science* **9**: 1771
- Hellens RP, Allan AC, Friel EN, Bolitho K, Grafton K, Templeton MD, Karunairetnam S, Gleave AP, Laing WA** (2005) Transient expression vectors for functional genomics, quantification of promoter activity and RNA silencing in plants. *Plant Methods* **1**: 13-13
- Hepler PK, Winship LJ** (2010) Calcium at the cell wall-cytoplasm interface. *Journal of Integrative Plant Biology* **52**: 147-160
- Hepworth C, Doheny-Adams T, Hunt L, Cameron DD, Gray JE** (2015) Manipulating stomatal density enhances drought tolerance without deleterious effect on nutrient uptake. *New Phytologist* **208**: 336-341
- Hoeflich KP, Ikura M** (2002) Calmodulin in action: diversity in target recognition and activation mechanisms. *Cell* **108**: 739-742
- Hong B, Ichida A, Wang Y, Scott Gens J, Pickard BG, Harper JF** (1999) Identification of a calmodulin-regulated Ca<sup>2+</sup>-ATPase in the endoplasmic reticulum. *Plant Physiology* **119**: 1165
- Hong Z, Lakkineni K, Zhang Z, Verma DP** (2000) Removal of feedback inhibition of delta(1)-pyrroline-5-carboxylate synthetase results in increased proline accumulation and protection of plants from osmotic stress. *Plant Physiology* **122**: 1129-1136
- Hooper CM, Tanz SK, Castleden IR, Vacher MA, Small ID, Millar AH** (2014) SUBAcon: a consensus algorithm for unifying the subcellular localization data of the Arabidopsis proteome. *Bioinformatics* **30**: 3356-3364
- Hrabak EM, Chan CWM, Gribskov M, Harper JF, Choi JH, Halford N, Kudla J, Luan S, Nimmo HG, Sussman MR, Thomas M, Walker-Simmons K, Zhu J-K, Harmon AC** (2003) The Arabidopsis CDPK-SnRK superfamily of protein kinases. *Plant Physiology* **132**: 666
- Hua XJ, van de Cotte B, Van Montagu M, Verbruggen N** (1997) Developmental regulation of pyrroline-5-carboxylate reductase gene expression in Arabidopsis. *Plant Physiology* **114**: 1215
- Huang FY, Philosop-Hadas S, Meir S, Callahan DA, Sabato R, Zelcer A, Hepler PK** (1997) Increases in cytosolic Ca<sup>2+</sup> in parsley mesophyll cells correlate with leaf senescence. *Plant Physiology* **115**: 51-60
- Hughes J, Hepworth C, Dutton C, Dunn JA, Hunt L, Stephens J, Waugh R, Cameron DD, Gray JE** (2017) Reducing stomatal density in barley improves drought tolerance without impacting on yield. *Plant Physiology* **174**: 776
- Ibarra-Caballero J, Villanueva-Verduzco C, Molina-GalÁN J, SÁNchez-De-JimÉNez E** (1988) Proline accumulation as a symptom of drought stress in maize: a tissue differentiation requirement. *Journal of Experimental Botany* **39**: 889-897
- Ishida H, Vogel HJ** (2006) Protein-peptide interaction studies demonstrate the versatility of calmodulin target protein binding. *Protein & Peptide Letters* **13**: 455-465
- Jahan MA, Harris B, Lowery M, Coburn K, Infante AM, Percifield RJ, Ammer AG, Kovinich N** (2019) The NAC family transcription factor GmNAC42-1 regulates biosynthesis of the anticancer and neuroprotective glyceollins in soybean. *BMC Genomics* **20**: 149
- Kang G, Yan D, Chen X, Yang L, Zeng R** (2020) HbWRKY82, a novel Ilc WRKY transcription factor from *Hevea brasiliensis* associated with abiotic stress tolerance and leaf senescence in Arabidopsis. *Physiologia Plantarum* **171**: 151-160
- Kant P, Gordon M, Kant S, Zolla G, Davydov O, Heimer YM, Chalifa-Caspi V, Shaked R, Barak S** (2008) Functional-genomics-based identification of genes that regulate

- Arabidopsis responses to multiple abiotic stresses. *Plant, Cell & Environment* **31**: 697-714
- Kaplan F, Kopka J, Sung DY, Zhao W, Popp M, Porat R, Guy CL** (2007) Transcript and metabolite profiling during cold acclimation of Arabidopsis reveals an intricate relationship of cold-regulated gene expression with modifications in metabolite content. *Plant Journal* **50**: 967-981
- Karimi M, Inzé D, Depicker A** (2002) GATEWAY vectors for Agrobacterium-mediated plant transformation. *Trends in Plant Science* **7**: 193-195
- Kaufmann K, Muiño JM, Østerås M, Farinelli L, Krajewski P, Angenent GC** (2010) Chromatin immunoprecipitation (ChIP) of plant transcription factors followed by sequencing (ChIP-SEQ) or hybridization to whole genome arrays (ChIP-CHIP). *Nature Protocols* **5**: 457-472
- Keinath NF, Waadt R, Brugman R, Schroeder Julian I, Grossmann G, Schumacher K, Krebs M** (2015) Live cell imaging with R-GECO1 sheds light on flg22- and chitin-induced transient  $[Ca^{2+}]_{cyt}$  patterns in Arabidopsis. *Molecular Plant* **8**: 1188-1200
- Kelly G, Lugassi N, Belausov E, Wolf D, Khamaisi B, Brandsma D, Kottapalli J, Fidel L, Ben-Zvi B, Egbaria A, Acheampong AK, Zheng C, Or E, Distelfeld A, David-Schwartz R, Carmi N, Granot D** (2017) The *Solanum tuberosum* KST1 partial promoter as a tool for guard cell expression in multiple plant species. *Journal of Experimental Botany* **68**: 2885-2897
- Kim HS, Park BO, Yoo JH, Jung MS, Lee SM, Han HJ, Kim KE, Kim SH, Lim CO, Yun DJ, Lee SY, Chung WS** (2007) Identification of a calmodulin-binding NAC protein as a transcriptional repressor in Arabidopsis. *Journal of Biological Chemistry* **282**: 36292-36302
- Kim MC, Chung WS, Yun D-J, Cho MJ** (2009) Calcium and Calmodulin-Mediated Regulation of Gene Expression in Plants. *Molecular Plant* **2**: 13-21
- Kim TH, Böhmer M, Hu H, Nishimura N, Schroeder JI** (2010) Guard cell signal transduction network: advances in understanding abscisic acid, CO<sub>2</sub>, and Ca<sup>2+</sup> signaling. *Annual Review of Plant Biology* **61**: 561-591
- Kiran U, Abdin MZ** (2012) Computational predictions of common transcription factor binding sites on the genes of proline metabolism in plants. *Bioinformatics* **8**: 886-890
- Kiyosue T, Yoshiba Y, Yamaguchi-Shinozaki K, Shinozaki K** (1996) A nuclear gene encoding mitochondrial proline dehydrogenase, an enzyme involved in proline metabolism, is upregulated by proline but downregulated by dehydration in Arabidopsis. *Plant Cell* **8**: 1323-1335
- Knight H, Trewavas AJ, Knight MR** (1996) Cold calcium signaling in Arabidopsis involves two cellular pools and a change in calcium signature after acclimation. *Plant Cell* **8**: 489-503
- Knight H, Trewavas AJ, Knight MR** (1997) Calcium signalling in *Arabidopsis thaliana* responding to drought and salinity. *Plant Journal* **12**: 1067-1078
- Knight MR, Campbell AK, Smith SM, Trewavas AJ** (1991) Transgenic plant aequorin reports the effects of touch and cold-shock and elicitors on cytoplasmic calcium. *Nature* **352**: 524-526
- Kocsy G, Laurie R, Szalai G, Szilágyi V, Simon-Sarkadi L, Galiba G, De Ronde JA** (2005) Genetic manipulation of proline levels affects antioxidants in soybean subjected to simultaneous drought and heat stresses. *Physiologia Plantarum* **124**: 227-235
- Köhler B, Hills A, Blatt MR** (2003) Control of guard cell ion channels by hydrogen peroxide and abscisic acid indicates their action through alternate signaling pathways. *Plant Physiology* **131**: 385

- Kolukisaoglu Ü, Weini S, Blazevic D, Batistic O, Kudla J** (2004) Calcium sensors and their interacting protein kinases: genomics of the Arabidopsis and rice CBL-CIPK signaling networks. *Plant Physiology* **134**: 43
- Koo JC, Lee IC, Dai C, Lee Y, Cho HK, Kim Y, Phee BK, Kim H, Lee IH, Choi SH, Park SJ, Jeon IS, Nam HG, Kwak JM** (2017) The protein trio RPK1-CaM4-RbohF mediates transient superoxide production to trigger age-dependent cell death in Arabidopsis. *Cell Reports* **21**: 3373-3380
- Kooyers NJ** (2015) The evolution of drought escape and avoidance in natural herbaceous populations. *Plant Science* **234**: 155-162
- Kovtun Y, Chiu WL, Tena G, Sheen J** (2000) Functional analysis of oxidative stress-activated mitogen-activated protein kinase cascade in plants. *Proceedings of the National Academy of Sciences of the United States of America* **97**: 2940-2945
- Kudla J, Becker D, Grill E, Hedrich R, Hippler M, Kummer U, Parniske M, Romeis T, Schumacher K** (2018) Advances and current challenges in calcium signaling. *New Phytologist* **218**: 414-431
- Kudla J, Xu Q, Harter K, Gruissem W, Luan S** (1999) Genes for calcineurin B-like proteins in Arabidopsis are differentially regulated by stress signals. *Proceedings of the National Academy of Sciences of the United States of America* **96**: 4718-4723
- Kumar S, Sachdeva S, Bhat KV, Vats S** (2018) Plant responses to drought stress: physiological, biochemical and molecular basis. In: S Vats, ed, biotic and abiotic stress tolerance in plants. Springer Singapore, Singapore, pp 1-25
- Kuromori T, Seo M, Shinozaki K** (2018) ABA transport and plant water stress responses. *Trends in Plant Science* **23**: 513-522
- Kushwaha R, Singh A, Chattopadhyay S** (2008) Calmodulin7 plays an important role as transcriptional regulator in Arabidopsis seedling development. *Plant Cell* **20**: 1747-1759
- La Verde V, Dominici P, Astegno A** (2018) Towards understanding plant calcium signaling through calmodulin-like proteins: a biochemical and structural perspective. *International Journal of Molecular Sciences* **19**: 1331
- Laemmli UK** (1970) Cleavage of structural proteins during the assembly of the head of bacteriophage T4. *Nature* **227**: 680-685
- Landoni M, De Francesco A, Galbiati M, Tonelli C** (2010) A loss-of-function mutation in Calmodulin2 gene affects pollen germination in *Arabidopsis thaliana*. *Plant Molecular Biology* **74**: 235-247
- Leckie CP, McAinsh MR, Allen GJ, Sanders D, Hetherington AM** (1998) Abscisic acid-induced stomatal closure mediated by cyclic ADP-ribose. *Proceedings of the National Academy of Sciences of the United States of America* **95**: 15837
- Lee K, Song EH, Kim HS, Yoo JH, Han HJ, Jung MS, Lee SM, Kim KE, Kim MC, Cho MJ, Chung WS** (2008) Regulation of MAPK phosphatase 1 (AtMKP1) by calmodulin in Arabidopsis. *Journal of Biological Chemistry* **283**: 23581-23588
- Lee S, Seo PJ, Lee HJ, Park CM** (2012) A NAC transcription factor NTL4 promotes reactive oxygen species production during drought-induced leaf senescence in Arabidopsis. *Plant Journal* **70**: 831-844
- Li J, Guo X, Zhang M, Wang X, Zhao Y, Yin Z, Zhang Z, Wang Y, Xiong H, Zhang H, Todorovska E, Li Z** (2018) OsERF71 confers drought tolerance *via* modulating ABA signaling and proline biosynthesis. *Plant Science* **270**: 131-139
- Li Y, Li H, Li Y, Zhang S** (2017) Improving water-use efficiency by decreasing stomatal conductance and transpiration rate to maintain higher ear photosynthetic rate in drought-resistant wheat. *Crop Journal* **5**: 231-239

- Lian H-L, Yu X, Ye Q, Ding X-S, Kitagawa Y, Kwak S-S, Su W-A, Tang Z-C** (2004) The role of aquaporin RWC3 in drought avoidance in rice. *Plant and Cell Physiology* **45**: 481-489
- Liang X, Zhang L, Natarajan SK, Becker DF** (2013) Proline mechanisms of stress survival. *Antioxidants & Redox Signaling* **19**: 998-1011
- Liese A, Romeis T** (2013) Biochemical regulation of in vivo function of plant calcium-dependent protein kinases (CDPK). *Biochimica Biophysica Acta* **1833**: 1582-1589
- Liu H-T, Li B, Shang Z-L, Li X-Z, Mu R-L, Sun D-Y, Zhou R-G** (2003) Calmodulin is involved in heat shock signal transduction in wheat. *Plant Physiology* **132**: 1186
- Liu H-T, Li G-L, Chang HUI, Sun D-Y, Zhou R-G, Li B** (2007) Calmodulin-binding protein phosphatase PP7 is involved in thermotolerance in Arabidopsis. *Plant, Cell & Environment* **30**: 156-164
- Liu X-s, Liang C-c, Hou S-g, Wang X, Chen D-h, Shen J-l, Zhang W, Wang M** (2020) The LRR-RLK protein HSL3 regulates stomatal closure and the drought stress response by modulating hydrogen peroxide homeostasis. *Frontiers in Plant Science* **11**: 548034
- Liu XY, Li B, Yang JH, Sui N, Yang XM, Meng QW** (2008) Overexpression of tomato chloroplast omega-3 fatty acid desaturase gene alleviates the photoinhibition of photosystems II and I under chilling stress. *Photosynthetica* **46**: 185
- Liu Y, Ji X, Nie X, Qu M, Zheng L, Tan Z, Zhao H, Huo L, Liu S, Zhang B, Wang Y** (2015) Arabidopsis AtbHLH12 regulates the expression of genes involved in abiotic stress tolerance by binding to their E-box and GCG-box motifs. *New Phytologist* **207**: 692-709
- Lowry DB, Willis JH** (2010) A widespread chromosomal inversion polymorphism contributes to a major life-history transition, local adaptation, and reproductive isolation. *PLOS Biology* **8**: e1000500
- Luan S** (2002) Signalling drought in guard cells. *Plant, Cell & Environment* **25**: 229-237
- Luo P, Shen Y, Jin S, Huang S, Cheng X, Wang Z, Li P, Zhao J, Bao M, Ning G** (2016) Overexpression of *Rosa rugosa* anthocyanidin reductase enhances tobacco tolerance to abiotic stress through increased ROS scavenging and modulation of ABA signaling. *Plant Science* **245**: 35-49
- Lynch J, Polito VS, Läuchli A** (1989) Salinity stress increases cytoplasmic Ca activity in maize root protoplasts. *Plant Physiology* **90**: 1271-1274
- Ma J, Hanssen M, Lundgren K, Hernández L, Delatte T, Ehlert A, Liu C-M, Schluempmann H, Dröge-Laser W, Moritz T, Smeekens S, Hanson J** (2011) The sucrose-regulated Arabidopsis transcription factor bZIP11 reprograms metabolism and regulates trehalose metabolism. *New Phytologist* **191**: 733-745
- Ma L, Xu X, Cui S, Sun D** (1999) The presence of a heterotrimeric G protein and its role in signal transduction of extracellular calmodulin in pollen germination and tube growth. *Plant Cell* **11**: 1351-1364
- Ma W** (2011) Roles of Ca<sup>2+</sup> and cyclic nucleotide gated channel in plant innate immunity. *Plant Science* **181**: 342-346
- Ma W, Smigel A, Walker RK, Moeder W, Yoshioka K, Berkowitz GA** (2010) Leaf senescence signaling: the Ca<sup>2+</sup>-conducting Arabidopsis cyclic nucleotide gated channel2 acts through nitric oxide to repress senescence programming. *Plant Physiology* **154**: 733-743
- Ma X-J, Yu T-F, Li X-H, Cao X-Y, Ma J, Chen J, Zhou Y-B, Chen M, Ma Y-Z, Zhang J-H, Xu Z-S** (2020) Overexpression of GmNFYA5 confers drought tolerance to transgenic Arabidopsis and soybean plants. *BMC Plant Biology* **20**: 123

- MacRobbie EAC, Brownlee C, Sanders D** (1992) Calcium and ABA-induced stomatal closure. *Philosophical Transactions of the Royal Society of London. Series B: Biological Sciences* **338**: 5-18
- Mair A, Pedrotti L, Wurzinger B, Anrather D, Simeunovic A, Weiste C, Valerio C, Dietrich K, Kirchler T, Nägele T, Vicente Carbajosa J, Hanson J, Baena-González E, Chaban C, Weckwerth W, Dröge-Laser W, Teige M** (2015) SnRK1-triggered switch of bZIP63 dimerization mediates the low-energy response in plants. *eLife* **4**: e05828
- Mansfield TA, Hetherington AM, Atkinson CJ** (1990) Some current aspects of stomatal physiology. *Annual Review of Plant Physiology and Plant Molecular Biology* **41**: 55-75
- McAinsh MR, Brownlee C, Hetherington AM** (1990) Abscisic acid-induced elevation of guard cell cytosolic Ca<sup>2+</sup> precedes stomatal closure. *Nature* **343**: 186-188
- McCormack E, Braam J** (2003) Calmodulins and related potential calcium sensors of Arabidopsis. *New Phytologist* **159**: 585-598
- McCormack E, Tsai YC, Braam J** (2005) Handling calcium signaling: Arabidopsis CaMs and CMLs. *Trends in Plant Science* **10**: 383-389
- Meyre D, Leonardi A, Brisson G, Vartanian N** (2001) Drought-adaptive mechanisms involved in the escape/tolerance strategies of Arabidopsis Landsberg erecta and Columbia ecotypes and their F1 reciprocal progeny. *Journal of Plant Physiology* **158**: 1145-1152
- Miller G, Honig A, Stein H, Suzuki N, Mittler R, Zilberstein A** (2009) Unraveling delta-1-pyrroline-5-carboxylate-proline cycle in plants by uncoupled expression of proline oxidation enzymes. *Journal of Biological Chemistry* **284**: 26482-26492
- Molinari HBC, Marur CJ, Filho JCB, Kobayashi AK, Pileggi M, Júnior RPL, Pereira LFP, Vieira LGE** (2004) Osmotic adjustment in transgenic citrus rootstock Carrizo citrange (*Citrus sinensis* Osb. x *Poncirus trifoliata* L. Raf.) overproducing proline. *Plant Science* **167**: 1375-1381
- Mona SA, Hashem A, Abd\_Allah EF, Alqarawi AA, Soliman DWK, Wirth S, Egamberdieva D** (2017) Increased resistance of drought by *Trichoderma harzianum* fungal treatment correlates with increased secondary metabolites and proline content. *Journal of Integrative Agriculture* **16**: 1751-1757
- Moore CA, Bowen HC, Scrase-Field S, Knight MR, White PJ** (2002) The deposition of suberin lamellae determines the magnitude of cytosolic Ca<sup>2+</sup> elevations in root endodermal cells subjected to cooling. *Plant Journal* **30**: 457-465
- Mruk K, Farley BM, Ritacco AW, Kobertz WR** (2014) Calmodulation meta-analysis: predicting calmodulin binding *via* canonical motif clustering. *Journal of General Physiology* **144**: 105-114
- Mueller-Roeber B, Pical C** (2002) Inositol phospholipid metabolism in Arabidopsis. Characterized and putative isoforms of inositol phospholipid kinase and phosphoinositide-specific phospholipase C. *Plant Physiology* **130**: 22-46
- Munemasa S, Muroyama D, Nagahashi H, Nakamura Y, Mori IC, Murata Y** (2013) Regulation of reactive oxygen species-mediated abscisic acid signaling in guard cells and drought tolerance by glutathione. *Frontiers in Plant Science* **4**: 472-472
- Munné-Bosch S, Alegre L** (2004) Die and let live: leaf senescence contributes to plant survival under drought stress. *Functional Plant Biology* **31**: 203-216
- Na JK, Metzger JD** (2017) Guard-cell-specific expression of Arabidopsis ABF4 improves drought tolerance of tomato and tobacco. *Molecular Breeding* **37**: 154

- Nakabayashi K, Okamoto M, Koshiba T, Kamiya Y, Nambara E** (2005) Genome-wide profiling of stored mRNA in *Arabidopsis thaliana* seed germination: epigenetic and genetic regulation of transcription in seed. *Plant Journal* **41**: 697-709
- Nakagawa T, Suzuki T, Murata S, Nakamura S, Hino T, Maeo K, Tabata R, Kawai T, Tanaka K, Niwa Y, Watanabe Y, Nakamura K, Kimura T, Ishiguro S** (2007) Improved Gateway binary vectors: high-performance vectors for creation of fusion constructs in transgenic analysis of plants. *Bioscience Biotechnology Biochemistry* **71**: 2095-2100
- Nakashima K, Satoh R, Kiyosue T, Yamaguchi-Shinozaki K, Shinozaki K** (1998) A gene encoding proline dehydrogenase is not only induced by proline and hypoosmolarity, but is also developmentally regulated in the reproductive organs of *Arabidopsis*. *Plant Physiology* **118**: 1233
- Nanjo T, Kobayashi M, Yoshiba Y, Kakubari Y, Yamaguchi-Shinozaki K, Shinozaki K** (1999) Antisense suppression of proline degradation improves tolerance to freezing and salinity in *Arabidopsis thaliana*. *FEBS Letters* **461**: 205-210
- Neill SJ, Desikan R, Clarke A, Hancock JT** (2002) Nitric oxide is a novel component of abscisic acid signaling in stomatal guard cells. *Plant Physiology* **128**: 13-16
- Ng CK, McAinsh MR** (2003) Encoding specificity in plant calcium signalling: hot-spotting the ups and downs and waves. *Annals of Botany* **92**: 477-485
- Nir I, Shohat H, Panizel I, Olszewski N, Aharoni A, Weiss D** (2017) The tomato DELLA protein PROCERA acts in guard cells to promote stomatal closure. *Plant Cell* **29**: 3186-3197
- O'Malley Ronan C, Huang S-shan C, Song L, Lewsey Mathew G, Bartlett A, Nery Joseph R, Galli M, Gallavotti A, Ecker Joseph R** (2016) Cistrome and epicistrome features shape the regulatory DNA landscape. *Cell* **165**: 1280-1292
- Onions J, Hermann S, Grundström T** (2000) A novel type of calmodulin interaction in the inhibition of basic helix-loop-helix transcription factors. *Biochemistry* **39**: 4366-4374
- Osmolovskaya N, Shumilina J, Kim A, Didio A, Grishina T, Bilova T, Keltsieva OA, Zhukov V, Tikhonovich I, Tarakhovskaya E, Frolov A, Wessjohann LA** (2018) Methodology of drought stress research: experimental setup and physiological characterization. *International Journal of Molecular Sciences* **19**: 4089
- Pandey N, Ranjan A, Pant P, Tripathi RK, Ateek F, Pandey HP, Patre UV, Sawant SV** (2013) CAMTA 1 regulates drought responses in *Arabidopsis thaliana*. *BMC Genomics* **14**: 216
- Parida AK, Dagaonkar VS, Phalak MS, Aurangabadkar LP** (2008) Differential responses of the enzymes involved in proline biosynthesis and degradation in drought tolerant and sensitive cotton genotypes during drought stress and recovery. *Acta Physiologiae Plantarum* **30**: 619-627
- Park CY, Lee JH, Yoo JH, Moon BC, Choi MS, Kang YH, Lee SM, Kim HS, Kang KY, Chung WS, Lim CO, Cho MJ** (2005) WRKY group IId transcription factors interact with calmodulin. *FEBS Letters* **579**: 1545-1550
- Parre E, Ghars MA, Leprince A-S, Thiery L, Lefebvre D, Bordenave M, Richard L, Mazars C, Abdely C, Saviouré A** (2007) Calcium signaling *via* phospholipase C is essential for proline accumulation upon ionic but not nonionic hyperosmotic stresses in *Arabidopsis*. *Plant Physiology* **144**: 503
- Patel JA, Vora AB** (1985) Free proline accumulation in drought-stressed plants. *Plant and Soil* **84**: 427-429
- Patil S, Takezawa D, Poovaiah BW** (1995) Chimeric plant calcium/calmodulin-dependent protein kinase gene with a neural visinin-like calcium-binding domain. *Proceedings of the National Academy of Sciences* **92**: 4897



- Pauly N, Knight MR, Thuleau P, van der Luit AH, Moreau M, Trewavas AJ, Ranjeva R, Mazars C** (2000) Control of free calcium in plant cell nuclei. *Nature* **405**: 754-755
- Poovaiah BW, Du L, Wang H, Yang T** (2013) Recent advances in calcium/calmodulin-mediated signaling with an emphasis on plant-microbe interactions. *Plant Physiology* **163**: 531-542
- Poutrain P, Guirimand G, Mahroug S, Burlat V, Melin C, Ginis O, Oudin A, Giglioli-Guivarc'h N, Pichon O, Courdavault V** (2011) Molecular cloning and characterisation of two calmodulin isoforms of the Madagascar periwinkle *Catharanthus roseus*. *Plant Biology* **13**: 36-41
- Qin X, Zeevaart JA** (1999) The 9-cis-epoxycarotenoid cleavage reaction is the key regulatory step of abscisic acid biosynthesis in water-stressed bean. *Proceedings of the National Academy of Sciences of the United States of America* **96**: 15354-15361
- Qiu Y, Xi J, Du L, Suttle JC, Poovaiah BW** (2012) Coupling calcium/calmodulin-mediated signaling and herbivore-induced plant response through calmodulin-binding transcription factor AtSR1/CAMTA3. *Plant Molecular Biology* **79**: 89-99
- Quan W, Hu Y, Mu Z, Shi H, Chan Z** (2018) Overexpression of AtPYL5 under the control of guard cell specific promoter improves drought stress tolerance in Arabidopsis. *Plant Physiology and Biochemistry* **129**: 150-157
- Raggenbass M** (1983) Effects of extracellular calcium and of light adaptation on the response to dim light in honey bee drone photoreceptors. *Journal of Physiology* **344**: 525-548
- Raineri J, Wang S, Peleg Z, Blumwald E, Chan RL** (2015) The rice transcription factor OsWRKY47 is a positive regulator of the response to water deficit stress. *Plant Molecular Biology* **88**: 401-413
- Ranty B, Aldon D, Cotelle V, Galaud J-P, Thuleau P, Mazars C** (2016) Calcium sensors as key hubs in plant responses to biotic and abiotic stresses. *Frontiers in Plant Science* **7**: 327-327
- Rauf M, Arif M, Dortay H, Matallana-Ramírez LP, Waters MT, Gil Nam H, Lim PO, Mueller-Roeber B, Balazadeh S** (2013) ORE1 balances leaf senescence against maintenance by antagonizing G2-like-mediated transcription. *EMBO Reports* **14**: 382-388
- Reddy VS, Ali GS, Reddy AS** (2002) Genes encoding calmodulin-binding proteins in the Arabidopsis genome. *Journal of Biological Chemistry* **277**: 9840-9852
- Reece-Hoyes JS, Marian Walhout AJ** (2012) Yeast one-hybrid assays: A historical and technical perspective. *Methods* **57**: 441-447
- Reguera M, Peleg Z, Abdel-Tawab YM, Tumimbang EB, Delatorre CA, Blumwald E** (2013) Stress-induced cytokinin synthesis increases drought tolerance through the coordinated regulation of carbon and nitrogen assimilation in rice. *Plant Physiology* **163**: 1609
- Ren Y, Miao M, Meng Y, Cao J, Fan T, Yue J, Xiao F, Liu Y, Cao S** (2018) DFR1-mediated inhibition of proline degradation pathway regulates drought and freezing tolerance in Arabidopsis. *Cell Reports* **23**: 3960-3974
- Riboni M, Galbiati M, Tonelli C, Conti L** (2013) GIGANTEA enables drought escape response via abscisic acid-dependent activation of the florigens and SUPPRESSOR OF OVEREXPRESSION OF CONSTANS. *Plant Physiology* **162**: 1706-1719
- Rudd JJ, Franklin-Tong VE** (1999) Calcium signaling in plants. *Cellular and Molecular Life Sciences CMLS* **55**: 214-232
- Ruf S, Forner J, Hasse C, Kroop X, Seeger S, Schollbach L, Schadach A, Bock R** (2019) High-efficiency generation of fertile transplastomic Arabidopsis plants. *Nature Plants* **5**: 282-289

- Saga H, Ogawa T, Kai K, Suzuki H, Ogata Y, Sakurai N, Shibata D, Ohta D** (2012) Identification and characterization of ANAC042, a transcription factor family gene involved in the regulation of camalexin biosynthesis in Arabidopsis. *Molecular Plant-Microbe Interactions* **25**: 684-696
- Sakuma Y, Maruyama K, Qin F, Osakabe Y, Shinozaki K, Yamaguchi-Shinozaki K** (2006) Dual function of an Arabidopsis transcription factor DREB2A in water-stress-responsive and heat-stress-responsive gene expression. *Proceedings of the National Academy of Sciences of the United States of America* **103**: 18822-18827
- Samach A, Onouchi H, Gold SE, Ditta GS, Schwarz-Sommer Z, Yanofsky MF, Coupland G** (2000) Distinct roles of CONSTANS target genes in reproductive development of Arabidopsis. *Science* **288**: 1613-1616
- Sathyanarayanan PV, Cremo CR, Poovaiah BW** (2000) Plant chimeric Ca<sup>2+</sup>/Calmodulin-dependent protein kinase. Role of the neural visinin-like domain in regulating autophosphorylation and calmodulin affinity. *Journal of Biological Chemistry* **275**: 30417-30422
- Satoh R, Fujita Y, Nakashima K, Shinozaki K, Yamaguchi-Shinozaki K** (2004) A novel subgroup of bZIP proteins functions as transcriptional activators in hypoosmolarity-responsive expression of the *ProDH* gene in Arabidopsis. *Plant Cell Physiology* **45**: 309-317
- Scarpeci TE, Frea VS, Zanol MI, Valle EM** (2017) Overexpression of AtERF019 delays plant growth and senescence, and improves drought tolerance in Arabidopsis. *Journal of Experimental Botany* **68**: 673-685
- Schertl P, Cabassa C, Saadallah K, Bordenave M, Saviouré A, Braun HP** (2014) Biochemical characterization of proline dehydrogenase in Arabidopsis mitochondria. *FEBS Journal* **281**: 2794-2804
- Schindelin J, Arganda-Carreras I, Frise E, Kaynig V, Longair M, Pietzsch T, Preibisch S, Rueden C, Saalfeld S, Schmid B, Tinevez J-Y, White DJ, Hartenstein V, Eliceiri K, Tomancak P, Cardona A** (2012) Fiji: an open-source platform for biological-image analysis. *Nature Methods* **9**: 676-682
- Schmid M, Davison TS, Henz SR, Pape UJ, Demar M, Vingron M, Schölkopf B, Weigel D, Lohmann JU** (2005) A gene expression map of *Arabidopsis thaliana* development. *Nature Genetics* **37**: 501-506
- Schymanski SJ, Or D, Zwieniecki M** (2013) Stomatal control and leaf thermal and hydraulic capacitances under rapid environmental fluctuations. *PLOS One* **8**: e54231-e54231
- Seo JS, Sohn HB, Noh K, Jung C, An JH, Donovan CM, Somers DA, Kim DI, Jeong S-C, Kim C-G, Kim HM, Lee S-H, Choi YD, Moon TW, Kim CH, Cheong J-J** (2012) Expression of the Arabidopsis AtMYB44 gene confers drought/salt-stress tolerance in transgenic soybean. *Molecular Breeding* **29**: 601-608
- Seo PJ, Lee SB, Suh MC, Park M-J, Go YS, Park C-M** (2011) The MYB96 transcription factor regulates cuticular wax biosynthesis under drought conditions in Arabidopsis. *Plant Cell* **23**: 1138
- Shahnejat-Bushehri S, Allu AD, Mehterov N, Thirumalaikumar VP, Alseekh S, Fernie AR, Mueller-Roeber B, Balazadeh S** (2017) Arabidopsis NAC transcription factor JUNGBRUNNEN1 exerts conserved control over gibberellin and brassinosteroid metabolism and signaling genes in tomato. *Frontiers in Plant Science* **8**: 214-214
- Shahnejat-Bushehri S, Mueller-Roeber B, Balazadeh S** (2012) Arabidopsis NAC transcription factor JUNGBRUNNEN1 affects thermomemory-associated genes and enhances heat stress tolerance in primed and unprimed conditions. *Plant Signaling & Behavior* **7**: 1518-1521

- Shahnejat-Bushehri S, Nobmann B, Devi Allu A, Balazadeh S** (2016) JUB1 suppresses *Pseudomonas syringae*-induced defense responses through accumulation of DELLA proteins. *Plant Signaling & Behavior* **11**: e1181245
- Shahnejat-Bushehri S, Tarkowska D, Sakuraba Y, Balazadeh S** (2016) Arabidopsis NAC transcription factor JUB1 regulates GA/BR metabolism and signaling. *Nature Plants* **2**: 16013
- Shang Z-l, Ma L-g, Zhang H-l, He R-r, Wang X-c, Cui S-j, Sun D-y** (2005) Ca<sup>2+</sup> influx into lily pollen grains through a hyperpolarization-activated Ca<sup>2+</sup>-permeable channel which can be regulated by extracellular CaM. *Plant and Cell Physiology* **46**: 598-608
- Sharma S, Verslues PE** (2010) Mechanisms independent of abscisic acid (ABA) or proline feedback have a predominant role in transcriptional regulation of proline metabolism during low water potential and stress recovery. *Plant Cell Environment* **33**: 1838-1851
- Sharma SS, Schat H, Vooijs R** (1998) In vitro alleviation of heavy metal-induced enzyme inhibition by proline. *Phytochemistry* **49**: 1531-1535
- Sharma UD, Rai VK** (1989) Modulation of osmotic closure of stomata, stomatal resistance and K<sup>+</sup> fluxes by exogenous amino acids in *Vicia faba* L. leaves. *Biochemie und Physiologie der Pflanzen* **185**: 369-376
- Shi J, Kim KN, Ritz O, Albrecht V, Gupta R, Harter K, Luan S, Kudla J** (1999) Novel protein kinases associated with calcineurin B-like calcium sensors in Arabidopsis. *Plant Cell* **11**: 2393-2405
- Shim JS, Oh N, Chung PJ, Kim YS, Choi YD, Kim J-K** (2018) Overexpression of OsNAC14 improves drought tolerance in rice. *Frontiers in Plant Science* **9**: 310
- Simon-Sarkadi L, Kocsy G, Várhegyi Á, Galiba G, De Ronde JA** (2006) Stress-induced changes in the free amino acid composition in transgenic soybean plants having increased proline content. *Biologia Plantarum* **50**: 793-796
- Sipari N, Lihavainen J, Shapiguzov A, Kangasjärvi J, Keinänen M** (2020) Primary metabolite responses to oxidative stress in early-senescing and paraquat resistant *Arabidopsis thaliana* RCD1 (Radical-Induced Cell Death1). *Frontiers in Plant Science* **11**: 194
- Sistrunk ML, Antosiewicz DM, Purugganan MM, Braam J** (1994) Arabidopsis TCH3 encodes a novel Ca<sup>2+</sup> binding protein and shows environmentally induced and tissue-specific regulation. *Plant Cell* **6**: 1553-1565
- Snedden WA, Fromm H** (2001) Calmodulin as a versatile calcium signal transducer in plants. *New Phytologist* **151**: 35-66
- Song Y, Miao Y, Song CP** (2014) Behind the scenes: the roles of reactive oxygen species in guard cells. *New Phytologist* **201**: 1121-1140
- Strizhov N, Abrahám E, Okrész L, Blickling S, Zilberstein A, Schell J, Koncz C, Szabados L** (1997) Differential expression of two P5CS genes controlling proline accumulation during salt-stress requires ABA and is regulated by ABA1, ABI1 and AXR2 in Arabidopsis. *Plant Journal* **12**: 557-569
- Sun DY, Bian YQ, Zhao BH, Zhao LY, Yu XM, Shengjun D** (1995) The effects of extracellular calmodulin on cell wall regeneration of protoplasts and cell division. *Plant and Cell Physiology* **36**: 133-138
- Sun Z, Qi X, Wang Z, Li P, Wu C, Zhang H, Zhao Y** (2013) Overexpression of TsGOLS2, a galactinol synthase, in *Arabidopsis thaliana* enhances tolerance to high salinity and osmotic stresses. *Plant Physiology and Biochemistry* **69**: 82-89
- Szabados L, Saviouré A** (2010) Proline: a multifunctional amino acid. *Trends in Plant Science* **15**: 89-97
- Székely G, Abrahám E, Csépló A, Rigó G, Zsigmond L, Csiszár J, Ayaydin F, Strizhov N, Jásik J, Schmelzer E, Koncz C, Szabados L** (2008) Duplicated *P5CS* genes of

- Arabidopsis play distinct roles in stress regulation and developmental control of proline biosynthesis. *Plant Journal* **53**: 11-28
- Szymanski DB, Liao B, Zielinski RE** (1996) Calmodulin isoforms differentially enhance the binding of cauliflower nuclear proteins and recombinant TGA3 to a region derived from the Arabidopsis *CaM3* promoter. *Plant Cell* **8**: 1069
- Tak H, Negi S, Ganapathi TR** (2017) Banana NAC transcription factor MusaNAC042 is positively associated with drought and salinity tolerance. *Protoplasma* **254**: 803-816
- Takabatake R, Karita E, Seo S, Mitsuhashi I, Kuchitsu K, Ohashi Y** (2007) Pathogen-induced calmodulin isoforms in basal resistance against bacterial and fungal pathogens in tobacco. *Plant and Cell Physiology* **48**: 414-423
- Takahashi F, Mizoguchi T, Yoshida R, Ichimura K, Shinozaki K** (2011) Calmodulin-dependent activation of MAP kinase for ROS homeostasis in Arabidopsis. *Molecular Cell* **41**: 649-660
- Takezawa D, Ramachandiran S, Paranjape V, Poovaiah BW** (1996) Dual regulation of a chimeric plant serine/threonine kinase by calcium and calcium/calmodulin. *Journal of Biological Chemistry* **271**: 8126-8132
- Tanaka Y, Sugano SS, Shimada T, Hara-Nishimura I** (2013) Enhancement of leaf photosynthetic capacity through increased stomatal density in Arabidopsis. *New Phytologist* **198**: 757-764
- Tanz SK, Castleden I, Small ID, Millar AH** (2013) Fluorescent protein tagging as a tool to define the subcellular distribution of proteins in plants. *Frontiers in Plant Science* **4**: 214-214
- Thiery L, Leprince AS, Lefebvre D, Ghars MA, Debarbieux E, Savouré A** (2004) Phospholipase D is a negative regulator of proline biosynthesis in *Arabidopsis thaliana*. *Journal of Biological Chemistry* **279**: 14812-14818
- Thirumalaikumar VP, Devkar V, Mehterov N, Ali S, Ozgur R, Turkan I, Mueller-Roeber B, Balazadeh S** (2018) NAC transcription factor JUNGBRUNNEN1 enhances drought tolerance in tomato. *Plant Biotechnology Journal* **16**: 354-366
- Thomas CD, Cameron A, Green RE, Bakkenes M, Beaumont LJ, Collingham YC, Erasmus BFN, de Siqueira MF, Grainger A, Hannah L, Hughes L, Huntley B, van Jaarsveld AS, Midgley GF, Miles L, Ortega-Huerta MA, Townsend Peterson A, Phillips OL, Williams SE** (2004) Extinction risk from climate change. *Nature* **427**: 145-148
- Townley HE, Knight MR** (2002) Calmodulin as a potential negative regulator of Arabidopsis COR gene expression. *Plant Physiology* **128**: 1169-1172
- Trewavas AJ, Malhó R** (1998) Ca<sup>2+</sup> signalling in plant cells: the big network! *Current Opinion in Plant Biology* **1**: 428-433
- Tuteja N, Mahajan S** (2007) Calcium signaling network in plants: an overview. *Plant Signaling & Behavior* **2**: 79-85
- Urban J, Ingwers MW, McGuire MA, Teskey RO** (2017) Increase in leaf temperature opens stomata and decouples net photosynthesis from stomatal conductance in *Pinus taeda* and *Populus deltoides* x *nigra*. *Journal of Experimental Botany* **68**: 1757-1767
- van der Luit AH, Olivari C, Haley A, Knight MR, Trewavas AJ** (1999) Distinct calcium signaling pathways regulate calmodulin gene expression in tobacco. *Plant Physiology* **121**: 705
- Veerabagu M, Kirchler T, Elgass K, Stadelhofer B, Stahl M, Harter K, Mira-Rodado V, Chaban C** (2014) The Interaction of the Arabidopsis response regulator ARR18 with bZIP63 mediates the regulation of *PROLINE DEHYDROGENASE* expression. *Molecular Plant* **7**: 1560-1577

- Verbruggen N, Hermans C** (2008) Proline accumulation in plants: a review. *Amino Acids* **35**: 753-759
- Verbruggen N, Hua XJ, May M, Van Montagu M** (1996) Environmental and developmental signals modulate proline homeostasis: evidence for a negative transcriptional regulator. *Proceedings of the National Academy of Sciences of the United States of America* **93**: 8787-8791
- Verslues PE, Agarwal M, Katiyar-Agarwal S, Zhu J, Zhu JK** (2006) Methods and concepts in quantifying resistance to drought, salt and freezing, abiotic stresses that affect plant water status. *Plant Journal* **45**: 523-539
- Verslues PE, Sharp RE** (1999) Proline accumulation in maize (*Zea mays* L.) primary roots at low water potentials. II. Metabolic source of increased proline deposition in the elongation zone. *Plant Physiology* **119**: 1349-1360
- Vráblová M, Vrábl D, Hronková M, Kubásek J, Šantrůček J** (2017) Stomatal function, density and pattern, and CO<sub>2</sub> assimilation in *Arabidopsis thaliana* tmm1 and sdd1-1 mutants. *Plant Biology* **19**: 689-701
- Waese J, Fan J, Pasha A, Yu H, Fucile G, Shi R, Cumming M, Kelley LA, Sternberg MJ, Krishnakumar V, Ferlanti E, Miller J, Town C, Stuerzlinger W, Provart NJ** (2017) ePlant: visualizing and exploring multiple levels of data for hypothesis generation in plant biology. *Plant Cell* **29**: 1806-1821
- Walter M, Chaban C, Schütze K, Batistic O, Weckermann K, Näke C, Blazevic D, Grefen C, Schumacher K, Oecking C, Harter K, Kudla J** (2004) Visualization of protein interactions in living plant cells using bimolecular fluorescence complementation. *Plant Journal* **40**: 428-438
- Wang J-P, Munyampundu J-P, Xu Y-P, Cai X-Z** (2015) Phylogeny of plant calcium and calmodulin-dependent protein kinases (CCaMKs) and functional analyses of tomato CCaMK in disease resistance. *Frontiers in Plant Science* **6**: 1075
- Wang L, Tsuda K, Sato M, Cohen JD, Katagiri F, Glazebrook J** (2009) Arabidopsis CaM binding protein CBP60g contributes to MAMP-induced SA accumulation and is involved in disease resistance against *Pseudomonas syringae*. *PLOS Pathogens* **5**: e1000301
- Wang M, Zou Z, Li Q, Sun K, Chen X, Li X** (2017) The CsHSP17.2 molecular chaperone is essential for thermotolerance in *Camellia sinensis*. *Scientific Reports* **7**: 1237
- Wang P, Song CP** (2008) Guard-cell signalling for hydrogen peroxide and abscisic acid. *New Phytologist* **178**: 703-718
- Wehner G, Balko C, Humbeck K, Zyprian E, Ordon F** (2016) Expression profiling of genes involved in drought stress and leaf senescence in juvenile barley. *BMC Plant Biology* **16**: 3
- Wei Y, Liu W, Hu W, Yan Y, Shi H** (2020) The chaperone MeHSP90 recruits MeWRKY20 and MeCatalase1 to regulate drought stress resistance in cassava. *New Phytologist* **226**: 476-491
- Weltmeier F, Ehlert A, Mayer CS, Dietrich K, Wang X, Schütze K, Alonso R, Harter K, Vicente-Carbajosa J, Dröge-Laser W** (2006) Combinatorial control of Arabidopsis proline dehydrogenase transcription by specific heterodimerisation of bZIP transcription factors. *EMBO Journal* **25**: 3133-3143
- Werner T, Nehnevajova E, Köllmer I, Novák O, Strnad M, Krämer U, Schmölling T** (2010) Root-specific reduction of cytokinin causes enhanced root growth, drought tolerance, and leaf mineral enrichment in Arabidopsis and tobacco. *Plant Cell* **22**: 3905-3920

- Winter D, Vinegar B, Nahal H, Ammar R, Wilson GV, Provart NJ** (2007) An “Electronic fluorescent pictograph” browser for exploring and analyzing large-scale biological data sets. *PLOS One* **2**: e718
- Woo HR, Kim HJ, Nam HG, Lim PO** (2013) Plant leaf senescence and death – regulation by multiple layers of control and implications for aging in general. *Journal of Cell Science* **126**: 4823-4833
- Woo HR, Kim JH, Nam HG, Lim PO** (2004) The delayed leaf senescence mutants of Arabidopsis, ore1, ore3, and ore9 are tolerant to oxidative stress. *Plant Cell Physiology* **45**: 923-932
- Wu A, Allu AD, Garapati P, Siddiqui H, Dortay H, Zanol MI, Asensi-Fabado MA, Munné-Bosch S, Antonio C, Tohge T, Fernie AR, Kaufmann K, Xue GP, Mueller-Roeber B, Balazadeh S** (2012) JUNGBRUNNEN1, a reactive oxygen species-responsive NAC transcription factor, regulates longevity in Arabidopsis. *Plant Cell* **24**: 482-506
- Wu FH, Shen SC, Lee LY, Lee SH, Chan MT, Lin CS** (2009) Tape-Arabidopsis sandwich - a simpler Arabidopsis protoplast isolation method. *Plant Methods* **5**: 16
- Xiang Y, Sun X, Bian X, Wei T, Han T, Yan J, Zhang A** (2021) The transcription factor ZmNAC49 reduces stomatal density and improves drought tolerance in maize. *Journal of Experimental Botany* **72**: 1399-1410
- Xiao XO, Zeng YM, Cao BH, Lei JJ, Chen QH, Meng CM, Cheng YJ** (2017) PSAG12-IPT overexpression in eggplant delays leaf senescence and induces abiotic stress tolerance. *Journal of Horticultural Science and Biotechnology* **92**: 349-357
- Xiong TC, Bourque S, Lecourieux D, Amelot N, Grat S, Brière C, Mazars C, Pugin A, Ranjeva R** (2006) Calcium signaling in plant cell organelles delimited by a double membrane. *Biochim Biophys Acta* **1763**: 1209-1215
- Xu B, Long Y, Feng X, Zhu X, Sai N, Chirkova L, Betts A, Herrmann J, Edwards EJ, Okamoto M, Hedrich R, Gilliam M** (2021) GABA signalling modulates stomatal opening to enhance plant water use efficiency and drought resilience. *Nature Communications* **12**: 1952
- Xu Z, Zhou G, Shimizu H** (2010) Plant responses to drought and rewatering. *Plant Signaling & Behavior* **5**: 649-654
- Xue X, Liu A, Hua X** (2009) Proline accumulation and transcriptional regulation of proline biosynthesis and degradation in *Brassica napus*. *BMB Reports* **42**: 28-34
- Yamada M, Morishita H, Urano K, Shiozaki N, Yamaguchi-Shinozaki K, Shinozaki K, Yoshida Y** (2005) Effects of free proline accumulation in petunias under drought stress. *Journal of Experimental Botany* **56**: 1975-1981
- Yang SL, Lan SS, Gong M** (2009) Hydrogen peroxide-induced proline and metabolic pathway of its accumulation in maize seedlings. *Journal of Plant Physiology* **166**: 1694-1699
- Yang T, Lev-Yadun S, Feldman M, Fromm H** (1998) Developmentally regulated organ-, tissue-, and cell-specific expression of calmodulin genes in common wheat. *Plant Molecular Biology* **37**: 109-120
- Yang T, Poovaiah BW** (2000) Molecular and biochemical evidence for the involvement of calcium/calmodulin in auxin action. *Journal of Biological Chemistry* **275**: 3137-3143
- Yang T, Poovaiah BW** (2002) Hydrogen peroxide homeostasis: activation of plant catalase by calcium/calmodulin. *Proceedings of the National Academy of Sciences of the United States of America* **99**: 4097-4102
- Yang Y, Shah J, Klessig DF** (1997) Signal perception and transduction in plant defense responses. *Genes & Development* **11**: 1621-1639

- Yap KL, Kim J, Truong K, Sherman M, Yuan T, Ikura M** (2000) Calmodulin Target Database. *Journal of Structural and Functional Genomics* **1**: 8-14
- Yin Q, Tian T, Kou M, Liu P, Wang L, Hao Z, Yue M** (2020) The relationships between photosynthesis and stomatal traits on the Loess Plateau. *Global Ecology and Conservation* **23**: e01146
- Yoo JH, Park CY, Kim JC, Heo WD, Cheong MS, Park HC, Kim MC, Moon BC, Choi MS, Kang YH, Lee JH, Kim HS, Lee SM, Yoon HW, Lim CO, Yun DJ, Lee SY, Chung WS, Cho MJ** (2005) Direct interaction of a divergent CaM isoform and the transcription factor, MYB2, enhances salt tolerance in *Arabidopsis*. *Journal of Biological Chemistry* **280**: 3697-3706
- Yoo S-D, Cho Y-H, Sheen J** (2007) *Arabidopsis* mesophyll protoplasts: a versatile cell system for transient gene expression analysis. *Nature Protocols* **2**: 1565-1572
- Zarattini M, Forlani G** (2017) Toward unveiling the mechanisms for transcriptional regulation of proline biosynthesis in the plant cell response to biotic and abiotic stress conditions. *Frontiers in plant science* **8**: 927-927
- Zeng H, Xu L, Singh A, Wang H, Du L, Poovaiah BW** (2015) Involvement of calmodulin and calmodulin-like proteins in plant responses to abiotic stresses. *Frontiers in Plant Science* **6**: 600
- Zhang H, Li Y, Zhu J-K** (2018) Developing naturally stress-resistant crops for a sustainable agriculture. *Nature Plants* **4**: 989-996
- Zhang H, Yang B, Liu W-Z, Li H, Wang L, Wang B, Deng M, Liang W, Deyholos MK, Jiang Y-Q** (2014) Identification and characterization of CBL and CIPK gene families in canola (*Brassica napus* L.). *BMC plant biology* **14**: 8-8
- Zhang S, Chen Y, Zhao L, Li C, Yu J, Li T, Yang W, Zhang S, Su H, Wang L** (2020) A novel NAC transcription factor, MdNAC42, regulates anthocyanin accumulation in red-fleshed apple by interacting with MdMYB10. *Tree Physiology* **40**: 413-423
- Zhang W, Zhou RG, Gao YJ, Zheng SZ, Xu P, Zhang SQ, Sun DY** (2009) Molecular and genetic evidence for the key role of AtCaM3 in heat-shock signal transduction in *Arabidopsis*. *Plant Physiology* **149**: 1773-1784
- Zhang X, Zhang L, Dong F, Gao J, Galbraith DW, Song CP** (2001) Hydrogen peroxide is involved in abscisic acid-induced stomatal closure in *Vicia faba*. *Plant Physiology* **126**: 1438-1448
- Zheng C, Wang Y, Ding Z, Zhao L** (2016) Global transcriptional analysis reveals the complex relationship between tea quality, leaf senescence and the responses to cold-drought combined stress in *Camellia sinensis*. *Frontiers in Plant Science* **7**: 1858
- Zhou L, Liu Z, Liu Y, Kong D, Li T, Yu S, Mei H, Xu X, Liu H, Chen L, Luo L** (2016) A novel gene *OsAHL1* improves both drought avoidance and drought tolerance in rice. *Scientific Reports* **6**: 30264
- Zhou S, Jia L, Chu H, Wu D, Peng X, Liu X, Zhang J, Zhao J, Chen K, Zhao L** (2016) *Arabidopsis* CaM1 and CaM4 promote nitric oxide production and salt resistance by inhibiting s-nitrosoglutathione reductase *via* direct binding. *PLOS Genetics* **12**: e1006255
- Zhou X, Jenks MA, Liu J, Liu A, Zhang X, Xiang J, Zou J, Peng Y, Chen X** (2014) Overexpression of transcription factor OsWR2 regulates wax and cutin biosynthesis in rice and enhances its tolerance to water deficit. *Plant Molecular Biology Reporter* **32**: 719-731
- Zia A, Walker BJ, Oung HMO, Charuvi D, Jahns P, Cousins AB, Farrant JM, Reich Z, Kirchhoff H** (2016) Protection of the photosynthetic apparatus against dehydration stress in the resurrection plant *Craterostigma pumilum*. *Plant Journal* **87**: 664-680

- Zielinski RE** (1998) Calmodulin and calmodulin-binding proteins in plants. Annual Review of Plant Physiology and Plant Molecular Biology **49**: 697-725
- Zimmermann P, Hirsch-Hoffmann M, Hennig L, Gruissem W** (2004) GENEVESTIGATOR. Arabidopsis microarray database and analysis toolbox. Plant Physiology **136**: 2621-2632



## 6. SUPPLEMENTAL DATA

**Supplemental Table S1. Primers used for cloning and genotyping.**

Primer	Sequence 5` to 3`	Description
CAM1-BP-F	GGGGACAAGTTTGTACAAAAAAGCAGGCTTAATGGCGGATCAACTCACT	Cloning full length <i>CaM1</i> CDS into pDONR207 or pDONR221 P1-P4
CAM1-BP-R	GGGGACCACTTTGTACAAGAAAGCTGGGTTTCACTTAGCCATCATAATCT	
CAM4-BP-F	GGGGACAAGTTTGTACAAAAAAGCAGGCTTAATGGCGGATCAGCTAACT	Cloning full length <i>CaM4</i> CDS into pDONR207 or pDONR221 P1-P4
CAM4-BP-R	GGGGACCACTTTGTACAAGAAAGCTGGGTTTCACTTAGCCATCATAATCT	
CAM1/4-WOstopBP-R	GGGGACCACTTTGTACAAGAAAGCTGGGTTCTTAGCCATCATAATCTTGA	Cloning full length <i>CaM1/4</i> CDS without a stop codon into pDONR207 or pDONR221 P1-P4
DREB2Apro-TA-F	GCACTGCAGGGGTTTGATAATGGATGT	Cloning 1 kb <i>DREB2A</i> promoter for TA into RD29A:LUC
DREB2Apro-TA-R	AACCCATGGCTCCTTCCCAGAAACAACA	
DREB2Apro-TA-InF-F	ttgatatcgaattcctgcagGGGGTTTGATAATGGATGTAAAGTAAC	Cloning 1 kb <i>DREB2A</i> promoter for TA into pGreenII 0800-LUC
DREB2Apro-TA-InF-R	ttttggcgtcttccatggGCTCCTTCCCAGAAACAACAC	
JUB1- BP-F	GGGGACAAGTTTGTACAAAAAAGCAGGCTTAATGAGTGGCGAAGGTAACT	Cloning full length <i>JUB1</i> CDS into pDONR207 or pDONR221 P2-P
JUB1- BP-R	GGGGACCACTTTGTACAAGAAAGCTGGGTTCTAGGGTTTAGTGTTGCCAT	
JUB1-WOstop-BP-R	GGGGACCACTTTGTACAAGAAAGCTGGGTTGGGTTTAGTGTTGCCATCTA	Cloning full length <i>JUB1</i> CDS without a stop codon into pDONR207
JUB1 <sub>Cterm</sub> -F-BP-F	GGGGACAAGTTTGTACAAAAAAGCAGGCTTAATGCATGAATTCCGCCTCC	Cloning <i>JUB1</i> <sub>Cterm</sub> part into pDONR221 P2-P3
JUB1 <sub>Nterm</sub> -BP-R	GGGGACCACTTTGTACAAGAAAGCTGGGTTGAGGCGGAATTCATGCATCA	Cloning <i>JUB1</i> <sub>Nterm</sub> part into pDONR221 P2-P3
bZIP63-BP-F	GGGGACAAGTTTGTACAAAAAAGCAGGCTTAATGGCCGACAACGACGG	Cloning full length <i>bZIP63</i> CDS without stop into pDONR207
bZIP63-BP-R	GGGGACCACTTTGTACAAGAAAGCTGGGTTACGTGGTTCGTGGTCGT	

Primer	Sequence 5' to 3'	Description
ANAC063- BP-F	GGGGACAACCTTTGTATAATAAAGTTGTAATGTCTCCTCCGTCGACGA	Cloning full length ANAC063 into pDONR221 P2-P3
ANAC063-BP-R	GGGGACCACTTTGTACAAGAAAGCTGGGTTGCATCCTTTTCCTTGGTCTG	
RFP for p2GWF7-InF-F	TGCGGACTCTAGCATGGCCGTTAGGCGCCGGTGGAGTGGC	Primers for cloning RFP (replacing GFP) into P2GWF7
RFP for p2GWF7- InF-R	TGTACAAAGTGGTGATATCAATGGCCTCCTCCGAGGACGT	
Myc for P2GWF7-InF-F	TGCGGACTCTAGCATGGCCGTTAAAGATCCTCCTCAGAAATCAACTTTTG	Primers for cloning Myc tag (replacing GFP) into P2GWF7
Myc for P2GWF7- InF-R	TGTACAAAGTGGTGATATCAATGGAGCAAAGTTGATTTCTGAGGAGGAT	
KST1pro-InF-F	GTACAAACTTGTGATATCACTAGTATTATATATTGCTGCTTCT	Primers for cloning <i>KST1</i> promoter (replacing 35S) into pK7FWG2.0
KST1pro-InF-R	CACAGATGGTTAGAGAGGCTAGAAAATGAAATGAAAAACA	
PDH2pro- Y1H-F	<u>ACGCGTGACTCACGAAGA</u>	Primers for cloning <i>PDH2pro</i> into pTUY1H
PDH2pro- Y1H-R	<u>CCGCGGCGTAATGAAAGTTA</u>	
MYB2pro- Y1H-F	<u>TCGCGAAGGGTCAAACCTTA</u>	Primers for cloning <i>MYB2pro</i> into pTUY1H
MYB2pro- Y1H-R	<u>CCGCGGAGATTTGAAGTGAT</u>	
bZIP63 Y1H-F	<u>ACGCGTCTTGTAGGACAGTG</u>	Primers for cloning <i>bZIP63pro</i> into pTUY1H
bZIP63 Y1H-R	<u>CCGCGGACACCATTAGTAGA</u>	
KST1pro-gent-F	CTAGAAAATGAAATGAAAAC	Primers for genotyping <i>KST1pro:JUB1-GFP</i> line
KST1pro-gent-R	TATTATATATTGCTGCTTCTT	
pGreen-Myc-gent -F	GTAAGTTTCTGCTTCTACCTT	Primers used for genotyping <i>JUB1-OX/CaM1-OX</i> , <i>JUB1-OX/CaM4-OX</i> lines
CaM1-gent-R	AGATCTGTTTCGTCAGTGAG	
CaM4-gent-R	TAGGTTTAAGAACTCAGGGAAG	
CaM1-crispr-gent-F	AAGATGGCGATGGTTAGATTACCTCTTC	
CaM4-crispr-gent-F	AAAGATGGAGATGGTTAGTCTCAA	Primers used for genotyping <i>cam1/cam4</i> knockout mutant
CaM1/4-crispr-gent-R	CTTAGCCATCATAATCTTGACAA	
JUB1pro-crispr-gent-F	CTAAAGAGATCGATGTAGTGAAGA	Primers used for genotyping <i>jub1 crispr</i> knockout mutant
JUB1-crispr-gent-R	GGGTTTAGTGTTGCCATCTATAA	

**Supplemental Table S2. Primers used for the generation of knockout mutants. sgRNAs are underlined.**

<b>Primer</b>	<b>Primer sequence (5` to 3`)</b>
CAM1 sgRNA1-F	accaGGTCTCaATTGGAGTGGGAAGAGATGATCCGTGgttttagagctagaaatagcaag
CAM1 sgRNA2-R	tggtGGTCTCtAAACCGTTGATCATGTCTTGGAGCcaatctcttagtcgactctacc
CAM4 sgRNA1-F	accaGGTCTCaATTGGCTACAAGACATGATCAACGgttttagagctagaaatagcaag
CAM4 sgRNA2-R	tggtGGTCTCtAAACCGTAGTTTATCTGACCATCTCcaatctcttagtcgactctacc
JUB1 sgRNA1-F	accaGGTCTCaATTGGCAGCGTCGGAGAAAAGGAGgttttagagctagaaatagcaag
JUB1 sgRNA2-R	tggtGGTCTCtAAACACACTTGTTCTAAGACCAGCcaatctcttagtcgactctacc

**Supplemental Table S3. Primers used for qRT-PCR and end-point PCR.**

<b>Transcript Identifier</b>	<b>Gene name</b>	<b>Forward primer sequence (5' to 3')</b>	<b>Forward primer sequence (5' to 3')</b>
AT3G18780	<i>Actin2</i>	TCCCTCAGCACATTCCAGCAGAT	AACGATTCCCTGGCCTGCCTCATC
AT1G13440	<i>5' GAPDH</i>	TCTCGATCTCAATTTTCGCAAAA	CGAAACCGTTGATTCCGATTC
AT1G13440	<i>3' GAPDH</i>	TTGGTGACAACAGGTCAAGCA	AAACTTGTTCGCTCAATGCAATC
AT5G37780	<i>CaM1</i>	AGCTATGGCGGATCAACTCACTG	TTGTGATGCAACCATCGCCATC
AT1G66410	<i>CaM4</i>	TTCGACAAAGATGGAGATGGTTG C	TGTTGGGTTCTGCCCTAGTGAC
AT2G43000	<i>JUB1</i>	TCTCCAGCTCAACAAGCAGAGGT A	CCGGTTTTTCGGTTTGGTGGTAAGA
AT5G05410	<i>DREB2A</i>	<i>CAGTGTTGCCAACGGTTCAT</i>	<i>AAACGGAGGTATTCCGTAGTTGAG</i>
AT2G39800	<i>P5CS1</i>	AGAGGATCACGAAGTTGCAGAGC	TGTGGAACACAGCAGCGCTATC
AT3G55610	<i>P5CS2</i>	ACCACGAGTACAGTTCCAAGGC	TGCAATCAGTGTGTGCACTTCC
AT5G14800	<i>P5CR</i>	AGGAGTAGCTGCTGGTTTACCC	ATCGTTGCAGCTCCAAGAACGG
AT3G30775	<i>PDH1</i>	TCTCCGACGCGCTTATGAGAAC	AAGTTCCATCCTCATGAGTTGACG
AT5G38710	<i>PDH2</i>	CGCATAACACAGACTCGGGTAAA C	TCCCGTAAAGCTGCGCAAATC
AT5G62530	<i>P5CDH</i>	AGGACCAGATGTTTCAGGAGGTTG	TTCTGTCCACTGCACGCGTATG
AT5G46180	<i>OAT</i>	TGCAGTGCTTGCTGATAAAGACG	AGGGTTACCACCAAATGTGCTTCC
AT5G28770	<i>bZIP63</i>	TCTTGCTTCTTCCAAAGCTACACC	TCACCAGAGAGCTCAGATCCAC
AT5G45890	<i>SAG12</i>	ACAAAGGCGAAGACGCTACTTG	ACCGGGACATCCTCATAACCTG
AT2G29350	<i>SAG13</i>	AGGGAGCATCGTGCTCATATCC	CCAGCTGATTCATGGCTCCTTTG
AT4G35770	<i>SEN1</i>	AAGACAGGTCTCGTCCCCTTC	CATTTGACCGCTCTCACAACCG
AT4G30270	<i>SEN4</i>	GTCATCGGCTATTTCTCCACCT	GTTGTCGTTGCTTTCCTCCATC
7011691	<i>GFP</i>	ACTGGCTGCTCAGGTAGTGG	CCTGAAGTTCATCTGCACCA
<b>Photosynthesis-associated genes</b>			
AT1G67090	<i>RBSC1A</i>	CCACCCGCAAGGCTAACAAC	TTCGGAATCGGTAAGGTCAGG
AT1G29930	<i>CAB1</i>	CCAGAGGCATTTCGCTGAGTTG	CCTTACCAGTGACGATGGCTTG
AT3G08940	<i>LHCB4.2</i>	CTATCACCGTCGAATGGCTCAC	ATCCATCCACTAGCTCTACCTTGC
AT3G27690	<i>LHCB2.4</i>	ACTCCTCAGAGCATCTGGTACG	TTTCTGGATCGGCTGAGAGACC
AT3G47470	<i>LHCA4</i>	ACCCGCTTAACTTTGCTCCTACG	AACATCGCCAACCTCCCGTTTG
AT5G54270	<i>LHCB3</i>	GTTTATCCGCAGACCCTGAAGC	CCATCTCCCATGGATCACCTCAAG
<b>Chlorophyll degradation</b>			
AT3G03470	<i>CYP89A9</i>	ACCATAAGGTCACACACGACACC	TAGTACCTTGGCGCGGAATGAG
AT4G13250	<i>NON-YC1</i>	GCTATTGTCACTTCCTGGCTAAGG	CTGCATATAACGCCCGTCCTTG
AT4G14690	<i>ELIP2</i>	CCACCAGTTAGCAAGCCTAAGGT G	TGGACCGCTAAACGCTAGCAAAT C
AT4G16690	<i>MES16</i>	CCAAAGCCCTCTTGAGGACGTAA C	TTGAAAGGCCCTCATAGGAGCAG
AT4G22920	<i>NY1</i>	ATCCTTCAACGCTCCCTAGGAC	TTGCCCATCCTTGCAACTGAG
<b>Knockout mutants</b>			
AT5G37780	<i>CaM1</i>	AGACACTGACTCCGAGGAAGAGC TA	TAGCTTCTCACCAAGATTGGTCAT CAC
AT1G66410	<i>CaM4</i>	CCCTGAGTTCTTAAACCTAATGGC TA	GCGAAGCTCTGCAGCGGATA

Transcript Identifier	Gene name	Forward primer sequence (5' to 3')	Forward primer sequence (5' to 3')
<b>End-point PCR</b>			
AT1G13440	GAPDH	GCAACATACGACGAAATCAAGAA	CGACACGAGAACTGTAACCCC
AT5G28770	bZIP63	GAAAAAGTTTTCTCCGACGAAGA	CTGATCCCCAACGCTTCGA
AT5G05410	DREB2A	ATGGCAGTTTATGATCAGAGT	TTAGTTCTCCAGATCCAAGTAACT
AT2G43000	JUB1	ATGAGTGGCGAAGGTAAGTCTTAG	GGGTTTAGTGTTGCCATCTATAA

**Supplemental Table S4. Oligonucleotides used for EMSA. Mutated nucleotides within the JUB1 binding site are shown in red. JUB1 binding site is underlined.**

Primer	Primer sequence (5' to 3')
bZIP63-F	GGACCAACTCTGAGTGTAG <u>CCG</u> TTGAATAGTCCATTCATC
bZIP63-R	GATGAATGGACTATTCAAC <u>GGC</u> TACACTCAGAGTTGGTCC
bZIP63 mutated -F	GGACCAACTCTGAGTGTAG <u>CC</u> <b>AA</b> TGAATAGTCCATTCATC
bZIP63 mutated -R	GATGAATGGACTATTCAAC <u>GG</u> <b>TT</b> TACACTCAGAGTTGGTCC

**Supplemental Table S5. Primers used for ChIP-qPCR.**

Primer	Primer sequence (5' to 3')
PDH2pro-ChIP-F1	TGACATCTCGTATGGTCACACAGG
PDH2pro-ChIP-R1	AAAGAGTAAGAGAAGAATTTTCGCCG
PDH2pro-ChIP-F2	CTTGGTGTCTCTGACTCGACTTT
PDH2pro-ChIP-R2	GAATTTTCGCCGTAATTTTCTGACAG
MYB2pro-ChIP-F1	CAAACAATTGACCAAATGGAGAGCT
MYB2pro-ChIP-R1	CTGGAACACGGCATAAGTGTTATG
MYB2pro-ChIP-F2	CACTTATGCCGTGTTCCAGTCAC
MYB2pro-ChIP-R2	GATTTGAAGTGATTAAGCAATGTGCG
bZIP63pro-ChIP-F1	CTTGTAGGACAGTGATTTTTCCGG
bZIP63pro-ChIP-R1	CGATGAATGGACTATTCAACGGC
bZIP63pro-ChIP-F2	GCCGTTGAATAGTCCATTCATCG
bZIP63pro-ChIP-R2	GACCTGGTGTGCATGTTTAAGGTTTAT
TA3pro-F	CTGCCGTGGAAGTCTGTCAA
TA3pro-R	CTATGCCACAGGGCAGTTTT

*PDH2pro* (AT5G38710) - 369 bp

**GACTCACGAAGA**CAAATCTTCATCAGAATTCTTACTTTTATTACTTTTCTATTAATAA  
TCATATCCATTAAATAATTCTATCTATCCAATGACATCTCGTATGGTCACACAGGTC  
ACGTCCTTGGTGTCTCTGACTCGACTTTCTTAATAGATTTTTGTTTTCCGAAACAA  
ATATGTTCTGTCAGAAAATT**ACGGC**GAAATTCTTCTTACTCTTTACTCCAAATTA  
ATTAGTTTTATTTCATTTTAGATTTTTGATTCCATTTCAATTGTTAAATCCTTATCTGC  
AAATATAATTATCACGTTTAGTAACTCTTGGGATTTACTATGCTTCAATCCGAATCT  
TATTTATCGCAT**TAACCTTCATTACG**

*MYB2pro* (AT2G47190) - 283 bp

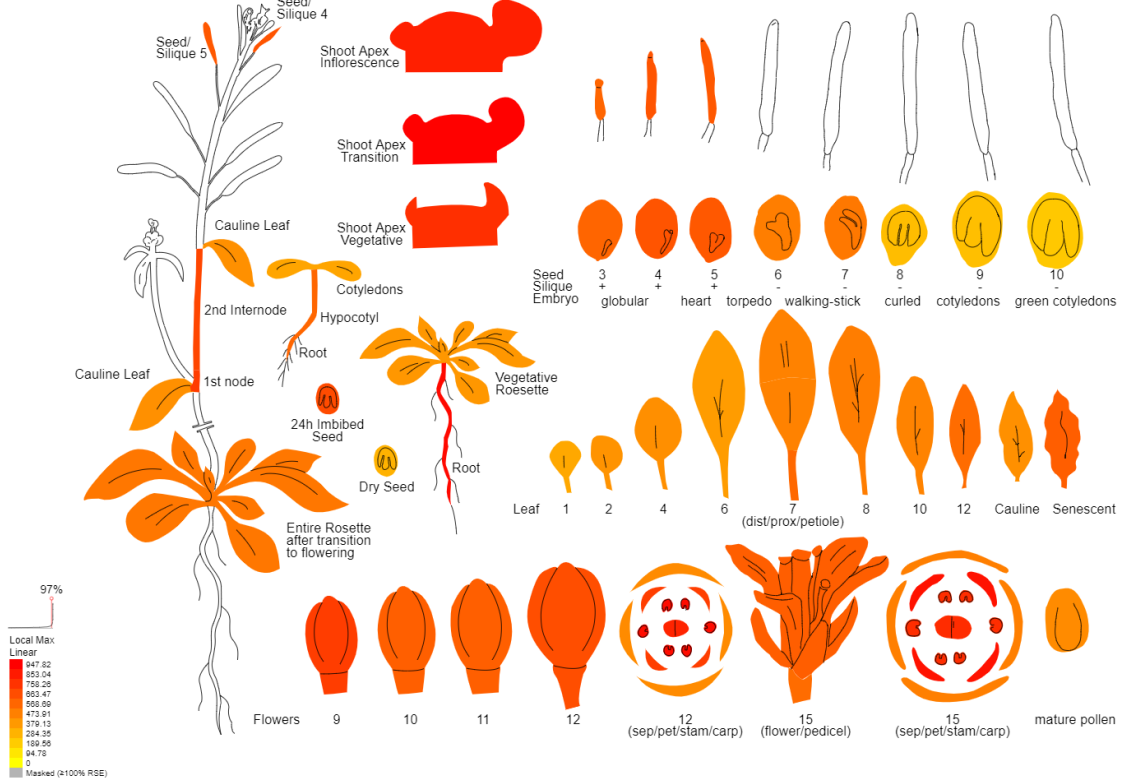
**AGGGTCAAACCTTA**GTATTTTAAAATTACACAAACAATTGACCAAATGGAGAGCTA  
ATTATGTTTAGCATAATTTACTATATAGTTGCAAAATTCACCTTTAGAAACAGAATA  
AAAAATAAAAATTGAACATAACACTTAT**GCCGT**GTTCCAGTCACTCTTCAACATTC  
TACTCATTTTCAAATATCCTTTTTATAAAATACTACTTTTAAAATTTATTGATTCTTAT  
GTTCTTCACTATATATATAAATATCGCACATTGCTTA**ATCACTTCAAATCT**

*bZIP63pro* (AT5G28770) - 343 bp

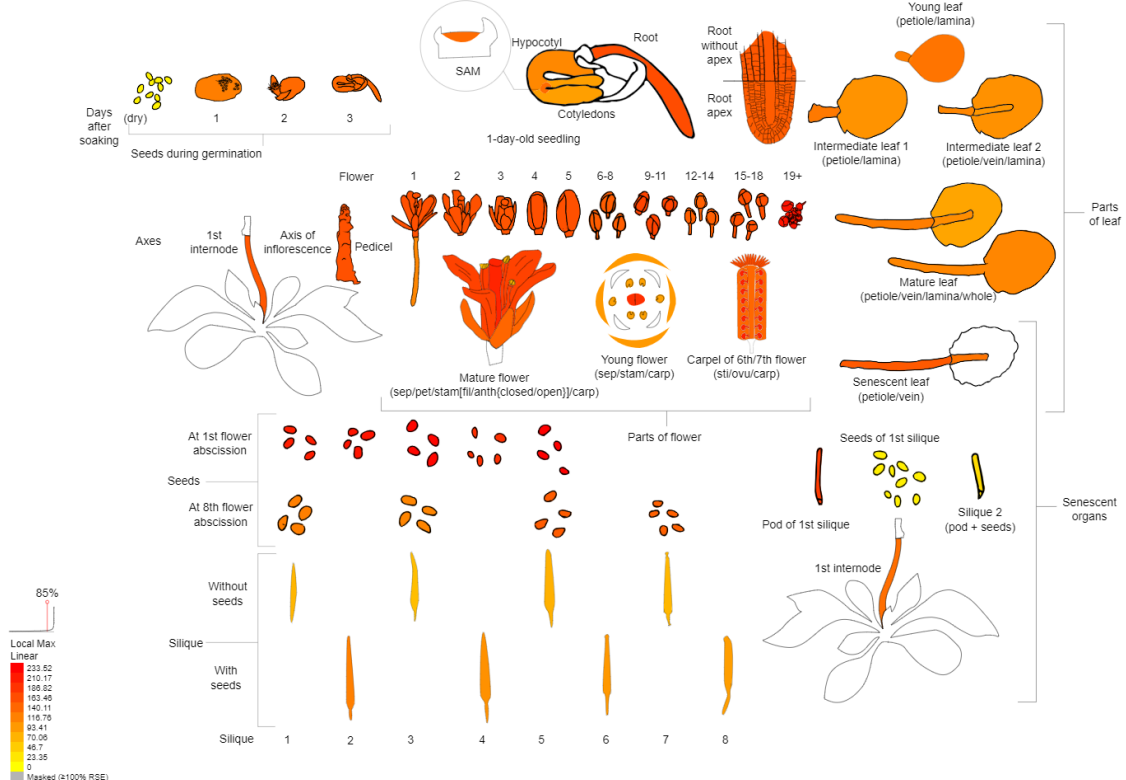
**CTTGTAGGACAGTG**ATTTTTCCGGGTTTTTTTTGTTTCTCATGTTATAGGTTTAAGTC  
TCCAATGCATCATTTTGCTATATTTTAAATATTTATAGGCAAAAAATATTTTGGGTTT  
TAGGACCAACTCTGAGTGTA**GCCGT**TGAATAGTCCATTCATCGGATTTTTAATAAA  
CCTTAAACATGACACCAGGTCAAATAAGAATGATTTAGAAATTGATTCATAACCT  
AACCTACATAATAATTCTTCCTAAAATAAGACAAAATGTCACACGAAATTATACAGT  
TTGAGATTTTTCTAAACCACTTTAACATAGAAAAGTCTACAAAAT**TCTACTAATGGT**  
**GT**

**Supplemental Figure S1. The sequences of the promoter regions are used in Y1H for the generation of bait constructs. JUB1 binding site is shown in yellow. The primer location used for PCR amplification is shown in green.**

AtGenExpress eFP: AT5G37780 / ACAM-1, CAM1, TCH1

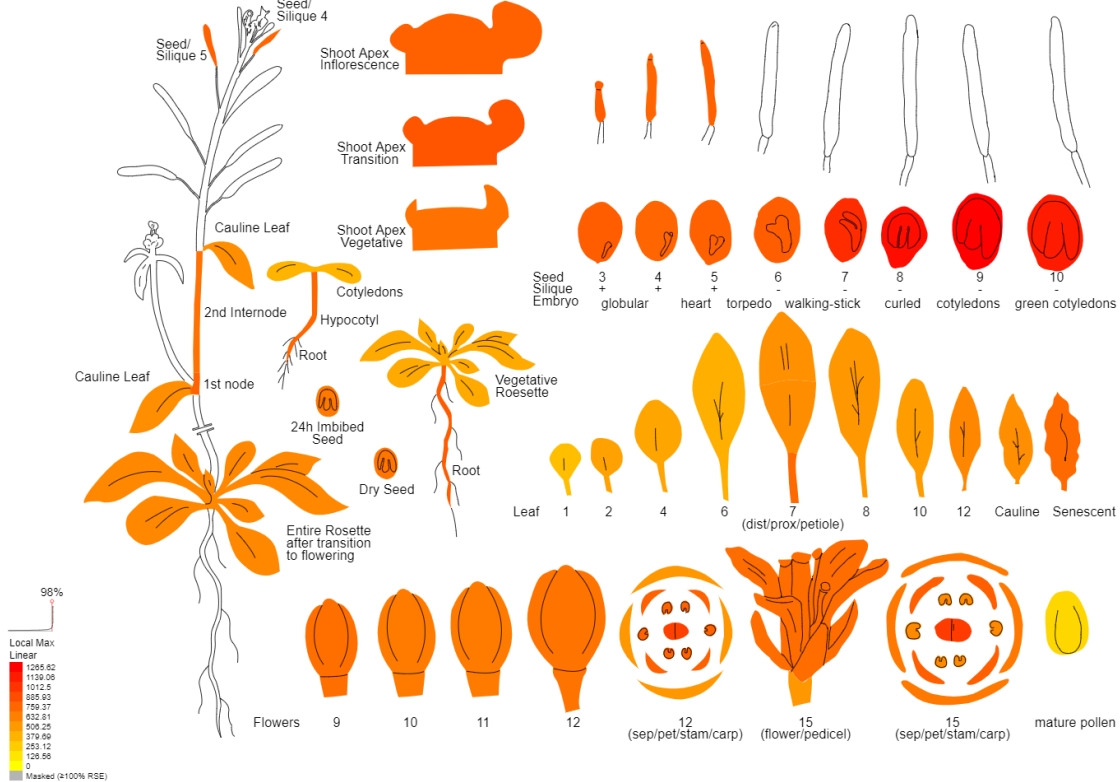


Klepikova eFP (RNA-Seq data): AT5G37780 / ACAM-1, CAM1, TCH1

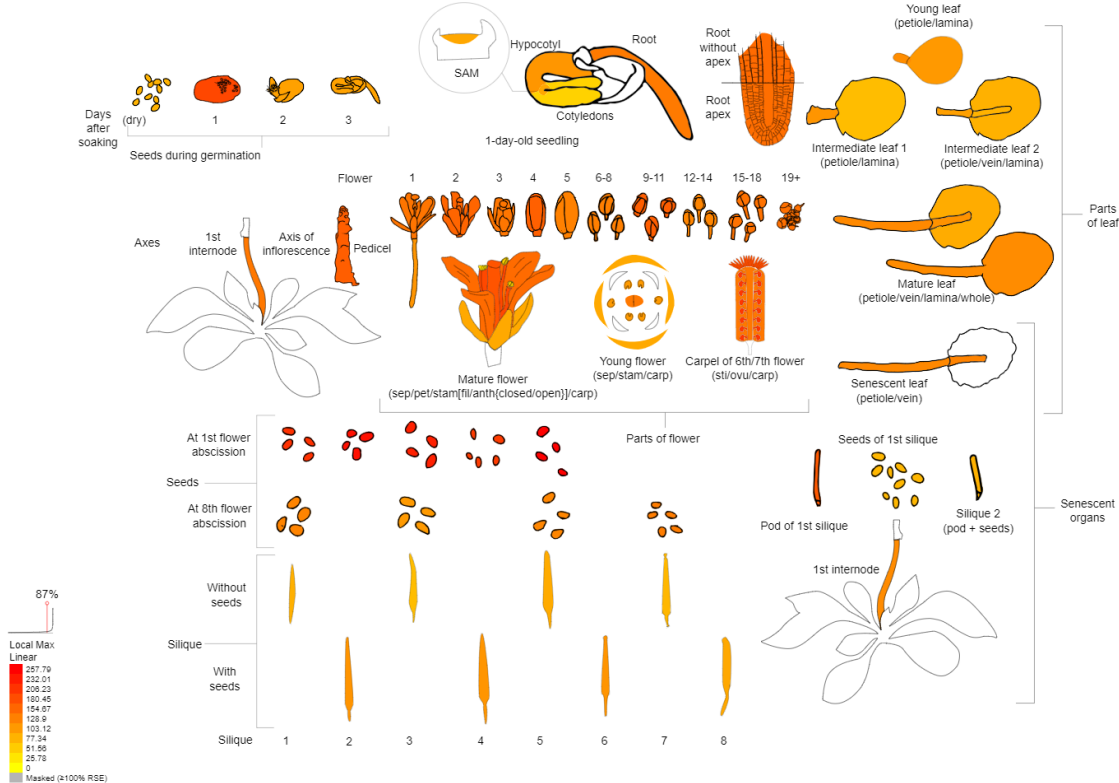


**Supplemental Figure S2. Expression pattern of *CaM1* gene.** The data come from (Nakabayashi et al., 2005; Schmid et al., 2005). Gene expression data generated by the Affymetrix ATH1 array are normalized by the GCOS method, TGT value of 100. Most tissues were sampled in triplicate. This image was generated with the AtGenExpress eFP at [bar.utoronto.ca/eplant](http://bar.utoronto.ca/eplant) (Waese et al., 2017)

AtGenExpress eFP: AT1G66410 / ACAM-4, CAM4



Klepikova eFP (RNA-Seq data): AT1G66410 / ACAM-4, CAM4



**Supplemental Figure S3. Expression pattern of *CaM4* gene.** The data come from (Nakabayashi et al., 2005; Schmid et al., 2005). Gene expression data generated by the Affymetrix ATH1 array are normalized by the GCOS method, TGT value of 100. Most tissues were sampled in triplicate. This image was generated with the AtGenExpress eFP at [bar.utoronto.ca/eplant](http://bar.utoronto.ca/eplant) (Waese et al., 2017).



## Publication and conference attendance

### Publication

Shuchao Dong, Danuse Tarkowska, Mastoureh Sedaghatmehr, **Maryna Welsch**, Saurabh Gupta, Bernd Mueller-Roeber, Salma Balazadeh. An *HB40- Jungbrunnen1 - GA 2-OXIDASE* regulatory module for gibberellin homeostasis in Arabidopsis. bioRxiv 2021.02.17.431590; doi: <https://doi.org/10.1101/2021.02.17.431590>

**Maryna Welsch**, ... Salma Balazadeh, Bernd Mueller-Roeber. JUB1 is a novel calmodulin-binding protein. (in preparation)

### Conference attendance

Conferences:

- Havel Spree Colloquium 2018 (Berlin, Germany; 13.04.2018): The Havel-Spree Colloquium is an annual symposium on plant biology. Attendance.
- Participation in International and Interdisciplinary Conference of the Arab-German Young Academy of Sciences and Humanities (AGYA) on Evolution of Mediterranean Agriculture (Barcelona, Spain; 23.-26.11.2018): Interdisciplinary Perspectives on Historical Developments and Future Visions. Poster presentation in Session Innovations in Agriculture.
- Havel Spree Colloquium 2019 (Berlin, Germany; 29.03.2019): The Havel-Spree Colloquium is an annual symposium on plant biology. Poster presentation.
- 9<sup>th</sup> International Symposium on Plant Senescence (Berlin, Germany; 01.-04.04.2019). Poster presentation, the poster received the Best Poster Award.
- Plants and People 2019 - Future Foods – Challenges for Global Food Security (3.-4.09.2019, Potsdam-Golm, Germany). Attendance. Organizing committee member.
- Plant Biology 2020 Worldwide Summit (PB20) (Online, 27.-31.07.2020). Attendance.


Scientific training:

- Institute of Plant Sciences Paris Saclay (IPS2) (Gif-sur-Yvette, France; 06.-10.08.2018). Supervisor Dr. Marie Boudsocq. Learned protoplasts isolation and transfection.
- PlantaSYST Metabolite profiling workshop (MPI-MP, Potsdam-Golm, Germany; 13-17.01.2020)

## **Eidesstattliche Erklärung**

Hiermit versichere ich, die vorliegende Arbeit selbstständig angefertigt und keine anderen als die angegebenen Quellen und Hilfsmittel verwendet zu haben. Ich versichere ebenfalls, dass die Arbeit an keiner anderen Hochschule als der Universität Potsdam eingereicht wurde.

**Potsdam, September 2021**



---

**Maryna Welsch**

## Acknowledgments

Firstly, I would like to express my sincere gratitude to my supervisors Prof. Dr. Bernd Müller-Röber and Prof. Dr. Salma Balazadeh, for giving me the opportunity to work on this exciting project, and for their support and supervision during both fruitful and challenging times of my doctorate. Furthermore, I am very grateful for all the opportunities and freedom they gave me to learn new methods and establish them in the scope of my PhD project.

Further, I want to acknowledge my PhD advisory committee Prof. Dr. Zoran Nikoloski, Dr. Dirk Hinch, and Dr. Friedrich Kragler, for the scientific discussions and constructive advice I received after each of our meetings. I want to express my gratitude to Dr. Friedrich Kragler and Prof. Dr. Wolfgang Dröge-Laser for kindly agreeing to review my thesis. A special and warm thanks to PhD and IMPRS coordinator Dr. Ina Talke for her tremendous organizational work and scientific support. I also want to thank Dr. Arun Sampathkumar for his great help with confocal microscope analysis, Dr. Karin Köhl and the Green Team for performing Arabidopsis infiltration and taking care of my plants on a regular basis.

I am grateful for the great support I received from all MPIMP service teams, especially the Photoservice team, qRT-PCR team, IT team, Administration team including HR, International and travel office team, Public relations, Cleaning & Media kitchen team, Library, LIMS, Store team, and Technical service team. Thank you all for being there every time I needed help or had a question. Thanks to PhD and PostDoc representatives, Krisenstaband, and Gender Equality Officers for making MPI a fantastic and safe workplace. I am thankful for the great help and events organization done by the Welcome Center, Potsdam Graduate School and Max Planck Academy.

I am grateful to the whole AG-Müller-Röber and AG-Balazadeh, current and previous lab colleagues Andy, Amit, Changqiong, Ewa, Gechemba, Iman K, Iman T, Karina, Mastoureh, Miao, Mindy (Shu Chao), Tobias, Vikas, Venkatesh, and Xuemin for a friendly atmosphere and support during my initial periods and the entire time of my PhD. Special thanks also to our lab manager Karina and our group technicians Antje, Eike, and Dagmar for their help during my research work. Thanks also to our group members at the University of Potsdam, Dr. Katrin Czempinski, Ines, and the whole AG-Müller-Röber. I am thankful to my interns Ange and Klaudia for their help during my PhD.

Thanks to all people who shared their knowledge, material, and consumables to help my project to succeed, especially Andy, Itzell, Magdalena, Joachim Forner, Joachim Fisahn, Reynel, Eleni, Feng, Irina, Erik and Kati and many others who have helped me in some ways and were

not mentioned here. I would like to thank Andy, Mike and Irina for their great help looking at my first drafts of the thesis and their suggestions, and Erik for helping me in writing the German summary for the thesis.

Furthermore, I would like to thank PlantaSYST project funding, European Union's Horizon 2020 research and innovation program under grant agreement No 664620 for providing financial support for my PhD and also the Max-Planck Institute of Molecular Plant Physiology (MPIMP) and Prof.Dr. Salma Balazadeh for providing an extension of my PhD funding.

I am grateful to Prof. Dr. Kazuko Yamaguchi-Shinozaki, Prof. Dr. Tina Romeis, Dr. Marie Boudsocq, and Dr. Joachim Forner for kindly providing seeds and vectors used in this study. Special thanks also to Dr. Marie Boudsocq for hosting me during my scientific training at the Institute of Plant Sciences Paris Saclay and teaching me protoplasts isolation and transfection. Last but not least, I want to say thank you to my family for their support and unconditional love that helped me to complete my thesis. I express my warm appreciation and love to my husband for always being there for me and accepting the long working hours and busy weekends as a part of life with a PhD student.